NEURONAL CIRCUIT MECHANISMS UNDERLYING FOOD INTAKE IN *DROSOPHILA MELANOGASTER*

A Dissertation

Presented to the Faculty of the Graduate School

of Cornell University

In Partial Fulfillment of the Requirements for the Degree of

Doctor of Philosophy

by

Xinyue Cui

December 2024

NEURONAL CIRCUIT MECHANISMS UNDERLYING FOOD INTAKE IN *DROSOPHILA MELANOGASTER*

Xinyue Cui, Ph. D.

Cornell University 2024

Proper regulation of food intake is essential for the survival of all animals, including humans. Although neural circuits that regulate food intake have been extensively investigated in rodent models, the entire sensorimotor circuits that regulate food intake have not been fully elucidated in any model organism. Previously, our lab has identified Ingestion Neuron 1 (IN1) as a regulator of food intake in adult *Drosophila melanogaster* (Yapici et al., 2016). Here, using optogenetics and two-photon calcium imaging, I revealed that IN1 neurons receive specific excitatory input from sugar-sensing enteric Gr43a neurons. We developed a new *in vivo* imaging method to record the activity of enteric neurons in behaving flies. Using this new method, we captured the acute response of Gr43a enteric neurons to sucrose ingestion and demonstrated that these neurons can activate IN1. In addition, I used the connectome of an entire adult fly brain to identify the major output neurons of IN1, crop innervating enteric motor (CEM) neurons. I showed that activation of CEM neurons can block the ingested food from entering the crop (a stomach-like organ). Furthermore, activation of IN1 neurons inhibits CEM neurons, allowing ingested food to be transported to the crop for storage, facilitating the later, slower process of regurgitation and digestion. Overall, my thesis research uncovered an IN1-centered sensory-motor neural circuit that acutely responds to the nutrient composition of ingested food, thereby directly influencing food ingestion in flies. By identifying this circuit's role in integrating sensory

information from ingested nutrients, we have gained insights into the real-time mechanisms by which the fly brain assesses and adjusts food intake based on nutritional quality. I anticipate that our research will yield a more comprehensive understanding of how food intake is precisely regulated through complex interactions between the central brain and the enteric nervous system. This work not only sheds light on the fundamental neurobiology of feeding but also provides a foundation for exploring similar sensory-motor pathways in other organisms, potentially offering broader insights into appetite control and nutrient-based decision-making.

BIOGRAPHICAL SKETCH

On the southern bank of the Long River (Yangtze River) lies a medium-sized city named Jiujiang, located at the northern end of Jiangxi Province, P.R. China. Xinyue Cui was born there in 1996 to a working-class family—Can Zhang and Guoping Cui. Like many Chinese children of that time, she had a joyful yet busy childhood, supported by and protected under the love of her parents, who did their best to provide for her despite their limited resources by today's standards. From a very young age, she had a wide range of interests and was curious about many aspects of life. At the age of 8, during her family's first visit to the newly opened musical instrument store in Jiujiang, she eagerly explored all the instruments, trying to figure out how each one made music. She overheard her parents jokingly remark that she had 'too many scattered interests,' but this didn't bother her. She was already busy exploring the next new thing she encountered.

Life wasn't always easy for Xinyue Cui. She developed a strong interest in biology while attending junior high school and aspired to participate in the Biology Olympiad when she entered Jiujiang No. 1 Middle School for high school. She was impressed by the knowledge her classmates gained while preparing for the Science Olympiad and wanted to challenge herself in the same way. However, from her first to second year in high school, she did not achieve very high scores in every Biology Olympiad team test. This led her to a heated confrontation with her parents, who urged her to abandon the Olympiad due to its uncertain prospects and focus instead on the more predictable path of preparing for college entrance exams. Despite this, Xinyue Cui remained determined to pursue the Olympiad, even if it meant failure. With the mediation and guidance of her biology teacher, Mr. Hongzhong Zhang, she eventually won first prize at the provincial level in the National Biology Olympiad in 2012, becoming the only student in her school to achieve this honor that year, and made peace with her parents.

While studying for the Biology Olympiad, she gradually came to appreciate the beauty of biology and other natural sciences. She also began to apply the knowledge and ideas she learned in these fields to think about increasingly philosophical and abstract problems. At times, she felt resentful that she had been brought into the world without her consent and thought that if she couldn't resist being part of the world's evolution, she should at least explore, discover, and even expose why the world is the way it is while she was still alive. Scientific research seemed to be one of the most effective ways to achieve this. With this sense of resistance toward accepting her destiny, she decided in her teenage years to dedicate herself to scientific research, with a particular interest in understanding the mechanisms of consciousness and its related problems.

In 2012, she won a prize in the Biology Olympiad and was guaranteed admission to Zhejiang University, Pursuit Science Class (Biomedical Sciences) after passing its entrance exam. At Zhejiang University, she met many friends and mentors who shared her scientific interests. Her undergraduate advisor, Dr. Zhefeng Gong, became her first guide on the path of scientific research. Despite being an undergraduate at the time, she was fortunate enough to join Dr. Gong's lab, where she experienced the entire process of a scientific research project—from the initial design to its implementation and completion—for the first time.

During the last year of her undergraduate education (August 2015 to Jun 2016), through a 3+1 joint program between Zhejiang University and the University of Edinburgh, she spent one year studying in Edinburgh, Scotland, U.K. During this time, she joined Dr. Mark Evans' lab at the School of Medicine and Veterinary Medicine, where she received rigorous training in cell culture and immunohistochemistry, successfully completing a research project and graduating with an MSc after one year.

In 2016, she applied for her first PhD program. Having realized that scientific advances are often driven by technological innovations, she aspired to develop non-invasive neural activity recording tools with single-neuron resolution on a whole-brain scale. However, probably due to her lack of background in biological engineering, she did not receive any acceptance offers that year.

In 2017, during her gap year, she returned to her undergraduate advisor Dr. Gong's lab as a research assistant. There, she successfully employed two-photon imaging and optogenetics to record IPC neuron responses to the activation of cold-sensing neurons in adult *Drosophila Melanogaster*. Meanwhile, she began her second round of application to PhD programs and was fortunate to receive an acceptance letter from the Department of Neurobiology and Behavior at Cornell University.

In August 2017, she began her PhD at Cornell University, where she met Dr. Nilay Yapici, a mentor who would significantly influence her life, as well as many lab mates from all around the world who became an important part of her journey. In September 2024, as she prepared for her PhD thesis, she wrote this autobiography

Dedicated to everyone

幸甚至哉

ACKNOWLEDGMENTS

First and foremost, this whole project wouldn't possibly exist without my P.I., Dr. Nilay Yapici. She was the one who discovered IN1 neurons and introduced this project to me at the very beginning of my Ph.D., and it was her original idea to add the gut neurons into the picture in this project, which later proved to be a remarkably visionary decision that greatly enhanced the impact of our work. It was her hard work that secured all the funding and apparatus supporting every experiment of this project, and it was her rigorous effort that polished the manuscript of this project up until the last minute of submission.

I benefited a lot from being a trainee in her lab over the past 7 years, and I feel immensely fortunate to be able to have that experience, for it was not only academically improving for me but also mind-opening and life-changing. I want to thank her for not laughing at all my seemingly foolish dreams and instead discussing them with me seriously, listening to me, and supporting me when I was going through the darker moments of life. I greatly appreciate every opportunity she gave me, every lesson she taught me, and everything she shared with me. And as is the ultimate way to express my gratitude, I know I will carry them on, as much as I can, to the next generation.

I am deeply grateful to my committee members—Dr. Joseph R. Fetcho, Dr. Ian Ellwood, and Dr. Chris Xu—for their invaluable guidance and insightful discussions that have enriched this project. Each committee meeting brought fresh perspectives that directly shaped and strengthened my work. I especially wish to thank Dr. Joseph R. Fetcho. My journey to Cornell began with the hope of joining his lab to pursue whole-brain imaging in zebrafish. Although he was unable to take me on as a PhD student, he graciously recommended me to other zebrafish labs, which was a kind gesture that went beyond my imagination at the time. After choosing to

join the Neurobiology and Behavior Department at Cornell, I was fortunate to spend a semester in my first year rotating in Dr. Fetcho's lab, where I gained firsthand experience with both the advantages and challenges of whole-brain neural activity recording. At the end of that rotation, Dr. Fetcho encouraged me to always keep sight of the 'big picture' in scientific research—a lesson that has benefited me ever since.

I would also like to thank all my lab mates. For me, they are not only lab mates, but more like life-mates. These 7 years of Ph.D. has been a long winding road with a lot of ups and downs, and I wouldn't be able to reach my current stage without the immense help I received from them. I want to thank Staci Thornton and Max Aragon for orientate me when I first joined the Yapici lab. I want to thank Dr. Matthew Meiselman for being my best bench mate during late-night work shifts. I want to especially thank Dr. Yuta Mabuchi, my Ph.D. littermate who witnessed the growth of both of us from each other's eye, for being an amazing friend, and making a huge impact on my life trajectory. I also want to sincerely thank Dr. Haein Kim, for his unwavering support for his colleagues over all these years; from him, I learned to view the world from a broader perspective. I want to thank Jamien Shea, who may seem quiet, even sometimes anonymous, but steadfastly supports everyone in the lab who needs help. I want to thank Dr. Deepthi Mahishi for being such a supportive friend during times when I needed strength, and for being a key role in our lab who brought us closer than ever. I want to thank Anna Gruzdeva, for being a great friend whenever I needed help, and for all her great advice whenever I face difficulties, in science or in life. I want to thank Naman Agrawal, for all the joyful moments we shared in and outside the lab, which I cherish as precious memories. Last but not least, I want to thank Wenshuai Jiang, for being such a reliable friend for me, and making me feel so fortunate to have developed such a sturdy friendship in the final years of my Ph.D. Besides these people, I

also want to thank all the undergraduate students and alumni of our lab, for being an irreplaceable part of our lab, and composing a community together.

I want to thank all members of the NBB community, including my office mates, lab neighbors, and the maintenance and administration staff, for all their own kind of support for me over all these years. Specially, I want to thank Dr. Micheal Smith, for providing me four light bulbs and one computer mouse for free in his SNEEB garage sale on 2017, because the only condition he asked in return is to acknowledge him for those items in an upcoming manuscript, and I honor my promises.

I also want to thank my friend Ying Sheng for introducing me to Cornell University. Her mention of Cornell's beautiful scenery drew my attention to the Neurobiology Ph.D. program, ultimately leading me to apply and gain admission. I am also grateful to my trainer and friend Kyle Allington for helping me maintain my health, which has been essential to my success in the Ph.D. program and beyond.

I want to thank my family, especially my parents, for all their support over all these years. I have been away from home for many years, and without their support, I would not be where I am today.

Lastly, I know there must be some people who helped me, but I forgot to mention them in the previous text. Here, I want to thank everyone who did not have to help me, but chose to. I appreciate every bit of kindness I received.

Finally, I want to thank all the fruit flies who lost their lives to this research project. It is their lives that enabled us to know more about this world shared by both human and fruit flies, together with all other living and non-living beings.

TABLE OF CONTENTS

LIST OF FIGURES

LIST OF ABBREVIATIONS

5-HT, Seretonin, or, 5-Hydroxytryptamine

AgRP, agouti-related peptide

AHL saline, adult hemolymph-like saline

ARC, arcuate nucleus

ATR, all-trans-retinal

CCK, cholecystokinin

CEM neurons, crop innervating enteric motor neurons

CNS, central nervous system

CPG, central pattern generator

DCSO, dorsal cibarial sense organs

Dh31, diuretic hormone 31

Dh44, diuretic hormone 44

DMV, dorsal motor nucleus of the vagus

DSK, drosulfakinin

ECP junction, esophagus, crop duct, and proventriculus junction

EM, electron microscopic

ENS, enteric nervous system

ENs>, Enteric neuron labelling split Gal4

FDHM, total duration at half maximum

HCG, hypocerebral ganglion

HGN-1, hindgut neuron 1

Ilp, insulin like peptide

IN1, Ingestion Neuron 1

IPCs, insulin-producing-cells

LSO, labral sense organ

Ms, Myosuppressin

NPF, neuropeptide F

NPY, mammalian neuropeptide Y

NTS, nucleus tractus solitarii

PG, proventriculus ganglion

PI, pars intercerebralis

PMT, photomultiplier tube

POMC, pro-opiomelanocortin

PVN, paraventricular nucleus

PYY, polypeptide YY

sNPF, short neuropeptide F

STG, stomagastric ganglion

STNS, stomagastric nervous system

TNT, tetanus toxin

VCSO, ventral cibarial sense organs

VGLUT, vesicular glutamate transporter

VNC, ventral nerve cord

CHAPTER 1

Literature Review and Introduction to the Thesis

As one of the most ancient and fundamental behaviors that characterizes the kingdom Animalia, food intake remains a critical aspect of the daily lives of many animal species, including humans (Odum & Barrett, 2005). Food intake in humans is densely regulated by neural circuits connecting the brain and gastrointestinal tract (GI tract), forming the famous gut-brain axis (Mayer, 2011), and so is the case in mice, rats, and flies. Mice and rats have a digestive system that is similar to humans; the food they ingest will first be transported to their stomachs, then to the small intestines and large intestines (DeSesso & Jacobson, 2001; Hugenholtz & de Vos, 2018). Many important discoveries about how the gut-brain axis can regulate food intake were made using rodent models. For example, it has been discovered that the mammalian GI tract contains a special type of endocrine cells, enteroendocrine cells, which can secret ~20 different hormones, including ghrelin, serotonin (5-HT), cholecystokinin (CCK), polypeptide YY (PYY), and glucagon-like peptide 1 (GLP1) (Gribble & Reimann, 2019; Latorre et al., 2016). Among these hormones, Ghrelin can directly act on the agouti-related peptide (AgRP) expressing neurons located at the arcuate nucleus in the brain to promote food intake (Wu et al., 2019), while CCK, PYY, and GLP1 can act on the afferent fiber of the vagus nerve, which will convey that stimulation first to the nodose ganglia, and then to *nucleus tractus solitarii* (NTS) in the brainstem (Latorre et al., 2016). In the brain, NTS provides efferent projections to the paraventricular nucleus (PVN), which contains MC4R neurons, and to the arcuate nucleus (ARC), which contains AgRP-expressing neurons and pro-opiomelanocortin (POMC) expressing

neurons (Jais & Brüning, 2022). Activation of PVH^{MC4R} and ARC^{POMC} neurons can promote satiety, whereas activation of ARC^{AgRP} neurons can promote hunger (Fenselau et al., 2017; Garfield et al., 2015; Jais & Brüning, 2022), although the exact mechanisms by which they promote satiety or hunger are not yet fully understood. After integrating the input information from the sensory branch of the vagus nerve with other input information from other parts of the brain, the brain can recruit the motor branch of the vagus nerve to send its output signals back to the GI tract. The projection of vagal motor neurons originates from the dorsal motor nucleus of the vagus (DMV) and ends at various locations of the GI tract, including the stomach, spleen, and intestine, with striking complexity and selectivity (Tao et al., 2021). Together, these gut-brain neural circuits integrate long-term internal state signals with short-term food intake cues to modulate decisions about when, what, and how much to eat. Although much research has revealed the food ingestion regulating mechanism in rodents and other mammals (Broberger, 2005; Challet, 2019; Ferrario et al., 2016; Sternson & Eiselt, 2017; Watts et al., 2022), the neural circuits underlying food intake behavior—from sensory input to behavioral output—have yet to be clearly mapped in any animal.

To elucidate sensorimotor circuits that regulate food intake, we chose to study the fruit fly *Drosophila melanogaster*. Compared to humans, mice, or rats, fruit flies have a much simpler central nervous system (CNS) and enteric nervous system (ENS) in terms of neuron count. Nonetheless, they can still perform complex tasks for regulating food intake, allowing them to effectively adapt to the challenges they face in their natural environments. Furthermore, the wiring diagram of a full adult fly brain has been recently completed and is open to public research in the FlyWire connectome database (Buhmann et al., 2021; Dorkenwald et al., 2023; Eckstein et al., 2023; Lin et al., 2024; Matsliah et al., 2024; Schlegel et al., 2023; Zheng et al.,

2018). FlyWire connectome (current version 783) is obtained by segmenting, proofreading, synapse detecting, and cellular annotating of electron microscopic (EM) fly brain images through a collaboration of human and artificial intelligence (AI) (Dorkenwald et al., 2023). The resolution of the FAFB EM dataset used for FlyWire is $4\times4\times40$ nm^3, which means it can offer a clear vision of every single synapse and many sub-cellular structures in almost every neuron in the adult fly brain (Dorkenwald et al., 2023). This new tool enables scientists, for the first time, to map the complete neural circuit for any behavior in flies, tracing each neuron from sensory input to motor output. Consequently, investigating the neural regulation of food intake in *Drosophila* offers a promising starting point that could ultimately lead to a comprehensive understanding of food intake circuits in humans and, eventually, in all animals.

The GI tract in adult flies consists of the foregut, midgut, and hindgut. Foregut in adult flies includes the esophagus, crop, and proventriculus (Miguel-Aliaga, Jasper, & Lemaitre, 2018). After the proboscis muscles pump the food liquid into the esophagus, the esophagus channels the food liquid through the brain, passing it to the three-way junction of the posterior esophagus, anterior crop duct, and anterior proventriculus which is immediately connected to the midgut (Hadjieconomou et al., 2020). For convenience, hereafter, this three-way junction will be referred to as the esophagus, crop duct, and proventriculus junction (ECP junction). In the acute phase of ingestion, most ingested food is transported into the crop and stored there, as it has been proposed that the expansion of the crop provides the negative pressure in the esophagus that is needed for food ingestion (Hadjieconomou et al., 2020). After the fly ceases feeding, a coordinated muscle-pumping cycle in the foregut transports small amounts of stored food from the crop back to the foregut, then moves it to the proventriculus and midgut for subsequent digestion and nutrient absorption (Stoffolano & Haselton, 2013). This pumping cycle likely

continues until all food stored in the crop is transported to the midgut. Due to its role in food storage, the crop in flies is often considered a partial functional equivalent of the human stomach (Sadaqat, Kaushik, & Kain, 2021).

Despite anatomical differences in the GI tract between flies and mammals, the mechanisms regulating food intake in flies share many similarities with those in mammals. For example, the homolog of mammalian cholecystokinin (CCK) in flies is drosulfakinin (DSK), and as activation of CCK neurons in the mammalian brain reduces food intake (D'Agostino et al., 2016), RNAi knock-down of DSK in insulin-producing-cells (IPCs) in the fly brain increases food intake (Söderberg, Carlsson, & Nässel, 2012). Similarly, just as the mammalian neuropeptide Y (NPY) promotes food preference in mice (Horio & Liberles, 2021), its fly homolog, short neuropeptide F (sNPF) enhances food intake in flies (Lee et al., 2004). Similar to mammals, flies have robust communication between the ENS and CNS. Many CNS neurons directly innervate the GI tract; for example, the foregut and midgut are innervated by insulin-like peptide-2 (Ilp-2) producing neurons in the pars celebralis, a region in the fly brain located in the central part of the brain near the protocerebrum (Nässel et al., 2013). Other CNS neurons that innervate the digestive tract include piezo-expressing neurons (Min et al., 2021), Diuretic hormone 44 (Dh44) expressing neurons (Dus et al., 2015; Min et al., 2021), Bitter-SEL neurons (Yao & Scott, 2022), and Myosuppressin (Ms) expressing neurons (Hadjieconomou et al., 2020). Furthermore, the fly hindgut is innervated by neurons projecting from the ventral nerve cord (VNC), a part of CNS in flies, including hindgut neuron 1 (HGN-1) and Ilp-7-producing neurons (Cognigni, Bailey, & Miguel-Aliaga, 2011). Last but not least, one important part of fly ENS is the hypocerebral ganglion (HCG) (also named proventriculus ganglion (PG)), a ganglion located just on top of the ECP junction. HCG contains the cell bodies of about 35 neurons, and many of

them innervate different segments of the foregut and midgut. Importantly, some of the HCG neurons have been shown to receive input from the brain or send their outputs to the brain, including enteric piezo neurons (Min et al., 2021; Wang et al., 2020), enteric 5-HT7 neurons (Yao & Scott, 2022), and, as we are about to reveal in this study, enteric Gr43a neurons (Miyamoto & Amrein, 2014). In summary, bidirectional neural communication exists between the CNS and ENS in flies, similar to that in mammals

Similar to mammals, the fly gut also contains enteroendocrine cells that can secret many signaling molecules, including neuropeptide F (NPF), Diuretic hormone 31 (Dh31), and CCHamide-2, and these molecules can act on CNS neurons to promote or inhibit food intake (Chopra, Kaushik, & Kain, 2022; Lin et al., 2022; Malita et al., 2022; Ren et al., 2015). Although the pharynx within the proboscis is typically not considered part of the GI tract in flies, it houses pharyngeal taste neurons located at the labral sense organ (LSO), ventral and dorsal cibarial sense organs (VCSO, DCSO), which send their sensory inputs to the brain. Additionally, pharyngeal muscles responsible for pumping food into the esophagus are innervated by motor neurons projecting from the brain. Altogether, the extensive neural circuits and molecular signaling pathways spanning across CNS and ENS dedicated to the regulation of food intake have once again demonstrated the remarkable importance of this behavior for survival.

In our previous study, we discovered that Ingestion Neuron 1 (IN1) located at the subesophageal zone (SEZ) of the fly brain can regulate the food intake behavior in *Drosophila melanogaster* (Yapici et al., 2016). Food intake of hungry flies is significantly reduced when IN1 synaptic transmission is inhibited. Calcium imaging experiments revealed that IN1 neurons are activated upon sucrose ingestion and maintain activation for at least 7 minutes in ~24-hour fasted

flies consuming 1M sucrose. However, this persistent activation is absent when hungry flies consume lower sucrose concentrations or in-fed flies (Yapici et al., 2016).

My thesis research systematically examined how IN1 neurons regulate food ingestion using two-photon in vivo calcium imaging and optogenetics. My results revealed that IN1 neurons regulate food intake via their bi-directional communication with the enteric nervous system. Thus, I uncovered a complete sensorimotor circuit dedicated to food ingestion in flies.

REFERENCES

Broberger, C. (2005). Brain regulation of food intake and appetite: Molecules and networks. In *Journal of Internal Medicine* (Vol. 258, pp. 301-327).

Buhmann, J., Sheridan, A., Malin-Mayor, C., Schlegel, P., Gerhard, S., Kazimiers, T., Krause, R., Nguyen, T. M., Heinrich, L., Lee, W.-C. A., Wilson, R., Saalfeld, S., Jefferis, G. S. X. E., Bock, D. D., Turaga, S. C., Cook, M., & Funke, J. (2021). Automatic detection of synaptic partners in a whole-brain Drosophila electron microscopy data set. *Nature Methods*, *18*(7), 771-774. https://doi.org/10.1038/s41592-021-01183-7

Challet, E. (2019). The circadian regulation of food intake. In *Nature Reviews Endocrinology* (Vol. 15, pp. 393-405): Nature Publishing Group.

Chopra, G., Kaushik, S., & Kain, P. (2022). Nutrient Sensing via Gut in Drosophila melanogaster. *Int J Mol Sci*, *23*(5). https://doi.org/10.3390/ijms23052694

Cognigni, P., Bailey, A. P., & Miguel-Aliaga, I. (2011). Enteric neurons and systemic signals couple nutritional and reproductive status with intestinal homeostasis. *Cell Metabolism*, *13*(1), 92-104. https://doi.org/10.1016/j.cmet.2010.12.010

D'Agostino, G., Lyons, D. J., Cristiano, C., Burke, L. K., Madara, J. C., Campbell, J. N., Garcia, A. P., Land, B. B., Lowell, B. B., Dileone, R. J., & Heisler, L. K. (2016). Appetite controlled by a cholecystokinin nucleus of the solitary tract to hypothalamus neurocircuit. *eLife*, *5*, e12225-e12225. https://doi.org/10.7554/eLife.12225

DeSesso, J. M., & Jacobson, C. F. (2001). Anatomical and physiological parameters affecting gastrointestinal absorption in humans and rats. *Food Chem Toxicol*, *39*(3), 209-228. https://doi.org/10.1016/s0278-6915(00)00136-8

Dorkenwald, S., Matsliah, A., Sterling, A. R., Schlegel, P., Yu, S.-c., McKellar, C. E., Lin, A., Costa, M., Eichler, K., Yin, Y., Silversmith, W., Schneider-Mizell, C., Jordan, C. S., Brittain, D., Halageri, A., Kuehner, K., Ogedengbe, O., Morey, R., Gager, J., . . . the

FlyWire, C. (2023). Neuronal wiring diagram of an adult brain. *bioRxiv*. https://doi.org/10.1101/2023.06.27.546656

Dus, M., Lai, J. S. Y., Gunapala, K. M., Min, S., Tayler, T. D., Hergarden, A. C., Geraud, E., Joseph, C. M., & Suh, G. S. B. (2015). Nutrient Sensor in the Brain Directs the Action of the Brain-Gut Axis in Drosophila. *Neuron*, *87*(1), 139-151. https://doi.org/10.1016/j.neuron.2015.05.032

Eckstein, N., Bates, A. S., Champion, A., Du, M., Yin, Y., Schlegel, P., Lu, A. K.-Y., Rymer, T., Finley-May, S., Paterson, T., Parekh, R., Dorkenwald, S., Matsliah, A., Yu, S.-C., McKellar, C., Sterling, A., Eichler, K., Costa, M., Seung, S., . . . Funke, J. (2023). Neurotransmitter Classification from Electron Microscopy Images at Synaptic Sites in Drosophila Melanogaster. *bioRxiv*. https://doi.org/10.1101/2020.06.12.148775

Fenselau, H., Campbell, J. N., Verstegen, A. M., Madara, J. C., Xu, J., Shah, B. P., Resch, J. M., Yang, Z., Mandelblat-Cerf, Y., Livneh, Y., & Lowell, B. B. (2017). A rapidly acting glutamatergic ARC-->PVH satiety circuit postsynaptically regulated by alpha-MSH. *Nat Neurosci*, *20*(1), 42-51. https://doi.org/10.1038/nn.4442

Ferrario, C. R., Labouèbe, G., Liu, S., Nieh, E. H., Routh, V. H., Xu, S., & O'Connor, E. C. (2016, 2016/11//). Homeostasis meets motivation in the battle to control food intake. Journal of Neuroscience,

Garfield, A. S., Li, C., Madara, J. C., Shah, B. P., Webber, E., Steger, J. S., Campbell, J. N., Gavrilova, O., Lee, C. E., Olson, D. P., Elmquist, J. K., Tannous, B. A., Krashes, M. J., & Lowell, B. B. (2015). A neural basis for melanocortin-4 receptor-regulated appetite. *Nat Neurosci*, *18*(6), 863-871. https://doi.org/10.1038/nn.4011

Gribble, F. M., & Reimann, F. (2019). Function and mechanisms of enteroendocrine cells and gut hormones in metabolism. In *Nature Reviews Endocrinology* (Vol. 15, pp. 226-237): Nature Publishing Group.

Hadjieconomou, D., King, G., Gaspar, P., Mineo, A., Blackie, L., Ameku, T., Studd, C., de Mendoza, A., Diao, F., White, B. H., Brown, A. E. X., Plaçais, P. Y., Préat, T., & Miguel-

Aliaga, I. (2020). Enteric neurons increase maternal food intake during reproduction. *Nature*, *587*(7834), 455-459. https://doi.org/10.1038/s41586-020-2866-8

Horio, N., & Liberles, S. D. (2021). Hunger enhances food-odour attraction through a neuropeptide Y spotlight. *Nature*, *592*(7853), 262-266. https://doi.org/10.1038/s41586-021-03299-4

Hugenholtz, F., & de Vos, W. M. (2018). Mouse models for human intestinal microbiota research: a critical evaluation. In *Cellular and Molecular Life Sciences* (Vol. 75, pp. 149-160): Birkhauser Verlag AG.

Jais, A., & Brüning, J. C. (2022). Arcuate Nucleus-Dependent Regulation of Metabolism-Pathways to Obesity and Diabetes Mellitus. In *Endocrine Reviews* (Vol. 43, pp. 314-328): Endocrine Society.

Latorre, R., Sternini, C., De Giorgio, R., & Greenwood-Van Meerveld, B. (2016). Enteroendocrine cells: A review of their role in brain-gut communication. In *Neurogastroenterology and Motility* (Vol. 28, pp. 620-630): Blackwell Publishing Ltd.

Lee, K. S., You, K. H., Choo, J. K., Han, Y. M., & Yu, K. (2004). Drosophila short neuropeptide F regulates food intake and body size. *Journal of Biological Chemistry*, *279*(49), 50781-50789. https://doi.org/10.1074/jbc.M407842200

Lin, A., Yang, R., Dorkenwald, S., Matsliah, A., Sterling, A. R., Schlegel, P., Yu, S.-c., McKellar, C. E., Costa, M., Eichler, K., Bates, A. S., Eckstein, N., Funke, J., Jefferis, G. S. X. E., & Murthy, M. (2024). Network Statistics of the Whole-Brain Connectome of Drosophila. *bioRxiv*. https://doi.org/10.1101/2023.07.29.551086

Lin, H. H., Kuang, M. C., Hossain, I., Xuan, Y., Beebe, L., Shepherd, A. K., Rolandi, M., & Wang, J. W. (2022). A nutrient-specific gut hormone arbitrates between courtship and feeding. *Nature*, *602*(7898), 632-638. https://doi.org/10.1038/s41586-022-04408-7

Malita, A., Kubrak, O., Koyama, T., Ahrentlov, N., Texada, M. J., Nagy, S., Halberg, K. V., & Rewitz, K. (2022). A gut-derived hormone suppresses sugar appetite and regulates food choice in Drosophila. *Nat Metab*, *4*(11), 1532-1550. https://doi.org/10.1038/s42255-022-00672-z

Matsliah, A., Yu, S.-c., Kruk, K., Bland, D., Burke, A., Gager, J., Hebditch, J., Silverman, B., Willie, K., Willie, R., Sorek, M., Sterling, A. R., Kind, E., Garner, D., Sancer, G., Wernet, M. F., Kim, S. S., Murthy, M., Seung, H. S., & the FlyWire, C. (2024). Neuronal parts list and wiring diagram for a visual system. *bioRxiv*. https://doi.org/10.1101/2023.10.12.562119

Mayer, E. A. (2011). Gut feelings: the emerging biology of gut-brain communication. *Nat Rev Neurosci*, *12*(8), 453-466. https://doi.org/10.1038/nrn3071

Miguel-Aliaga, I., Jasper, H., & Lemaitre, B. (2018). Anatomy and physiology of the digestive tract of drosophila melanogaster. *Genetics*, *210*(2), 357-396. https://doi.org/10.1534/genetics.118.300224

Min, S., Oh, Y., Verma, P., Whitehead, S. C., Yapici, N., Van Vactor, D., Suh, G. S. B., & Liberles, S. D. (2021). Control of feeding by piezo-mediated gut mechanosensation in drosophila. *eLife*, *10*, 1-30. https://doi.org/10.7554/eLife.63049

Miyamoto, T., & Amrein, H. (2014). Diverse roles for the Drosophila fructose sensor Gr43a. *Fly*, *8*(1), 19-25. https://doi.org/10.4161/fly.27241

Nässel, D. R., Kubrak, O. I., Liu, Y., Luo, J., & Lushchak, O. V. (2013). Factors that regulate insulin producing cells and their output in drosophila. *Frontiers in Physiology*, *4 SEP*. https://doi.org/10.3389/fphys.2013.00252

Odum, E. P., & Barrett, G. W. (2005). *Fundamentals of ecology* (5th ed.). Thomson Brooks/Cole. Contributor biographical information http://www.loc.gov/catdir/enhancements/fy1103/2004101400-b.html
Publisher description http://www.loc.gov/catdir/enhancements/fy1103/2004101400-d.html
Table of contents only http://www.loc.gov/catdir/enhancements/fy1103/2004101400-t.html

Ren, G. R., Hauser, F., Rewitz, K. F., Kondo, S., Engelbrecht, A. F., Didriksen, A. K., Schjott, S. R., Sembach, F. E., Li, S., Sogaard, K. C., Sondergaard, L., & Grimmelikhuijzen, C. J. (2015). CCHamide-2 Is an Orexigenic Brain-Gut Peptide in Drosophila. *PLoS One*, *10*(7), e0133017. https://doi.org/10.1371/journal.pone.0133017

Sadaqat, Z., Kaushik, S., & Kain, P. (2021). Gut Feeding the Brain: Drosophila Gut an Animal Model for Medicine to Understand Mechanisms Mediating Food Preferences. In E. Purevjav, J. F. Pierre, & L. Lu (Eds.), *Preclinical Animal Modeling in Medicine*. IntechOpen. https://doi.org/10.5772/intechopen.96503

Schlegel, P., Yin, Y., Bates, A. S., Dorkenwald, S., Eichler, K., Brooks, P., Han, D. S., Gkantia, M., dos Santos, M., Munnelly, E. J., Badalamente, G., Capdevila, L. S., Sane, V. A., Pleijzier, M. W., Tamimi, I. F. M., Dunne, C. R., Salgarella, I., Javier, A., Fang, S., . . . Jefferis, G. S. X. E. (2023). Whole-brain annotation and multi-connectome cell typing quantifies circuit stereotypy in Drosophila. *bioRxiv*. https://doi.org/10.1101/2023.06.27.546055

Söderberg, J. A. E., Carlsson, M. A., & Nässel, D. R. (2012). Insulin-producing cells in the Drosophila brain also express satiety-inducing cholecystokinin-like peptide, drosulfakinin. *Frontiers in endocrinology*, *3*, 109-109.

Sternson, S. M., & Eiselt, A. K. (2017). Three Pillars for the Neural Control of Appetite. In *Annual Review of Physiology* (Vol. 79, pp. 401-423): Annual Reviews Inc.

Stoffolano, J. G., & Haselton, A. T. (2013). The adult dipteran crop: A unique and overlooked organ. In *Annual Review of Entomology* (Vol. 58, pp. 205-225): Annual Reviews Inc.

Tao, J., Campbell, J. N., Tsai, L. T., Wu, C., Liberles, S. D., & Lowell, B. B. (2021). Highly selective brain-to-gut communication via genetically defined vagus neurons. *Neuron*, *109*(13), 2106-2115 e2104. https://doi.org/10.1016/j.neuron.2021.05.004

Wang, P., Jia, Y., Liu, T., Jan, Y. N., & Zhang, W. (2020). Visceral Mechano-sensing Neurons Control Drosophila Feeding by Using Piezo as a Sensor. *Neuron*, *108*(4), 640-650.e644. https://doi.org/10.1016/j.neuron.2020.08.017

Watts, A. G., Kanoski, S. E., Sanchez-Watts, G., & Langhans, W. (2022). THE PHYSIOLOGICAL CONTROL OF EATING: SIGNALS, NEURONS, AND NETWORKS. In *Physiological Reviews* (Vol. 102, pp. 689-813): American Physiological Society.

Wu, C. S., Bongmba, O. Y. N., Lee, J. H., Tuchaai, E., Zhou, Y., Li, D. P., Xue, B., Chen, Z., & Sun, Y. (2019). Ghrelin receptor in agouti-related peptide neurones regulates metabolic adaptation to calorie restriction. *J Neuroendocrinol*, *31*(7), e12763. https://doi.org/10.1111/jne.12763

Yao, Z., & Scott, K. (2022). Serotonergic neurons translate taste detection into internal nutrient regulation. *Neuron*, *110*(6), 1036-1050.e1037. https://doi.org/10.1016/j.neuron.2021.12.028

Yapici, N., Cohn, R., Schusterreiter, C., Ruta, V., & Vosshall, L. B. (2016). A Taste Circuit that Regulates Ingestion by Integrating Food and Hunger Signals. *Cell*, *165*(3), 715-729. https://doi.org/10.1016/j.cell.2016.02.061

Zheng, Z., Lauritzen, J. S., Perlman, E., Robinson, C. G., Nichols, M., Milkie, D., Torrens, O., Price, J., Fisher, C. B., Sharifi, N., & others. (2018). A complete electron microscopy volume of the brain of adult Drosophila melanogaster. *Cell*, *174*(3), 730-743.

CHAPTER 2

A Gut-Brain-Gut Interoceptive Circuit Loop Gates Sugar Ingestion in Drosophila

Abstract

The communication between the brain and digestive tract is critical for optimizing nutrient preference and food intake, yet the underlying neural mechanisms remain poorly understood (Cui et al., 2022; Miguel-Aliaga, Jasper, & Lemaitre, 2018; Naslund & Hellstrom, 2007; Prescott & Liberles, 2022; Simpson & Bernays, 1983; Stoffolano & Haselton, 2013; Yu, Xu, & Chang, 2020). Here, we show that a gut-brain-gut circuit loop gates sugar ingestion in flies. We discovered that brain neurons regulating food ingestion, IN1 (Yapici et al., 2016), receive excitatory input from enteric sensory neurons, which innervate the esophagus and express the sugar receptor *Gr43a*. These enteric sensory neurons monitor the sugar content of food within the esophagus during ingestion and send positive feedback signals to IN1s, stimulating the consumption of high-sugar foods. Connectome analyses reveal that IN1s form a core ingestion circuit. This interoceptive circuit receives synaptic input from enteric afferents and provides synaptic output to enteric motor neurons, which modulate the activity of muscles at the entry segments of the crop, a stomach-like food storage organ. While IN1s are persistently activated upon ingestion of sugar-rich foods, enteric motor neurons are continuously inhibited, causing the crop muscles to relax and enabling flies to consume large volumes of sugar. Our findings reveal a key interoceptive mechanism that underlies the rapid sensory monitoring and motor control of sugar ingestion within the digestive tract, optimizing the diet of flies across varying metabolic states.

Introduction

Most animals regulate food intake via a complex network of sensory, homeostatic, and hedonic physiological processes that are under the control of neural circuits within the central and enteric nervous systems. Communication between the brain and gastrointestinal tract is essential for assessing the body's metabolic status, regulating the ingestion of specific nutrients, and triggering satiety responses when energy reserves are replenished (Miguel-Aliaga, Jasper, & Lemaitre, 2018; Naslund & Hellstrom, 2007; Prescott & Liberles, 2022; Yu, Xu, & Chang, 2020). Recent studies highlight the critical roles of gut-brain circuits in regulating homeostatic and hedonic aspects of food intake across species, including invertebrates (Cognigni, Bailey, & Miguel-Aliaga, 2011; Hadjieconomou et al., 2020; Min et al., 2021; Oh et al., 2021; Wang et al., 2020) and mammals (Borgmann et al., 2021; Chen et al., 2020; Han et al., 2018; Kaelberer et al., 2018; Li et al., 2022; McDougle et al., 2024; Tan et al., 2020; Williams et al., 2016). In mammals, the vagus nerve serves as one of the primary pathways for bidirectional communication between the gastrointestinal tract and the brain. As part of the parasympathetic nervous system, it extensively innervates multiple compartments of the digestive tract, including the esophagus, stomach, small intestine, and parts of the large intestine (Prescott & Liberles, 2022; Yu, Xu, & Chang, 2020). This broad network of innervation allows the vagus nerve to play critical roles in regulating food ingestion, nutrient preference, and various digestive processes, such as swallowing, gastric secretions, and gut motility (Bai et al., 2019; Borgmann et al., 2021; Kaelberer et al., 2018; Li et al., 2022; Lowenstein et al., 2023; McDougle et al., 2024; Prescott & Liberles, 2022; Puizillout, 2005; Tan et al., 2020; Yu, Xu, & Chang, 2020). Despite the critical roles of the gut-brain axis in regulating food intake and metabolism, the interoceptive

circuits that translate sensory signals from the gut into motor actions that control nutrient preference and ingestion remain poorly understood. It remains a challenge to address this knowledge gap in mammals due to the complexity of their enteric nervous system. The small enteric nervous system of *Drosophila* shares many functions with its vertebrate counterparts (Cui et al., 2022; Miguel-Aliaga, Jasper, & Lemaitre, 2018; Simpson & Bernays, 1983), providing a valuable model for studying the functional principles of gut-brain circuits.

The fly digestive tract is innervated by neurons originating from the stomatogastric nervous system, which encompasses the hypocerebral ganglion (HCG) and central neurons located in the brain and the ventral nerve cord (Hadjieconomou et al., 2020; Miguel-Aliaga, Jasper, & Lemaitre, 2018; Stoffolano & Haselton, 2013). Neurons with cell bodies located in the pars intercerebralis (PI) region of the brain and HCG innervate the crop and the anterior regions of the midgut. Meanwhile, neurons in the abdominal ganglia of the ventral nerve cord extend their arborizations to the posterior regions of the midgut, as well as to the hindgut (Cognigni, Bailey, & Miguel-Aliaga, 2011; Miguel-Aliaga, Jasper, & Lemaitre, 2018). Recent studies have revealed that the PI and enteric sensory neurons expressing the mechanosensory channel Piezo sense crop distension and mediate food ingestion and nutrient preference in flies(Min et al., 2021; Oh et al., 2021; Wang et al., 2020). Another class of enteric neurons expressing the neuropeptide myosuppressin is remodeled by steroid hormones after mating, enabling females to consume large amounts of food (Hadjieconomou et al., 2020). These findings indicate that, as in humans and other mammals, the gut-brain axis plays significant roles in regulating nutrient preference and food ingestion in *Drosophila*.

Previously, we identified ~12 local interneurons (IN1, for ‘‘ingestion neurons’’) in the taste processing center of the fly brain, subesophageal zone (SEZ), as a critical regulator of food

intake (Yapici et al., 2016). IN1s are persistently activated in hungry flies consuming high concentrations of sucrose but not those consuming low concentrations (Yapici et al., 2016). Furthermore, IN1 activity is essential for the rapid and precise regulation of sugar ingestion, suggesting these neurons serve as a central node in neural circuits that process taste sensory information and govern food intake (Yapici et al., 2016). Here, we use IN1s as a gateway to identify and characterize a gut-brain-gut interoceptive circuit that gates sugar ingestion across varying metabolic states.

Results

IN1s receive excitatory input from enteric sensory neurons expressing Gr43a

To identify neurons that provide sensory input to IN1s, we used a previously validated approach to map functional connectivity within the *Drosophila* nervous system (Hoopfer et al., 2015; Mabuchi et al., 2023; Strother et al., 2017). We stimulated candidate sensory neurons with a red-shifted channelrhodopsin, Chrimson (Hoopfer et al., 2015; Klapoetke et al., 2014), while imaging the activity of IN1s using a genetically encoded calcium indicator GCaMP6s (Chen et al., 2013) (Figs. 2.1a, b). Optogenetic activation of sugar-sensing neurons expressing Gr64f (Jiao et al., 2008; Wang et al., 2004) strongly excited IN1s. In contrast, optogenetic stimulation of other sensory neurons, such as bitter-sensing (Gr66a(Lee, Kim, & Montell, 2010; Moon et al., 2006; Weiss et al., 2011)), water-sensing (ppk28(Cameron et al., 2010)), or mechanosensory neurons (TMC (Wu et al., 2019; Zhang et al., 2016)), did not elicit the same responses (Figs. 2.1c-h, Extended Data Figs. 2.1a-g). Next, we aimed to identify which group of sugar-sensing neurons provides sensory input to IN1s. In flies, most sugar-sensing neurons express Gr64f. These neurons are located in multiple chemosensory organs, including the labellum, legs,

pharynx (Chen & Dahanukar, 2017; Dahanukar et al., 2007; Fujii et al., 2015; Jiao et al., 2008; LeDue et al., 2015; Slone, Daniels, & Amrein, 2007; Wang et al., 2004), brain (Dus et al., 2015; Miyamoto et al., 2012) , and enteric nervous system (Miyamoto & Amrein, 2014). We stimulated various subsets of Gr64f neurons labeled by other *Gr-GAL4s* and simultaneously recorded IN1 activity. Optogenetic stimulation of sugar-sensing neurons expressing *Gr5a (Chyb et al., 2003), Gr64a (Dahanukar et al., 2007; Fujii et al., 2015)* , or *Gr64d (Chen & Dahanukar, 2017; Uchizono et al., 2017)* did not elicit a significant response (Figs. 2.2a-c). However, stimulation of neurons expressing *Gr43a* (labeled by *Gr43a*^{GAL4}, a knock-in insertion to *Gr43a* locus*)* strongly activated IN1s (Figs. 2.2d, g). To further narrow down the Gr43a neurons required for IN1 activation, we used two additional transgenic lines, *ChAT-GAL80 (Kitamoto, 2002)* and *Gr43a-GAL4* (an enhancer-GAL4*)*, to label subsets of Gr43a neurons. Neurons labeled by *Gr43a-GAL4* or Gr*43a*^{GAL4} combined with *ChAT-GAL80* were not able to activate IN1s upon optogenetic stimulation (Figs. 2.2e-f). The main difference among these transgenic flies was their expression in the HCG: only Gr*43a*^{GAL4} labeled multiple enteric sensory neurons (Figs. 2.2g-i, Extended Data Figs. 2.2a-d). Our results indicate that enteric sensory neurons expressing *Gr43a* are required for IN1 activation.

Enteric Gr43a neurons penetrate the gut lumen and monitor sucrose ingestion

Since our results suggest that IN1s receive excitatory input from enteric Gr43a neurons, we hypothesized that these neurons would also respond to sucrose ingestion similarly to IN1s. Gr43a is one of the most conserved insect taste receptors specifically activated by the monosaccharide fructose(Ma et al., 2024). It is expressed not only in chemosensory neurons but also in other organs, such as the brain and digestive tract (Miyamoto & Amrein, 2014) (Fig. 2.2g). Although Gr43a is a fructose receptor (Ma et al., 2024), neurons expressing Gr43a have been shown to

respond to multiple sugars, including sucrose (Miyamoto & Amrein, 2014; Miyamoto et al., 2012). To test our hypothesis, we captured the activity of enteric Gr43a neurons during sucrose ingestion. Since the cell bodies of these enteric neurons are located in the HCG next to the proventriculus (Miyamoto & Amrein, 2014), we developed a novel preparation that allowed us to gain optical access to these neurons (Figs. 2.3a, b). By combining rapid volumetric two-photon imaging with our new surgical preparation, we successfully recorded the activity of enteric neurons *in vivo* during ingestion (Supplementary Video 1). In these experiments, some enteric Gr43a neurons (cell count=~3-4) rapidly responded to the ingestion of high-concentration sucrose (~1M), measured by GCaMP6s fluorescence in their cell bodies. In contrast, other enteric Gr43a neurons were tonically active throughout the imaging session (cell count=~2-3) (Figs. 2.3c, d). The activity of sugar-responsive Gr43a neurons was transient, remaining elevated only during the period of ingestion (Fig. 2.3e). We then investigated whether Gr43a neural responses to sugar ingestion are dependent on the metabolic state or sugar concentration by recording their activity in fed and fasted flies offered high-concentration (~1M) or low-concentration (~100mM) sucrose. The sugar-evoked peak activity of Gr43a neurons was similar across all conditions (Figs. 2.3e, f). However, Gr43a neural activity persisted longer when flies consumed high-concentration sucrose compared to low-concentration (Figs. 2.3e, g). Interestingly, the persistent activity of Gr43a neurons is positively correlated with sugar concentration but is independent of the flies' metabolic state. These results indicate that a subset of enteric Gr43a neurons monitor the sugar content of food during ingestion and convey this information to IN1s within seconds.

Next, we examined the anatomical differences among enteric Gr43a neurons that might explain their distinct responses to sucrose ingestion. To do this, we acquired high-resolution

images of Gr43a neural processes along the fly digestive tract (Figs. 2.3h, i, Extended Data Figs. 2.3j, k). Our morphological analysis revealed two classes of enteric Gr43a neurons: those that penetrate the foregut lumen at the junction of the crop duct and proventriculus (foregut lumen neurons) (Figs. 2.3h, i) and those that send projections along the midgut muscles (midgut surface neurons) (Extended Data Figs. 2.3j, k). The foregut lumen Gr43a neurons are ideally positioned to detect ingested sucrose, as their processes have direct access to the nutrients within the gut lumen (Figs. 2.3i). In contrast, midgut surface Gr43a neurons innervate the gut muscles, and their processes do not penetrate the midgut muscles (Extended Data Figs. 2.3k). Our findings demonstrate that foregut lumen Gr43a neurons directly monitor the sugar content of food within the gut lumen and relay this information to IN1s. This rapid sensory feedback mechanism enables flies to assess the nutrient content of food as they ingest it, allowing them to decide whether to continue or stop eating.

IN1s receive excitatory input from two classes of enteric sensory neurons expressing *Gr43a*

Based on our anatomical and functional analysis, we propose that Gr43a neurons that penetrate the foregut lumen respond to sucrose ingestion and activate IN1s in the brain. To investigate this further, we generated split-GAL4 (Luan et al., 2006; Pfeiffer et al., 2010) lines targeting distinct classes of Gr43a neurons using enhancers expressed in the enteric nervous system (Extended Data Figs. 2.3a-i). Split-GAL4s were first screened for expression in the enteric nervous system, then used in functional connectivity analysis using optogenetics coupled with two-photon functional imaging (Fig. 2.4a). Out of the 20 split-GAL4 lines generated, 15 labeled enteric sensory neurons, and of these 7, significantly activated IN1s upon optogenetic stimulation (Fig. 2.4b, Extended Data Figs. 2.4a-o). Next, we explored whether all enteric neurons capable of activating IN1s also respond to sucrose ingestion. Only enteric neurons labeled by *EN-13>* were

activated by sucrose ingestion. In contrast, the others showed no sugar-evoked responses (Fig. 2.4d). Our anatomical analysis revealed that *EN-13>* labels enteric Gr43a neurons whose processes penetrate the gastrointestinal tract (foregut lumen neurons), enabling them to detect sucrose within the gut lumen during ingestion (Figs. 2.4e, f). These findings support our hypothesis that Gr43a neurons in the foregut lumen can monitor the sucrose content of ingested food and send positive feedback signals to IN1s to sustain sugar intake. Interestingly, we have identified other enteric sensory neurons that can induce IN1 activity, yet they do not respond to sugar ingestion. These neurons may detect other nutrients or mechanical stimuli in the gut lumen, potentially regulating various aspects of feeding behavior or metabolic processes.

IN1s receive synaptic input from enteric afferents and are anatomically distant from feeding initiation circuits

Next, we used connectomics to characterize the anatomical organization of IN1s and their interactions with different classes of gustatory receptor neurons (GRNs) and neurons that regulate feeding initiation. Recently, the whole-brain connectome of an adult fly has been completed and released to the *Drosophila* community through the online FlyWire platform, describing the synaptic organization of ~130,000 neurons (Buhmann et al., 2021; Dorkenwald et al., 2023; Dorkenwald et al., 2022; Schlegel et al., 2023). Flywire uses the full adult female brain (FAFB) dataset, the first electron microscopy (EM) volume of an adult fly brain (Zheng et al., 2018), which contains the neurons in the primary taste processing center of the fly brain, SEZ(Engert et al., 2022; Shiu et al., 2022). FAFB volume has recently been segmented automatically, allowing computer-based detection of synapses (Buhmann et al., 2021; Li et al., 2019). Using the FAFB connectome, we first identified four putative IN1s (IN1-1, IN1-2, IN1-3, and IN1-4) based on their cell body locations, projection patterns, and synaptic organizations

(Extended Data Figs. 2.5a, b). Synaptic network analysis revealed that putative IN1s have a similar number of presynaptic (n=825±20) and postsynaptic (n=585±32) connections. Interestingly, we found that IN1s are connected to each other (Extended Data Fig. 2.5d). This synaptic organization might indicate feed-forward excitation among IN1s, which could play a crucial role in generating their persistent activity upon sugar ingestion.

Using the connectome, we further investigated the synaptic distance of IN1s to different classes of GRNs that are annotated in the FlyWire data analysis platform Codex (Connectome Data Explorer: codex.flywire.ai) (Engert et al., 2022; Lin et al., 2024) (Extended Data Fig. 2.5e). Our analysis demonstrated that IN1s do not receive direct synaptic input from any of the labellar GRNs or the majority of pharyngeal GRNs (Extended Data Figs. 2.5g-i). Since our functional connectivity experiments revealed that IN1s receive functional input from enteric Gr43a neurons (Figs. 2, 3), we next investigated whether enteric afferents provide direct synaptic input to IN1s. We first annotated putative enteric afferents in the FAFB connectome based on their characteristic projections in the prow area of the SEZ (Extended Data Figs. 2.5e, f). We found that several putative enteric afferents provide direct synaptic input to IN1s (Extended Data Fig. 2.5f), further supporting their role in regulating food ingestion rather than initiating feeding behavior.

Next, we investigated the connectivity between IN1s and neurons that regulate feeding initiation. Recent studies have identified neural circuits in the adult fly brain governing this behavior. These sensorimotor circuits connect GRNs to motor neurons that innervate the proboscis muscles(Shiu et al., 2022; Shiu et al., 2023). Most neurons in this pathway respond to sugar ingestion and can induce proboscis extension, a behavior associated with feeding initiation (Shiu et al., 2022; Shiu et al., 2023). Our analysis showed no direct synaptic connections

between IN1s and second-order, third-order, or pre-motor neurons that regulate feeding initiation (Extended Data Figs. 2.6a, b). Overall, our connectome analysis revealed that IN1s are synaptically distant from sensory and central neurons regulating feeding initiation. Instead, as our functional connectivity analysis also demonstrated (Figure 4), they receive direct synaptic input from enteric sensory neurons linked to food ingestion.

IN1s are synaptically connected to local SEZ neurons

Since IN1s are not directly connected to neurons that regulate feeding initiation, we asked which circuits they are connected to in the fly brain. All four putative IN1s (IN1-1, IN1-2, IN1-3, and IN1-4) received presynaptic and postsynaptic connections from a comparable number of neurons (n=55.75±1.4 and n=29.75±1.1 respectively). Interestingly, most of these neurons were intrinsic to SEZ, with few exceptions that project outside this region (Extended Data Figs. 2.7a-h, Extended Data Figs. 2.8a-h). We first characterize the IN1 presynaptic neurons. Our connectomics analysis showed that four local SEZ neurons contributed the highest count of input synapses to IN1s. PRW.10 contributed the most, with 82.5±4 synapses per IN1, followed by PRW.70, with an average of 63.75±3, PRW.9, with an average of 49.25±1.6, and PRW.GNG.8 with an average of 47.75±5 synapses (Extended Data Figs. 2.7b, d, f, h). All of these IN1 presynaptic neurons are predicted to be cholinergic(Eckstein et al., 2024), and they have processes within the prow region of the SEZ (Extended Data Figs. 2.7i). Next, we examined IN1 postsynaptic neurons. Similar to presynaptic inputs, the primary outputs of IN1s appear to be neurons with cell bodies within the SEZ: PRW.248 (54±13 synapses), PRW.249 (63±4 synapses), PRW.263 (82.5±2.5), PRW.274 (55.5±13.5), PRW.281 (67.5±2.5), PRW.310 (57.5±2.5) and Doublescoop(Sterne et al., 2021) (55±4) (Extended Data Figs. 2.8a-h). PRW.248, PRW.249, PRW.263, PRW.274, PRW.281, and PRW.310 belong to the same class of SEZ

neurons (previously dubbed “Peep” neurons(Sterne et al., 2021)) with dendrites located in the prow and no evident axons within the brain, suggesting they are putative motor neurons. These neurons represent the primary synaptic output of IN1s, accounting for 28-35% of their output synapses. The second class of IN1 output neurons consists of those previously dubbed as Doublescoop neurons (Sterne et al., 2021). Doublescoop neurons have cell bodies in mediolateral SEZ and send projections toward the midline, where IN1 processes are located (Extended Data Figs. 2.8b, d, f & h). These neurons are predicted to be cholinergic (Eckstein et al., 2024), and like the IN1 presynaptic neurons, their processes are intrinsic to the SEZ. Our connectome analysis revealed that IN1s’ main synaptic inputs and outputs are local SEZ neurons, most of which have not been previously described. Furthermore, the major synaptic output of IN1s is motor neurons that project outside of the brain (Extended Data Fig. 2.8i). We hypothesized that IN1 motor output neurons are most critical for their functions in regulating fly ingestion, leading us to focus our further investigation on these neurons.

IN1s inhibit the activity of enteric motor neurons that innervate the crop duct

To further investigate the relationship between IN1s and their motor output neurons (PRW.248, PRW.249, PRW.263, PRW.274, PRW.281, and PRW.310), we first generated split-GAL4(Luan et al., 2006; Pfeiffer et al., 2010) lines to gain genetic access to them (Figs. 2.5a, b). Our anatomical characterization verified that these neurons extend long projections outside the brain to the gastrointestinal tract, where they innervate the entry segments of the crop duct. (Fig. 2.5c). We renamed these neurons as Crop-innervating Enteric Motor (CEM) neurons to more precisely reflect their anatomical organization. CEM neurons do not appear sexually dimorphic and exist in both male (Fig. 2.5b) and female brains (Extended Data Figs. 2.9a, b). The axons of these neurons project outside the brain along the esophagus and branch at the junction between the

crop duct and the entry of the proventriculus (Figs. 2.5b, c, Extended Data Figs. 2.9a, b). Immunohistochemical analysis showed that the synaptic boutons of CEM neurons express the vesicular glutamate transporter (VGLUT), confirming they are indeed glutamatergic motor neurons (Fig. 2.5c). To further examine the functional connectivity between CEM neurons and IN1s, we performed two-photon functional imaging coupled with optogenetic stimulation. Optogenetic activation of IN1s inhibited the activity of CEM neurons. This inhibitory effect was modest during the short (1-second) optogenetic trials but became more pronounced in longer (10-second) ones (Figs. 2.5d, e). Our results demonstrated that IN1s provide inhibitory synaptic input to CEM neurons.

Next, we investigated the activity of CEM neurons during sugar ingestion. Given that IN1s are excited by sugar ingestion and exhibit state- and stimulus-specific responses(Yapici et al., 2016), we hypothesized that CEM neurons might reflect IN1 activity and would be inhibited by sugar ingestion due to their inhibitory synaptic inputs from IN1s. Supporting this hypothesis, our functional imaging experiments showed that CEM neurons were persistently inhibited upon the ingestion of high-concentration sucrose in both fed and 24-hour-fasted conditions (Fig. 2.5f, Supplementary Video 2). The inhibitory response to sucrose was transient when 24-hour-fasted flies consumed low-concentration sucrose (Fig. 2.5f). Our quantitative analysis revealed that the peak response in CEM neurons was similar across all conditions (Fig. 2.5g). However, we observed that the persistence of inhibition was significantly reduced in 24-hour-fasted flies consuming low-concentration sucrose compared to those consuming high-concentrations (Fig. 2.5h). Our findings revealed an inverse correlation between the activity of CEM neurons and IN1s: IN1s remain persistently activated during the ingestion of high-concentration sucrose(Yapici et al., 2016), while CEM neurons are continuously inhibited. Moreover, this

persistent activation of IN1s(Yapici et al., 2016) and inhibition of CEM neurons depend on sugar concentration, occurring only when flies ingest high-concentration sucrose but not low-concentration.

IN1 ingestion circuit mediates sugar intake by controlling food entry to the crop

In *Drosophila* and other insects, ingestion is regulated by a series of peristaltic muscle contractions that pump the food into the gastrointestinal tract(Dethier, 1976; Manzo et al., 2012; Miguel-Aliaga, Jasper, & Lemaitre, 2018). After the ingested food passes through the esophagus, it reaches the crop duct and proventriculus, where it must be sorted to either enter the crop, a stomach-like storage organ, or proceed to the midgut through the proventriculus. Mosquitoes transport meals with low sugar content directly to the midgut, whereas sugar-enriched meals are stored in the crop (Friend, 1981; Trembley, 1952). However, the neural circuits that regulate sugar transport within the gastrointestinal tract are unknown. We hypothesized that the IN1 ingestion circuit might regulate sugar intake by mediating the transport of sugar-enriched foods into the crop. To test this hypothesis, we first investigated whether flies regulate the transport of ingested food based on its sugar content, similar to other insects. We developed an *in vivo* imaging assay to monitor the food entry into different gastrointestinal compartments in body-fixed flies. In this assay, a fluorescent dye, fluorescein, was mixed with high and low-concentration sucrose and fed to 24-hour fasted flies. Using *in vivo* two-photon imaging, we then tracked the movement of the fluorescent food within the esophagus and crop during and after ingestion. (Fig. 2.6a, Extended Data Fig. 2.10a). When flies ingested high-concentration sucrose, the crop duct remained persistently open, as indicated by the sustained fluorescent signal, allowing continuous food passage into the crop. In contrast, when they consumed low-concentration sucrose, the crop duct opened only briefly, resulting in a short-lived fluorescent

signal (Figs. 2.6b, c). These differences in food transport were not apparent in the esophagus (Extended Data Figs. 2.10b, c), indicating flies can modulate the transport of food to their crop based on its sugar content.

Building on our findings, we then tested whether the activity of IN1s or CEM neurons is required for sugar transport into the crop. Using two-photon imaging, we monitored the flow of high sucrose and fluorescein mixture to different digestive compartments while manipulating the activity of these neurons. Inhibiting synaptic vesicle release by expressing tetanus toxin light chain (Sweeney et al., 1995) in IN1s (*IN1>TNT*) blocked the entry of high-concentration sucrose into the crop (Figs. 2.6d, e) without affecting the food transport to the esophagus (Extended Data Figs. 2.10d, e). These results explain why *IN1>TNT* flies can only consume small volumes of food, as we previously demonstrated (Yapici et al., 2016). We then manipulated the activity of CEM neurons to determine if their activity is also required for sugar transport to the crop. Since IN1s inhibit CEM neurons during sugar ingestion (Fig. 2.5f), we hypothesized that activating CEM neurons during ingestion might mimic the effects of IN1 inhibition. To test this, we expressed the red-shifted channelrhodopsin Chrimson (Hoopfer et al., 2015; Klapoetke et al., 2014) in CEM neurons and photoactivated them during ingestion. Under continuous optogenetic stimulation, flies were unable to transport sucrose into their crop (Figs. 2.6g, h, Supplementary Video 3). However, once the optogenetic stimulation stopped, sucrose was able to enter the crop, allowing the flies to resume ingestion (Supplementary Video 3). Importantly, this effect on food ingestion was not due to red light stimulation, as control flies of the same genotype that were not fed all-trans-retinal (ATR), a co-factor essential for Chrimson activity, showed no impairments in food transportation from the esophagus to the crop (Figs. 2.6i, j, Supplementary Video 3). Our findings indicate that the coordinated activity of IN1s and CEM neurons is essential for

transporting sugar-rich foods into the crop and thereby optimizing flies' ingestive behaviors. When the activity of these neurons is disrupted, ingested food cannot be moved into the crop. This impairment restricts flies' ability to consume and store large volumes of sugar, highlighting the critical role of this gut-brain-gut interoceptive circuit in controlling sugar ingestion.

Discussion

Gut-brain circuits have been linked to nutrient preference and food ingestion in humans (Burneo et al., 2002; Kral, 1978), rodents (Bai et al., 2019; Chen et al., 2020; Li et al., 2022; McDougle et al., 2024; Tan et al., 2020), and insects (Cognigni, Bailey, & Miguel-Aliaga, 2011; Dethier, 1976; Hadjieconomou et al., 2020; Min et al., 2021; Oh et al., 2021; Stoffolano & Haselton, 2013; Wang et al., 2020). In mammals, these circuits sense nutrients (Kaelberer et al., 2018; McDougle et al., 2024; Tan et al., 2020) or stretch (Bai et al., 2019; Williams et al., 2016) within the stomach or intestinal lumen and send feedback signals to central and motor circuits, which mediate swallowing, digestion and gut motility (Bai et al., 2019; Lowenstein et al., 2023; Prescott & Liberles, 2022; Puizillout, 2005; Yu, Xu, & Chang, 2020). Here, we reveal a gut-brain-gut interoceptive circuit that regulates state and concentration-specific sugar ingestion in *Drosophila*. Our data support a model in which sugar-responsive enteric sensory neurons in the gut provide real-time nutrient information to the brain, specifically to IN1s that are synaptically connected to enteric motor neurons. When food-deprived flies consume sugar-rich foods, these enteric sensory neurons rapidly convey the sugar stimulus to IN1s, leading to their persistent activation and, consequently, inhibition of enteric motor neurons that innervate the crop duct muscles. This coordinated activity allows flies to open their crop duct and continuously transport food from the esophagus into the crop, thereby enhancing their capacity to ingest and store large

volumes of sugar-rich foods. The dynamic regulation of this interoceptive circuit by metabolic state and sugar concentration is crucial for flies to quickly assess the nutritional value of ingested foods and adjust their digestive processes accordingly, either stimulating or halting their food intake as needed. We propose that this gut-brain-gut interoceptive circuit plays a crucial role in enabling flies to optimize their dietary intake by prioritizing the ingestion and storage of foods enriched in sugar, which provides a quick and efficient energy source. This adaptive feeding behavior is likely to contribute to the survival and fitness of flies by maximizing their energy acquisition in environments where food quality fluctuates.

Our study reveals that the interoceptive gut-brain circuit we have identified here in flies closely parallels the vagal sensorimotor circuits that mediate gut-brain communication in mammals. In mice, vagal sensory neurons reside in the nodose ganglia, where they transmit nutrient-derived signals (e.g., sugars, fats) from the gut to the hindbrain, specifically targeting the brainstem nuclei, the nucleus of the solitary tract (NTS) (Bai et al., 2019; Prescott & Liberles, 2022; Yu, Xu, & Chang, 2020). Recently, vagal sensory neurons that stimulate sugar preference and intake have been identified in mice (Chen et al., 2020; Tan et al., 2020). In contrast, the cell bodies of vagal motor neurons are located in the dorsal motor nucleus of the vagus (DMV) in the brainstem. These neurons project to various regions of the gastrointestinal tract, including the stomach, small intestine, large intestine, gallbladder, and pancreas, where they exert control over digestive processes (Tao et al., 2021). Our results demonstrate that in *Drosophila*, enteric sensory neurons located in the hypocerebral ganglion (HCG, analogous structure to mammalian nodose ganglia) detect sugars in the gut lumen and relay this information to the IN1s in the brain. INs are located in the subesophageal zone (SEZ) of the fly brain, which processes gustatory sensory information similarly to the mammalian brainstem, particularly the NTS. The major

synaptic output of IN1s is enteric motor neurons that project to the digestive tract, innervating the entry segments of the fly crop, a stomach-like organ. Activation of this gut-brain-gut circuit opens crop muscles, allowing flies to ingest large volumes of sugar-rich foods. Our findings reveal striking anatomical and functional parallels between the vagal sensory and motor neurons in mice and the enteric sensory and motor neurons in flies, suggesting conserved neural mechanisms for processing gut-derived sensory signals across evolutionarily distinct species.

Another notable finding in our study is the demonstration that the IN1 ingestion circuit is anatomically distinct and synaptically distant from the feeding initiation circuits within the fly brain (Shiu et al., 2022; Shiu et al., 2023). Recent whole-brain imaging studies in flies have provided compelling evidence for the presence of a functional map within the SEZ (Munch, Goldschmidt, & Ribeiro, 2022). Parallel investigations in mammalian models, particularly in mice, have similarly identified topographic and functional representations within the brainstem nuclei, NTS (Ran et al., 2022; Zhao et al., 2022) , and DMV (Tao et al., 2021). Our connectome analysis of the IN1 gut-brain interoceptive circuit further supports the idea of functional segregation within feeding-related neural circuits in the fly brain. This separation suggests a hierarchical organization, where distinct but interconnected neural circuits process each step of food intake, from sensory detection of food to feeding initiation and sustained ingestion. Understanding this interconnected network could reveal fundamental principles underlying feeding behavior across species and provide insights into the conserved neural computations that regulate food intake and interoception in the brain. In the long term, this knowledge may pave the way for novel therapeutic strategies to treat human disorders related to gut-brain dysregulation, such as obesity and eating disorders.

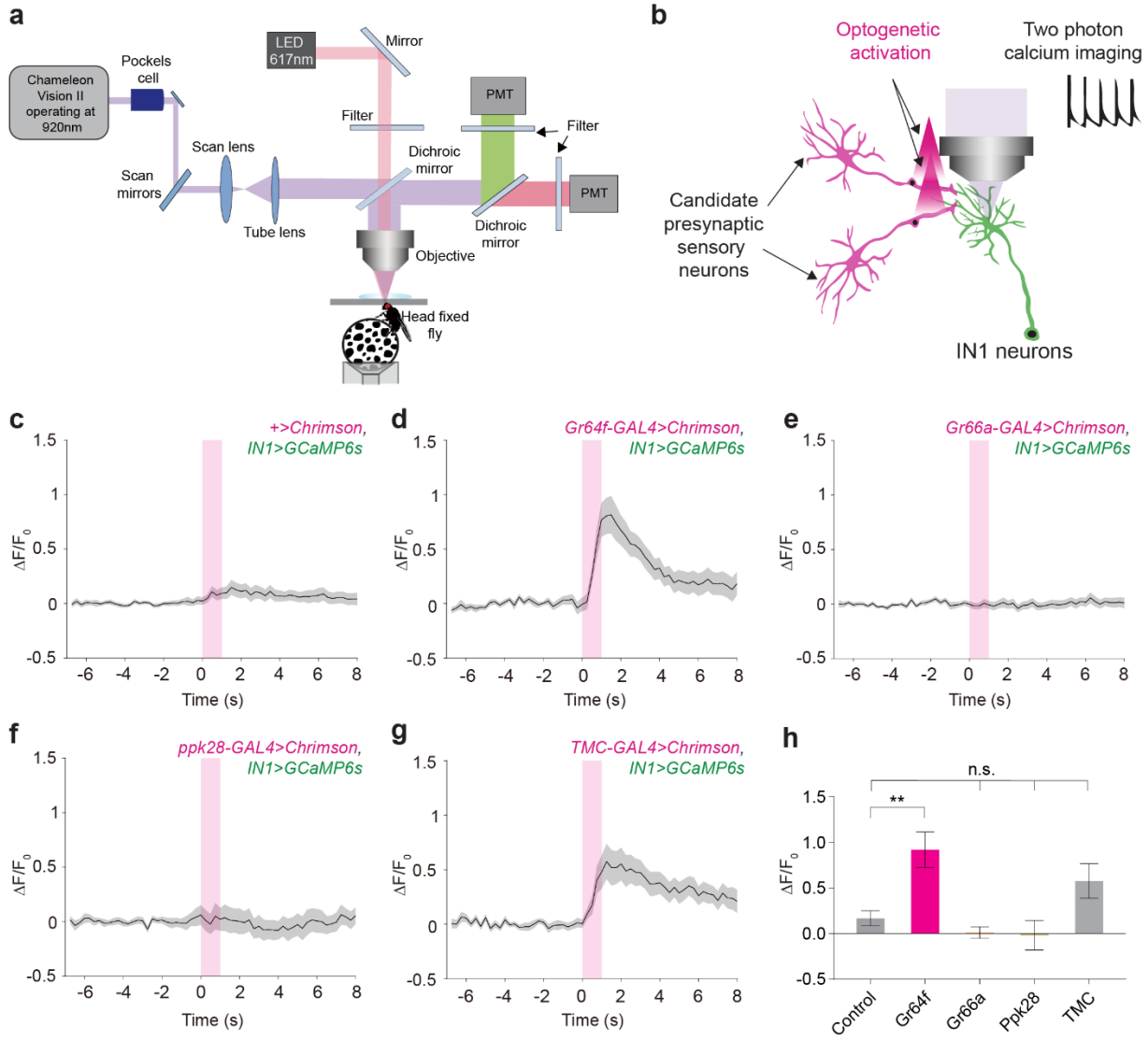
a
Chameleon Vision II operating at 920nm
Pockels cell
LED 617nm
Mirror
Filter
PMT
Filter
Scan lens
Scan mirrors
Dichroic mirror
PMT
Tube lens
Dichroic mirror
Objective
Head fixed fly
b
Optogenetic activation
Two photon calcium imaging
Candidate presynaptic sensory neurons
IN1 neurons
c
+>Chrimson, IN1>GCaMP6s
d
Gr64f-GAL4>Chrimson, IN1>GCaMP6s
e
Gr66a-GAL4>Chrimson, IN1>GCaMP6s
f
ppk28-GAL4>Chrimson, IN1>GCaMP6s
g
TMC-GAL4>Chrimson, IN1>GCaMP6s
ΔF/F0
Time (s)
h
n.s.
**
Control
Gr64f
Gr66a
Ppk28
TMC

Fig. 2. 1| IN1s receive excitatory input from sugar-sensing neurons expressing *Gr64f*.
a, Schematic of the two-photon microscope setup coupled with optogenetic stimulation. A male fly is standing on top of an air-suspended spherical treadmill (PMT, photomultiplier tube).
b, Schematic showing the strategy used for optogenetic stimulation coupled with two-photon calcium imaging. GCaMP6s is expressed in IN1s, while red-shifted opsin, Chrimson, is expressed in candidate IN1 sensory input neurons.
c-g, Averaged normalized ($\Delta F/F_0$) GCaMP6s fluorescence in IN1s before and after optogenetic stimulation of candidate sensory neurons: Control group (**c**), sugar sensing neurons, Gr64f (**d**), bitter sensing neurons, Gr66a (**e**), water sensing neurons, ppk28 (**f**), and mechanosensory neurons, TMC (**g**). The optogenetic stimulation period is shown in a magenta-shaded area (mean ± SEM, stimulation = 1s, continuous, power = ~0.75mW). (See also Extended Data Figs. 1a-g).
h, Averaged normalized peak responses of IN1s in indicated genotypes upon optogenetic stimulation (n = 5-7 flies and five trials per fly, mean ± SEM, one-way ANOVA with Bonferroni post hoc test, $^{**}p < 0.01$, not significant (n.s.)). IN1s responded to the activation of sugar-sensing neurons but not to other sensory neurons. Although TMC neurons appeared to activate IN1s weakly, this response did not reach statistical significance.

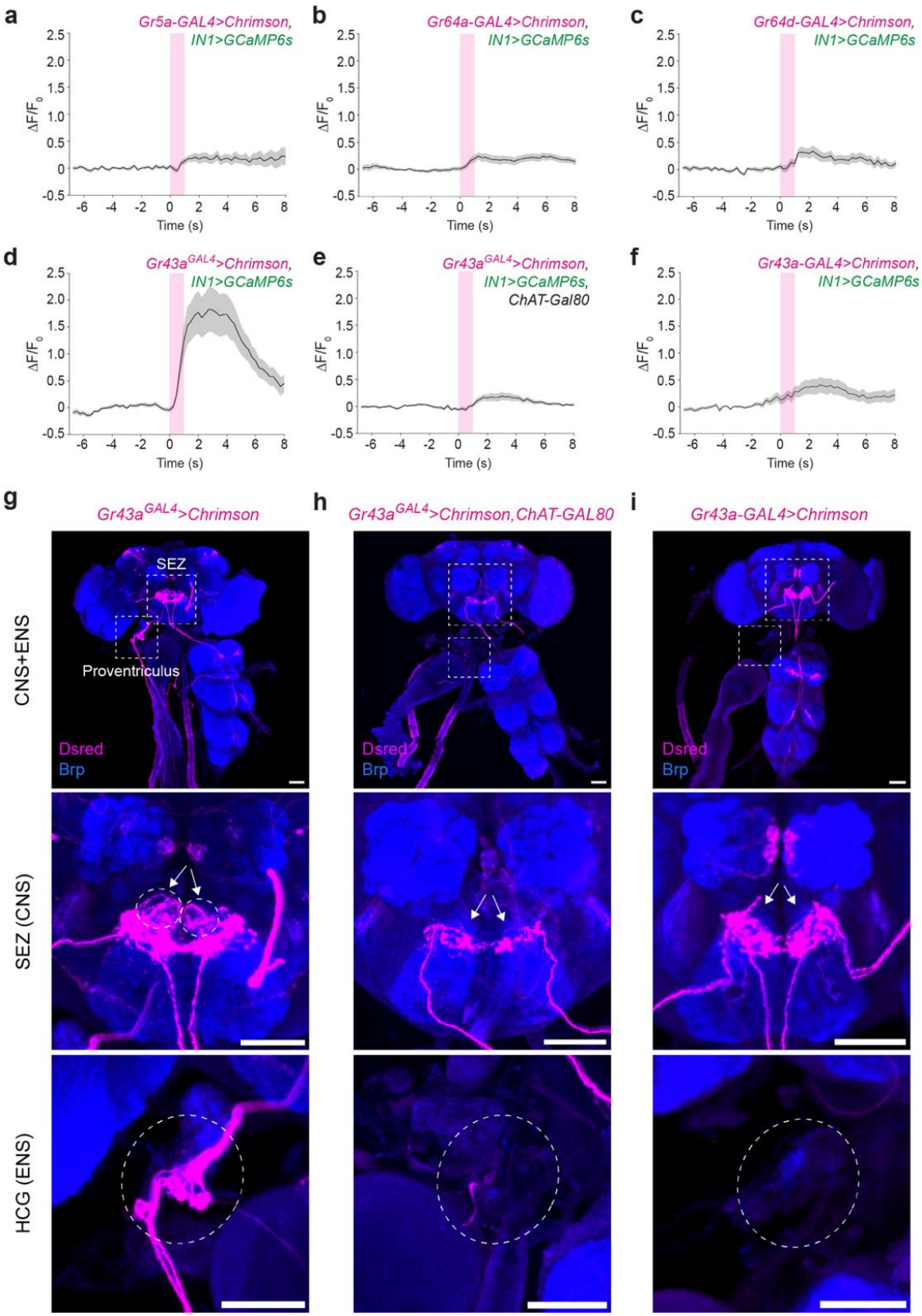
a
Gr5a-GAL4>Chrimson,
IN1>GCaMP6s
b
Gr64a-GAL4>Chrimson,
IN1>GCaMP6s
c
Gr64d-GAL4>Chrimson,
IN1>GCaMP6s
d
Gr43a^GAL4>Chrimson,
IN1>GCaMP6s
e
Gr43a^GAL4>Chrimson,
IN1>GCaMP6s,
ChAT-Gal80
f
Gr43a-GAL4>Chrimson,
IN1>GCaMP6s
ΔF/F0
Time (s)
g
Gr43a^GAL4>Chrimson
h
Gr43a^GAL4>Chrimson, ChAT-GAL80
i
Gr43a-GAL4>Chrimson
CNS+ENS
SEZ (CNS)
HCG (ENS)
SEZ
Proventriculus
Dsred
Brp

Fig. 2. 2| IN1s receive excitatory input from enteric sensory neurons expressing *Gr43a*.
a-c, Averaged normalized ($\Delta F/F_0$) GCaMP6s fluorescence in IN1s before and after optogenetic stimulation of different classes of sugar-sensing neurons. IN1s do not respond to the activation of neurons expressing *Gr5a* (**a**), *Gr64a* (**b**), or *Gr64d* (**c**) (n = 5-7 male flies; mean ± SEM). The optogenetic stimulation period is shown in a magenta-shaded area (stimulation = 1s, continuous, power = ~0.75mW out of objective).
d-f, Stimulation of different classes of Gr43a neurons results in different responses in IN1s. IN1s are strongly activated only when enteric neurons express Chrimson (n = 6 male flies, mean ± SEM). (See also Extended Data Figs. 2a-d).
g-i, Expression patterns of Gr43a transgenic flies expressing Chrimson (magenta) in the CNS+ENS (top), SEZ (middle) and HCG (ENS) (bottom). (**g**) *Gr43a*^{GAL4} knock-in labels enteric sensory neurons in the HCG and strongly activates IN1s (**d**). (**h**) Combining *Gr43a*^{GAL4} with *ChAT-Gal80* suppresses the expression in HCG and the responses in IN1s (**e**)**.** (**i**) *Gr43a-GAL4* transgenic strain does not label enteric neurons and does not activate INs (**f**) (scale bars = 50 μm, white circles indicate enteric neuron cell bodies in HCG, white arrows indicate their projections in the SEZ.)

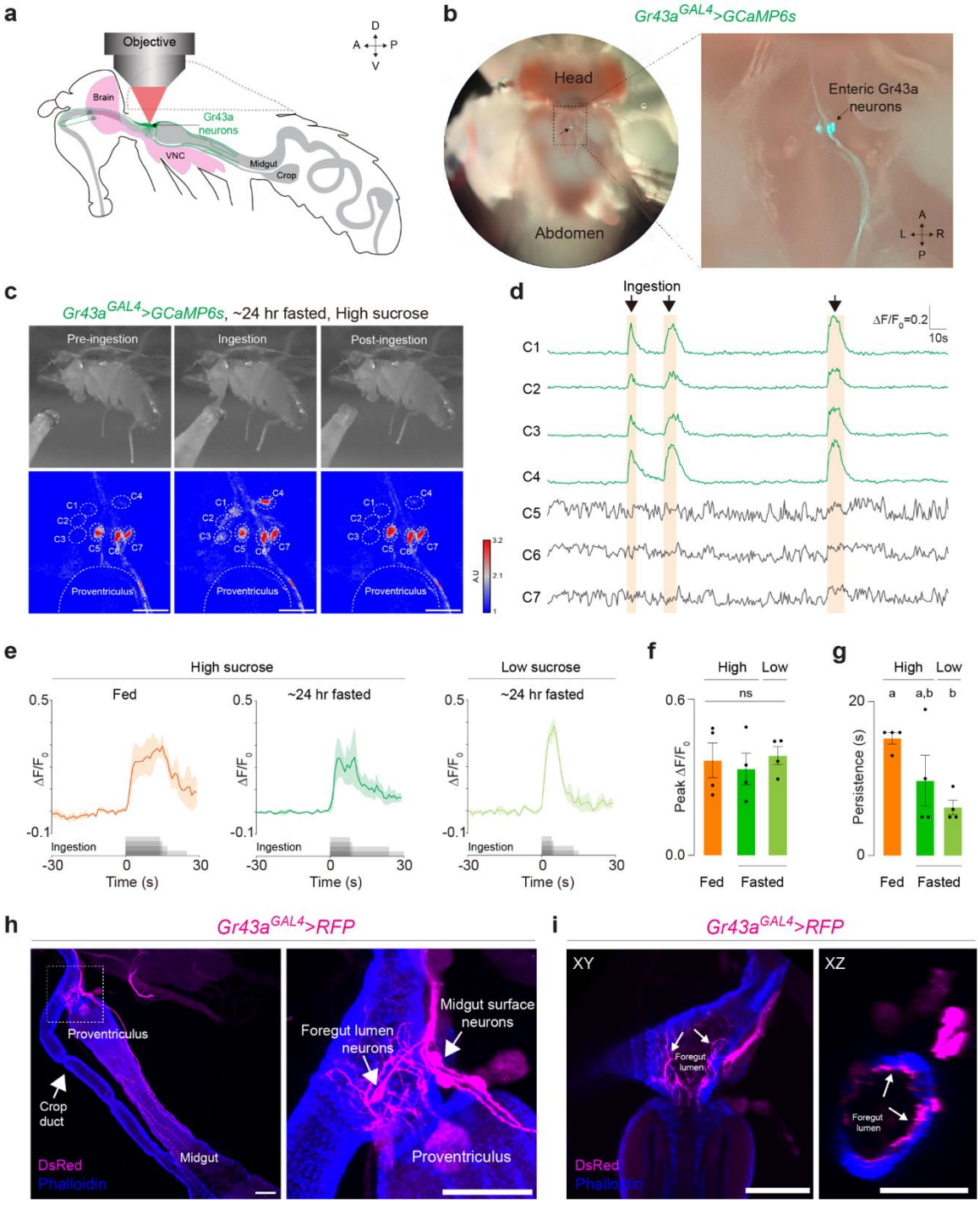
a
Objective
D
A
P
V
Brain
Gr43a neurons
VNC
Midgut
Crop
b
Gr43a^GAL4>GCaMP6s
Head
Abdomen
Enteric Gr43a neurons
A
L
R
P
c
Gr43a^GAL4>GCaMP6s, ~24 hr fasted, High sucrose
Pre-ingestion
Ingestion
Post-ingestion
C1
C2
C3
C4
C5
C6
C7
Proventriculus
A.U.
3.2
2.1
1
d
Ingestion
ΔF/F0=0.2
10s
C1
C2
C3
C4
C5
C6
C7
e
High sucrose
Low sucrose
Fed
~24 hr fasted
~24 hr fasted
ΔF/F0
0.5
-0.1
Ingestion
-30
0
30
Time (s)
f
High
Low
ns
Peak ΔF/F0
0.6
0.0
Fed
Fasted
g
High
Low
a
a,b
b
Persistence (s)
20
0
Fed
Fasted
h
Gr43a^GAL4>RFP
Proventriculus
Crop duct
Midgut
DsRed
Phalloidin
Foregut lumen neurons
Midgut surface neurons
Proventriculus
i
Gr43a^GAL4>RFP
XY
XZ
Foregut lumen
Foregut lumen
DsRed
Phalloidin

Fig. 2. 3| Enteric sensory neurons expressing *Gr43a* respond to sugar ingestion.

a, Schematic showing the enteric neuron imaging prep. Anterior (A), posterior (P), dorsal (D), ventral (V). The dashed line indicates the tissue removed. Adapted from Pauls, Dennis, et al., 2018 (Pauls et al., 2018).

b, Top view of the enteric Gr43a sensory neurons expressing *GCaMP6s*. Anterior (A), posterior (P), left (L), right (R). The arrows indicate the enteric Gr43a neurons.

c, Representative GCaMP6s responses of Gr43a enteric sensory neurons recorded in the same 24-hr-fasted male fly before (left), during (middle), and after (right) ~1M sucrose ingestion. Still images were captured by a video camera (top). Heatmap of Gr43a enteric sensory neuron activity in response to sucrose ingestion (bottom). Dashed white circles indicate seven separate cell bodies (C1-C7) of enteric Gr43a neurons (A.U., arbitrary units).

d, Normalized ($\Delta F/F_0$) GCaMP6s fluorescence in individual Gr43a cell bodies. Neurons that respond to ~1M sugar ingestion (C1-C4) are colored in green; neurons that are not activated during sugar ingestion (C5-C7) are colored in grey. The sugar ingestion period is shown as an orange-shaded area.

e, Normalized ($\Delta F/F_0$) GCaMP6s fluorescence in active Gr43a enteric sensory neurons in response to high (~1M and low sucrose (~100mM) ingestion in fed and ~24-hour fasted conditions (n = 4 male flies, mean ± SEM). The sugar ingestion is shown in grey.

f, Averaged normalized ($\Delta F/F_0$) peak responses of Gr43a enteric sensory neurons in indicated conditions (n =4 male flies, mean ± SEM, one-way ANOVA, $p = 0.8083$).

g, Persistence of Gr43a normalized ($\Delta F/F_0$) responses in indicated conditions (n =4 male flies, mean ± SEM, one-way ANOVA with Bonferroni post hoc test, $p < 0.05$).

h, Detailed anatomical visualization of enteric Gr43a neurons (magenta). A subset of Gr43a enteric sensory neurons penetrate the foregut and arborize in the inner surfaces of the gut lumen (foregut lumen neurons). Other Gr43a enteric sensory neurons do not penetrate the foregut and send their projections to the midgut (midgut surface neurons) (scale bars = 50μm) (See also Extended Data Figs. 3j-k).

i, Cross-sectional images of Gr43a foregut lumen neurons (magenta) in different axes: XY (left) and XZ (right). Arrows indicate enteric Gr43a neurites penetrating the gut lumen (scale bars = 50μm).

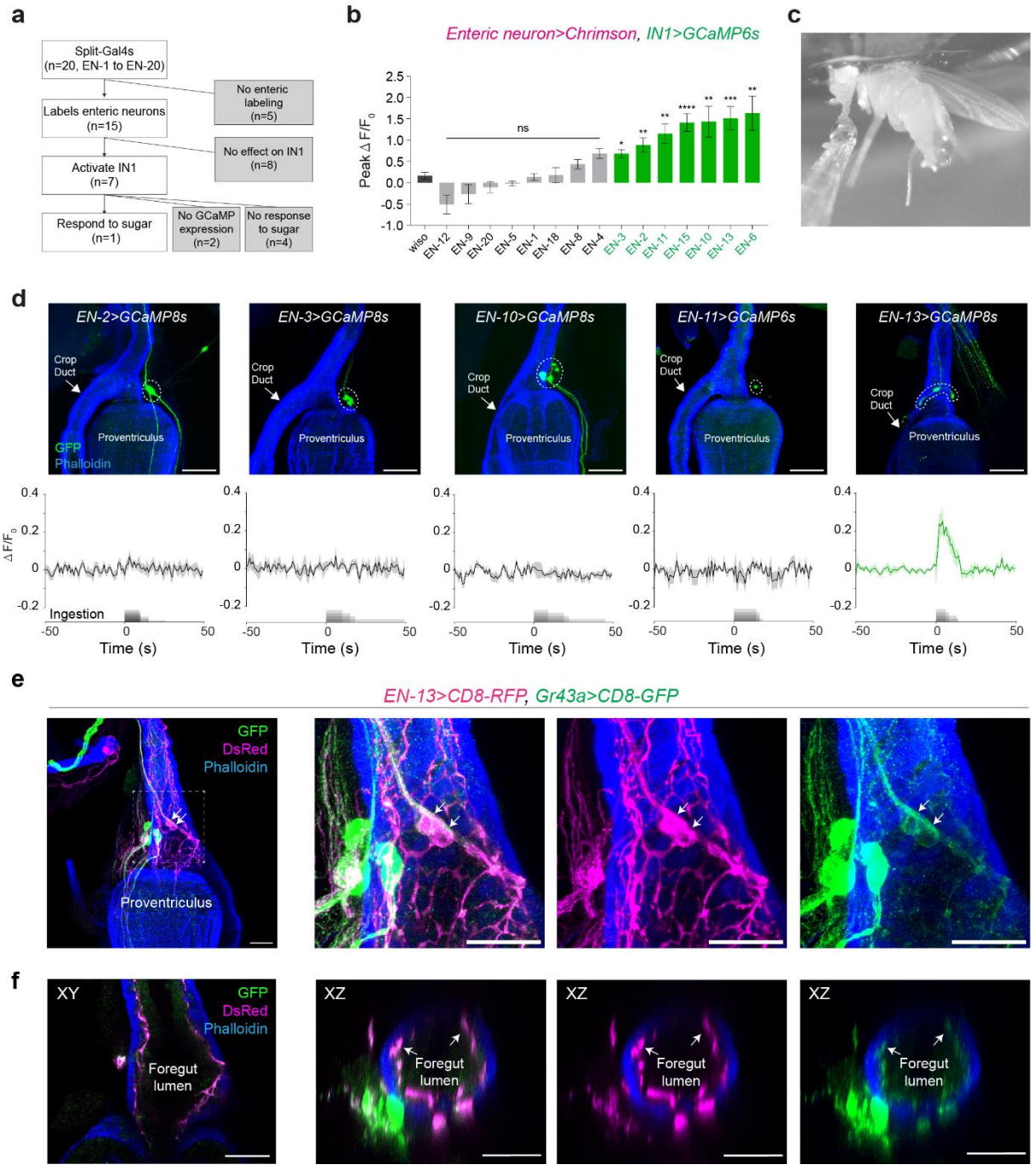
a
Split-Gal4s (n=20, EN-1 to EN-20)
No enteric labeling (n=5)
Labels enteric neurons (n=15)
No effect on IN1 (n=8)
Activate IN1 (n=7)
Respond to sugar (n=1)
No GCaMP expression (n=2)
No response to sugar (n=4)
b
Enteric neuron>Chrimson, IN1>GCaMP6s
Peak Δ F/F0
ns
wiso
EN-12
EN-9
EN-20
EN-5
EN-1
EN-18
EN-8
EN-4
EN-3
EN-2
EN-11
EN-15
EN-10
EN-13
EN-6
c
d
EN-2>GCaMP8s
EN-3>GCaMP8s
EN-10>GCaMP8s
EN-11>GCaMP6s
EN-13>GCaMP8s
Crop Duct
Proventriculus
GFP
Phalloidin
ΔF/F0
Ingestion
Time (s)
e
EN-13>CD8-RFP, Gr43a>CD8-GFP
GFP
DsRed
Phalloidin
Proventriculus
f
XY
XZ
Foregut lumen

Fig. 2. 4| Different classes of enteric sensory neurons can activate IN1s.

a, Overview of the enteric sensory neuron two-photon functional imaging screen. We generated 20 split-GAL4s (see also Extended Data Figs. 3a-i). Fifteen of these split-GAL4s labelled different populations of enteric sensory neurons. Optogenetic activation of seven enteric split-GAL4s (*ENs>*) activated IN1s, and one of these lines also responded to sugar ingestion.

b, Averaged normalized ($\Delta F/F_0$) peak responses of IN1s upon optogenetic stimulation of enteric split-GAL4s (*ENs>*). Positive ENs are shown in green; negative ENs are shown in grey; the control group is shown in black. (n = 5-7 male flies and five trials per fly, mean ± SEM, Kruskal Wallis test with Dunn's post hoc test, $*p < 0.05$, $**p < 0.01$, $***p < 0.001$, $****p < 0.0001$) (see also Extended Data Fig. 4).

c, A representative image showing enteric sensory neuron imaging during sugar ingestion. A male fly is fixed from its thorax underneath the imaging objective. Sugar stimulus is delivered using a pulled glass pipette.

d, Confocal images showing the expression of GCaMP6s or GCaMP8s in each *ENs>* (green). Dashed white circles indicate the ROIs used to quantify the GCaMP6s fluorescence (scale bars = 50μm.) (top). Normalized ($\Delta F/F_0$) GCaMP6s fluorescence in *ENs>* in response to high sucrose (~1M) ingestion in 24-hour fasted flies (n = 4-7 male flies; mean ± SEM), with sugar ingestion shown in grey (bottom).

e, Immunohistochemical analysis of neurons labelled by *EN-13>* (magenta) and *Gr43a>* (green) in the HCG. White arrows indicate the enteric sensory neurons labeled by both transgenic lines (scale bars = 25μm).

f, Cross-sectional images of neurons labelled by *EN-13>* (magenta) and *Gr43a>* (green) in different axes: XY (left) and XZ (middle-right). Arrows indicate enteric sensory arbours penetrating the gut lumen (scale bars = 25μm).

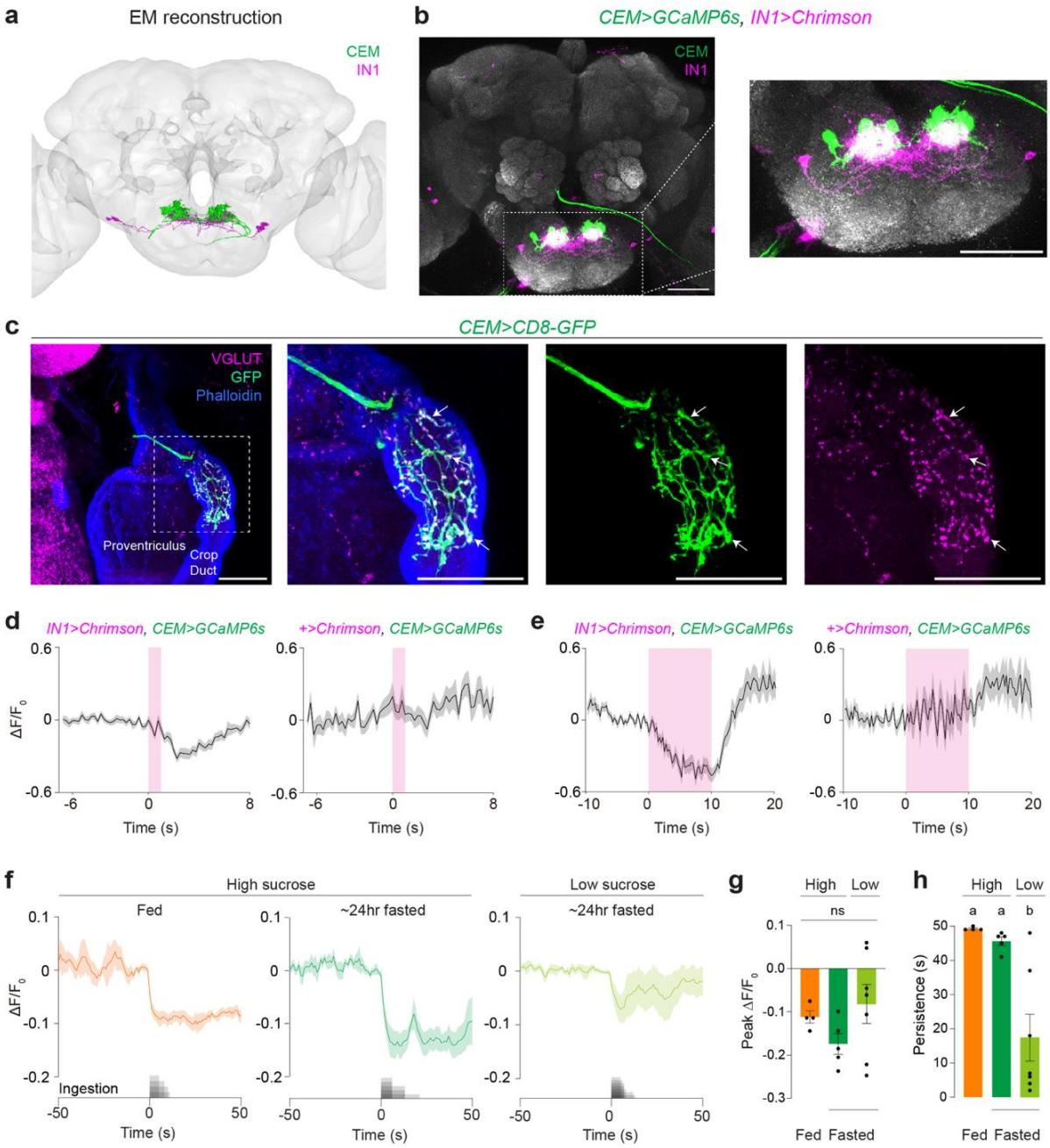
a
EM reconstruction
CEM
IN1
b
CEM>GCaMP6s, IN1>Chrimson
CEM
IN1
c
CEM>CD8-GFP
VGLUT
GFP
Phalloidin
Proventriculus
Crop
Duct
d
IN1>Chrimson, CEM>GCaMP6s
+>Chrimson, CEM>GCaMP6s
ΔF/F0
Time (s)
e
IN1>Chrimson, CEM>GCaMP6s
+>Chrimson, CEM>GCaMP6s
Time (s)
f
High sucrose
Low sucrose
Fed
~24hr fasted
~24hr fasted
ΔF/F0
Ingestion
Time (s)
g
High
Low
ns
Peak ΔF/F0
Fed
Fasted
h
High
Low
a
a
b
Persistence (s)
Fed
Fasted

Fig. 2. 5| IN1s inhibit CEM neurons upon sucrose ingestion.

a, Electron microscopy (EM) reconstruction of putative INs (magenta) and the CEM neurons (green).

b, Confocal images of IN1s (magenta) and CEM neurons (green) in the brain (left). IN1 and CEM arbors are intermingled in the SEZ (right) (scale bars = 50μm).

c, Staining of CEM axonal terminals with VGLUT and GFP antibodies in *CEM>CD8-GFP* flies. White arrows indicate the co-labelling of CEM synaptic terminals in the crop duct with VGLUT (magenta) and GFP (green) (scale bars = 25μm).

d-e, Optogenetic stimulation of INs inhibits the activity of CEM neurons. (n = 5-8 male flies; mean ± SEM). The optogenetic stimulation period is shown in a magenta-shaded area (stimulation = 1s (**d**) or 10s (**e**), continuous, power = ~0.75mW).

f, Normalized ($\Delta F/F_0$) GCaMP6s fluorescence in CEM neurons in response to high (~1M) and low (~100mM) sucrose ingestion in fed and ~24-hour fasted conditions (n = 4-7 male flies; mean ± SEM). The sugar ingestion is shown in grey.

g, Averaged normalized ($\Delta F/F_0$) peak responses of CEM neurons in indicated conditions (n = 4-7 male flies, mean ± SEM, one-way ANOVA, $p = 0.2353$).

h, Persistence of CEM normalized ($\Delta F/F_0$) responses in indicated conditions (n =4-7 male flies, mean ± SEM, one-way ANOVA with Bonferroni post hoc test, $p < 0.05$).

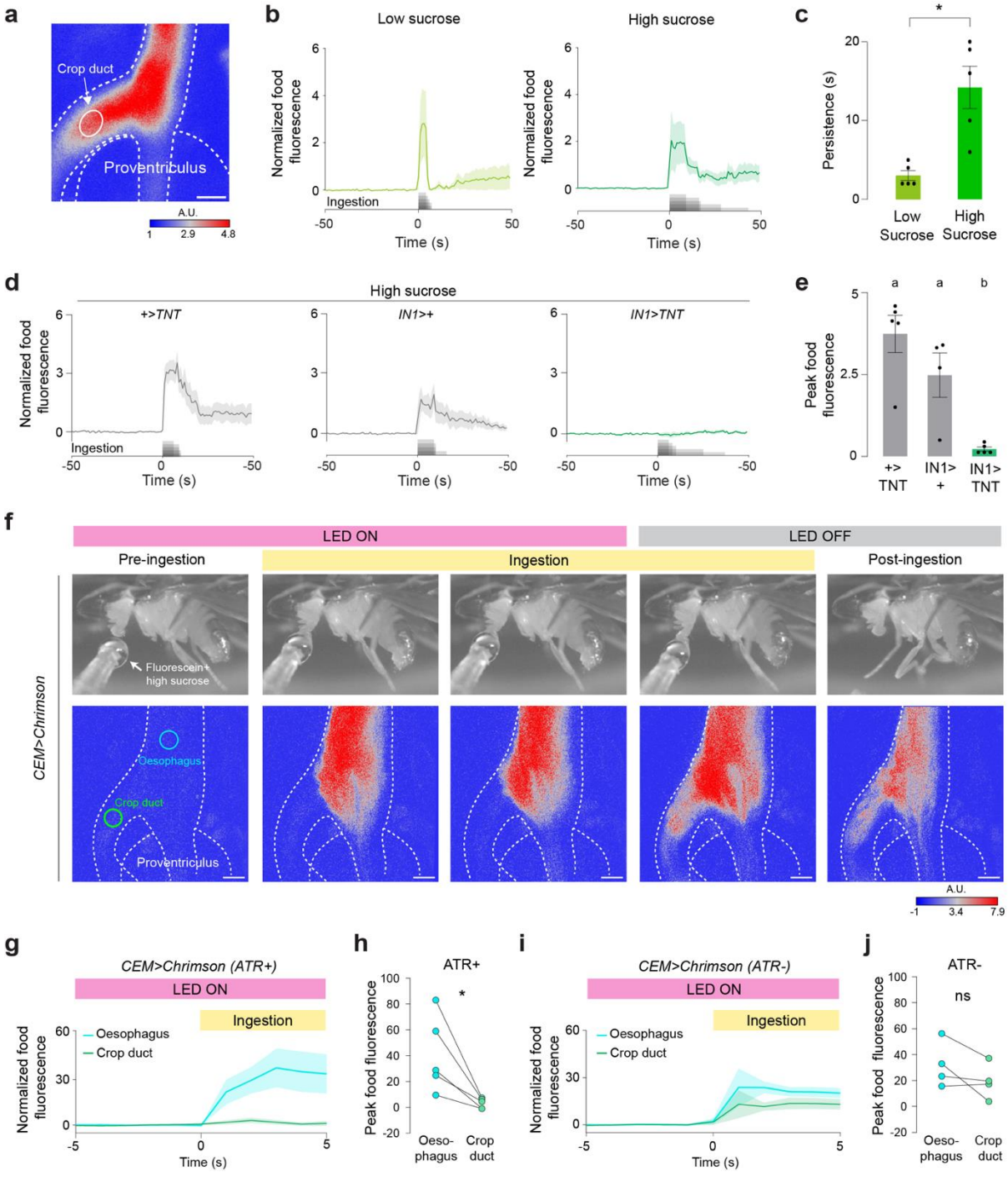
a
Crop duct
Proventriculus
A.U.
1
2.9
4.8
b
Low sucrose
High sucrose
Normalized food fluorescence
Ingestion
Time (s)
c
Persistence (s)
Low Sucrose
High Sucrose
d
High sucrose
+>TNT
IN1>+
IN1>TNT
e
Peak food fluorescence
+> TNT
IN1> +
IN1> TNT
f
LED ON
LED OFF
Pre-ingestion
Ingestion
Post-ingestion
CEM>Chrimson
Fluorescein+ high sucrose
Oesophagus
Crop duct
Proventriculus
A.U.
g
CEM>Chrimson (ATR+)
Oesophagus
Crop duct
h
ATR+
Oeso- phagus
Crop duct
i
CEM>Chrimson (ATR-)
j
ATR-
ns

Fig. 2. 6| CEM neurons gate the entry of sucrose into the crop during ingestion.

a, A representative image showing the ROI in the crop-duct during ingestion of high-sucrose containing fluorescein (scale bar = 25μm. A.U., arbitrary unit).

b, Normalized food fluorescence in the crop duct before and after ingestion of low (~100mM) (left) and high (~1M) (right) sucrose (n = 5 male flies, mean ± SEM). The sugar stimulus was provided *ad libitum*.

c, Persistence of normalized food fluorescence when flies are ingesting low (~100mM) or high (~1M) sucrose (n = 5 male flies, mean ± SEM, Unpaired t-test with Welch's correction, $*p < 0.05$).

d, Normalized food fluorescence in the crop duct before and after ingestion of high sucrose (~1M) in flies with indicated genotypes (n = 4-5 male flies, mean ± SEM).

e, Peak food fluorescence in the crop duct after ingesting high sucrose (~1M) in flies with indicated genotypes. The food volume that enters the crop duct is significantly reduced when IN1 neurons are inhibited (n = 4-5 male flies, mean ± SEM, one-way ANOVA with Bonferroni post hoc test, $p < 0.05$).

f, Representative images (top) and food fluorescence in the crop duct and esophagus (bottom) of a 24-hr-fasted *CEM>Chrimson* male fly before (pre-ingestion), during (ingestion), and after (post-ingestion) high sucrose ingestion, and with and without optogenetic stimulation of CEM neurons. High sucrose (~1M) solution cannot enter the crop duct until the CEM optogenetic activation is turned OFF (LED OFF). Cyan and green circles indicate ROIs in the esophagus and crop duct, respectively (scale bars = 25μm, A.U., arbitrary unit).

g-j, Normalized food fluorescence in the esophagus (cyan) and crop duct (green) of *CEM>Chrimson* flies during optogenetic stimulation with ATR (**g**, test group) and without ATR (**i,** control group). (**h**) Optogenetic stimulation reduces the amount of sucrose that can enter the crop duct in the test group quantified by peak food fluorescence. (**j**) However, control flies are not affected by optogenetic stimulation (n = 4-5 male flies, mean ± SEM, paired t-test, ns, $*p<0.05$).

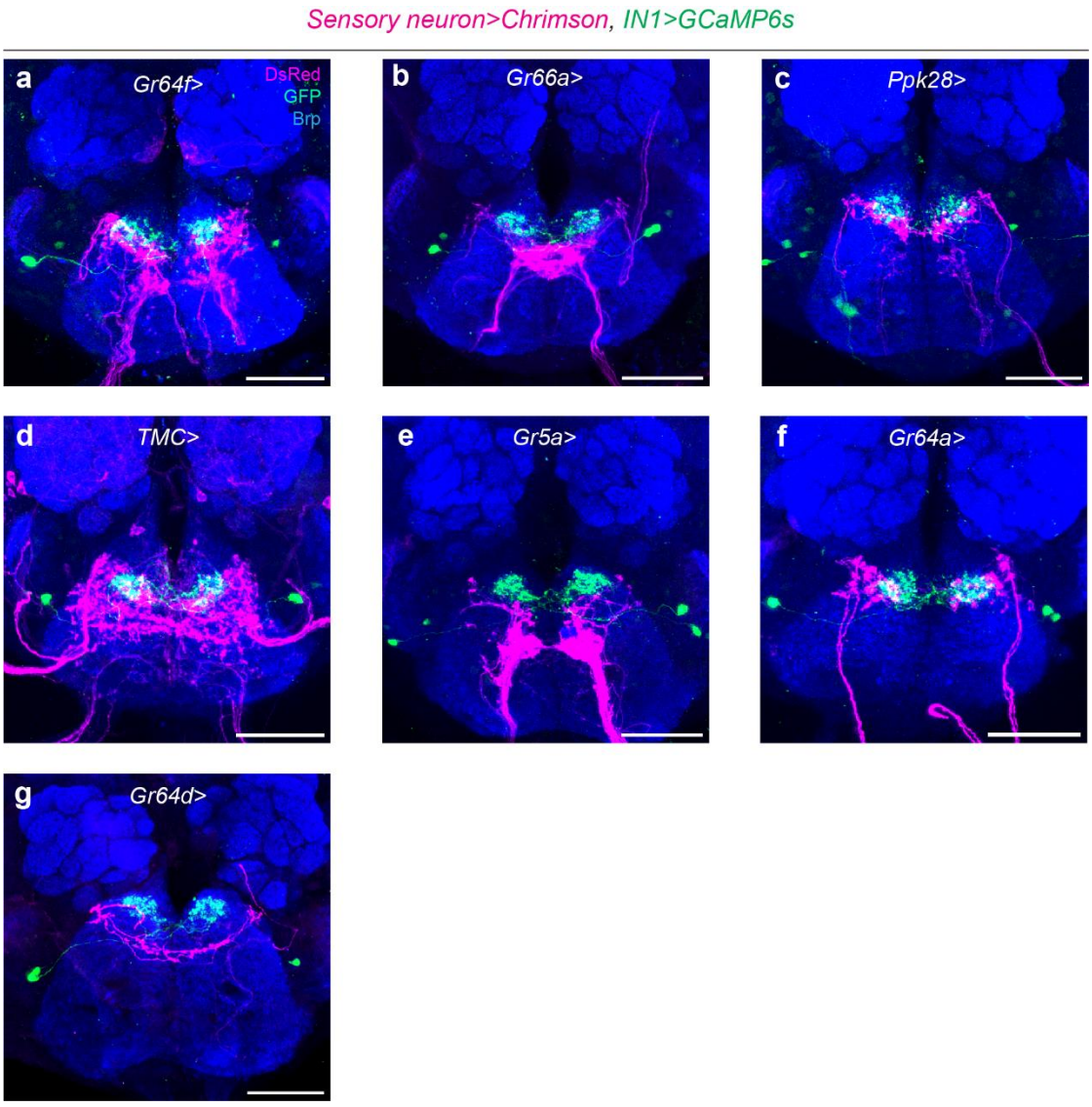

Extended Data Fig. 2. 1| Expression patterns of GAL4 lines in SEZ labeling different classes of sensory neurons.

a-g, Confocal images of sensory neuron afferents (magenta) and IN1 arbors (green) in the anterior SEZ. The sensory neurons are labeled by *Gr64f>* (**a**), *Gr66a>* (**b**), *ppk28>* (**c**), *TMC>* (**d**), *Gr5a>* (**e**), *Gr64a>* (**f**), *Gr64d>* (**g**). (scale bars = 50μm).

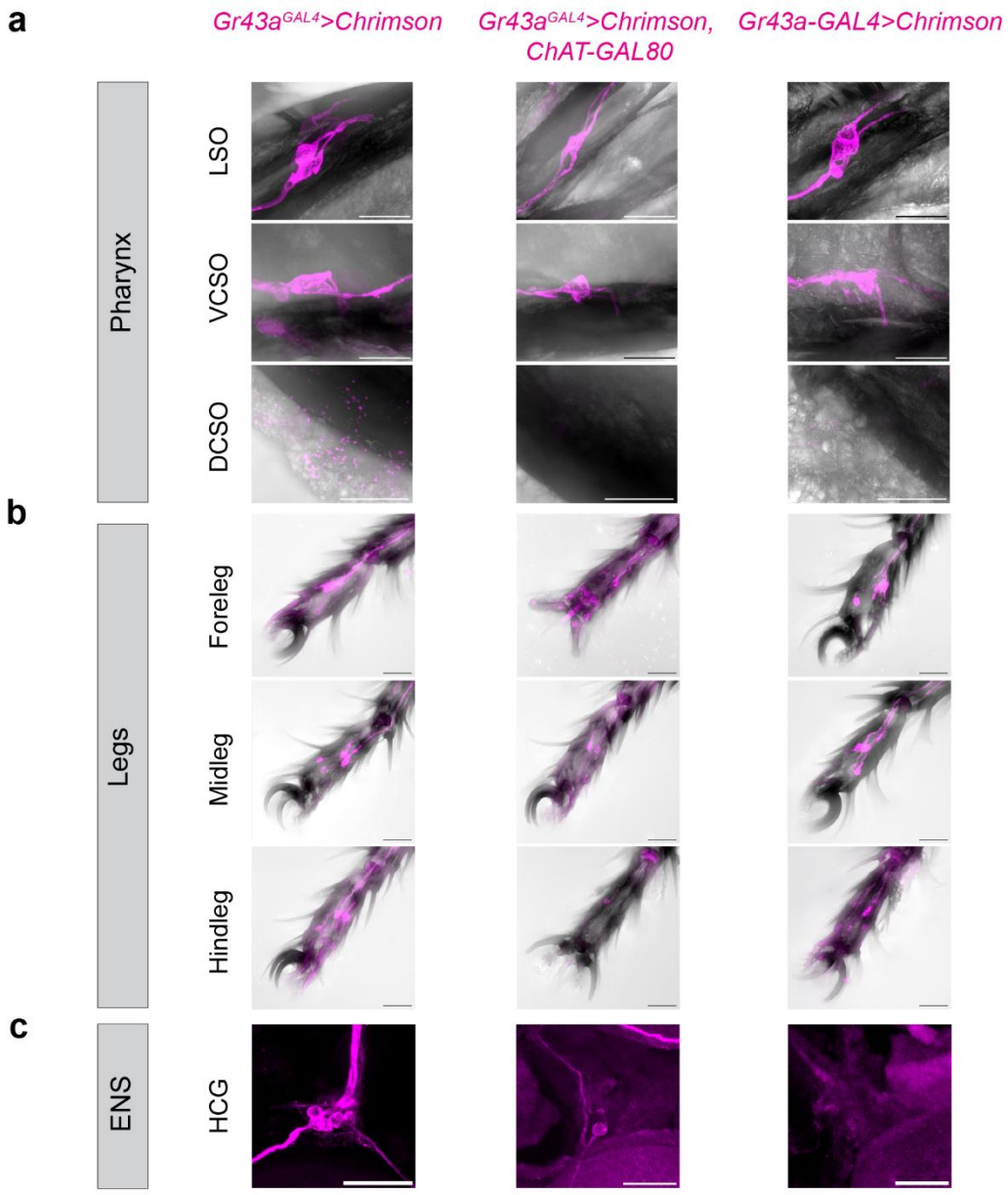

d

# of neurons per tissue, per genotype		*Gr43a^{GAL4}>Chrimson*	*Gr43a^{GAL4}>Chrimson, ChAT-GAL80*	*Gr43a-GAL4>Chrimson*
Brain		7.67±0.67	8.33±0.33	0
HCG		6.67±0.33	0.67±0.33	0
VNC		0	0	0
Pharynx	LSO	2	2	2
	VCSO	2	1.25±0.25	2
	DCSO	0.67±0.33	0.5±0.29	0.5±0.29
Legs	Foreleg	5	2.33±0.33	4.67±0.33
	Midleg	4	1.5±0.29	4
	Hindleg	4	0.75±0.48	3±0.58

Extended Data Fig. 2. 2| Expression patterns of Gr43a transgenic lines in the chemosensory and enteric neurons

a-c, Expression patterns of different transgenes labeling distinct classes of Gr43a neurons (magenta) in various chemosensory organs and the enteric nervous system (scale bars = 25μm). **d**, Quantification of Gr43a neurons in flies carrying the indicated transgenes in the CNS, ENS, and various chemosensory organs (HCG, hypocerebral ganglion; VNC, ventral nerve cord; LSO, labral sense organ, VCSO, ventral cibarial sense organs, DCSO, dorsal cibarial sense organs). For legs and pharyngeal organs, LSO, VCSO, and DCSO, we report the number of neurons unilaterally (n = 3-4 male flies per group, mean ± SEM).

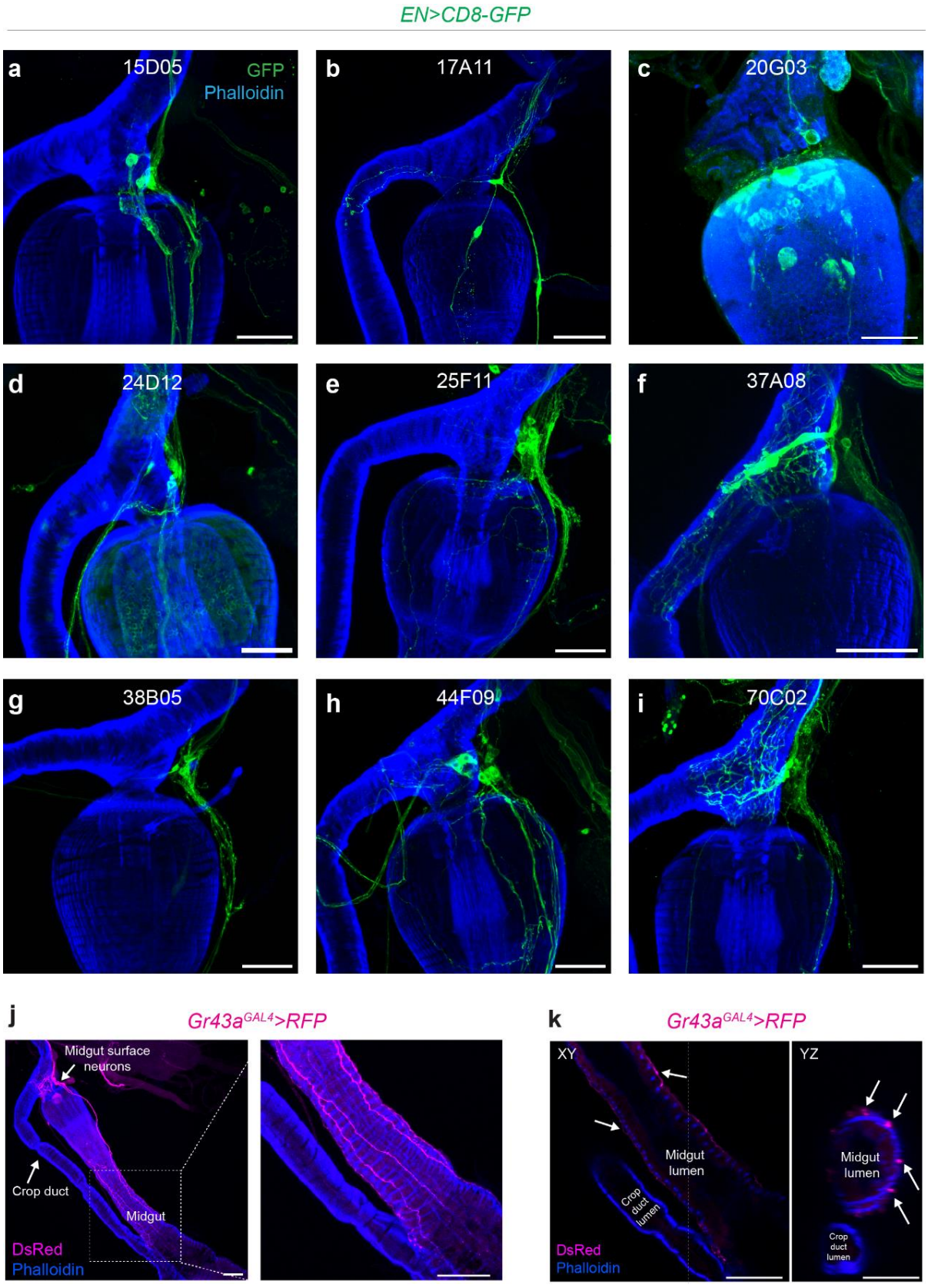
EN>CD8-GFP
a
15D05
GFP
Phalloidin
b
17A11
c
20G03
d
24D12
e
25F11
f
37A08
g
38B05
h
44F09
i
70C02
j
Gr43a^GAL4>RFP
Midgut surface neurons
Crop duct
Midgut
DsRed
Phalloidin
k
Gr43a^GAL4>RFP
XY
Midgut lumen
Crop duct lumen
DsRed
Phalloidin
YZ
Midgut lumen
Crop duct lumen

Extended Data Fig. 2. 3| GAL4 lines labeling different classes of enteric neurons.

a-i, Confocal images of enteric neurons (green) labeled by selected GAL4 lines whose promoters are used to generate the EN-split GAL4s (scale bars = 50μm).

j, Confocal images of enteric Gr43a neurons that project to the midgut (magenta). The upper white arrow indicates the midgut surface neuron cell bodies and the lower white arrow indicates the crop duct (left). Notice the midgut surface neurons arborize along the surface of the midgut muscle (blue) (right) (scale bars = 50μm)

k, Cross-sectional images of Gr43a midgut surface neurons in different axes: XY (left) and XZ (right). Arrows indicate the neurites of Gr43a midgut surface neurons (magenta) innervating the gut muscles (blue) (scale bars = 50μm).

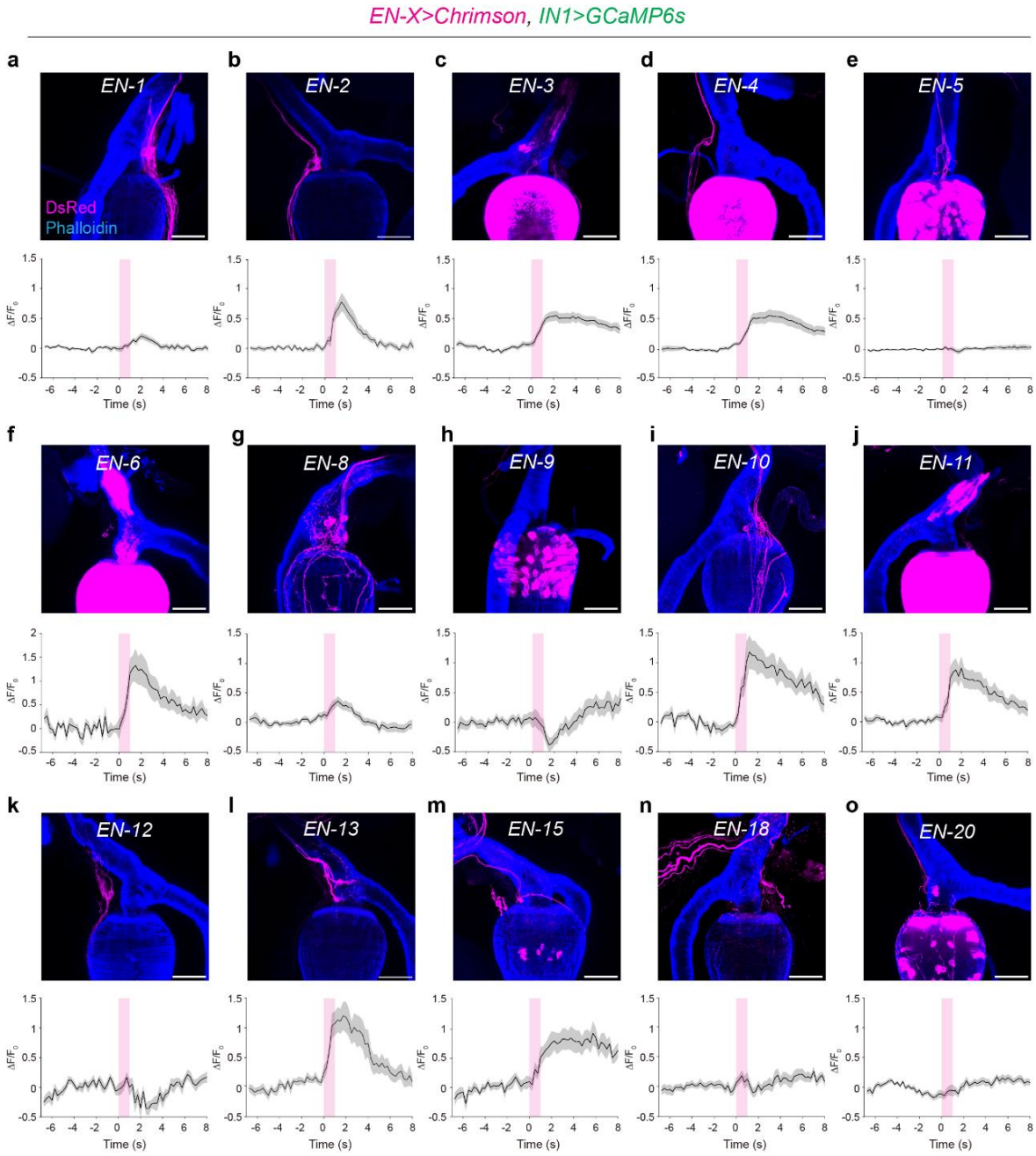

Extended Data Fig. 2. 4| IN1s receive excitatory input from different classes of enteric neurons.

a-o, Confocal images showing the expression patterns of EN split GAL4 lines expressing Chrimson (*ENs> Chrimson*) (magenta) in the HCG (top) (scale bars = 50μm). Normalized ($\Delta F/F_0$) GCaMP6s fluorescence in INs before and after optogenetic stimulation of different classes of enteric neurons (bottom) (n = 5-7 male flies, five trials per fly mean ± SEM).

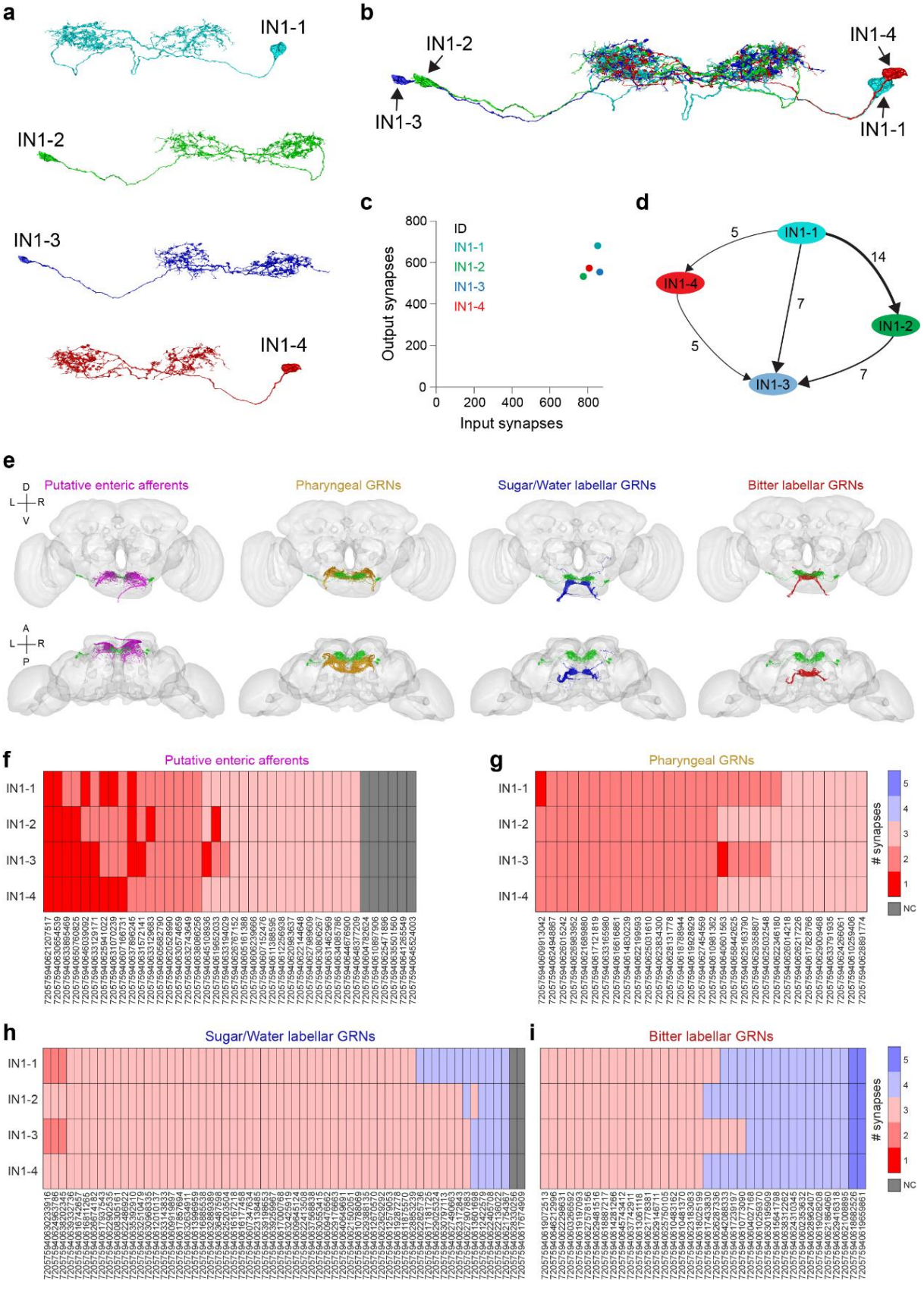
a
IN1-1
IN1-2
IN1-3
IN1-4
b
IN1-2
IN1-4
IN1-3
IN1-1
c
ID
IN1-1
IN1-2
IN1-3
IN1-4
Output synapses
Input synapses
0
200
400
600
800
d
IN1-1
IN1-2
IN1-3
IN1-4
5
14
7
5
7
e
Putative enteric afferents
Pharyngeal GRNs
Sugar/Water labellar GRNs
Bitter labellar GRNs
D
L
R
V
A
P
f
Putative enteric afferents
g
Pharyngeal GRNs
h
Sugar/Water labellar GRNs
i
Bitter labellar GRNs
synapses
NC

Extended Data Fig. 2. 5| EM analysis of IN1s and their synaptic connectivity with different classes of GRNs and putative enteric neurons

a-**b**, EM reconstruction of putative IN1s (n=4) in the FAFB connectome is shown individually (**a**) or together (**b**).

c, Total number of input and output synapses of putative IN1s in the FAFB connectome.

d, Synaptic connectivity of IN1s to each other with arrows indicating the direction of connections (from presynaptic to postsynaptic neurons). The total number of synapses is shown on top of the arrows.

e, EM reconstruction of putative IN1s (green) together with different classes of GRN (yellow, pharyngeal GRNs; blue, sweet/water labellar GRNs; red, bitter labellar GRNs) or putative enteric afferents (magenta) in the FAFB connectome. The front view (top) and top view (bottom) are shown. (L, left; R, right; D, dorsal; V, ventral; A, anterior; P, posterior).

f-i, Heatmap showing the connectivity network between IN1s and different classes of GRNs or putative enteric afferents (NC, no path). IN1s are synaptically closer to putative enteric afferents than pharyngeal or labellar GRNs. A threshold of 5 synapses is used to determine connectivity between pairs of neurons.

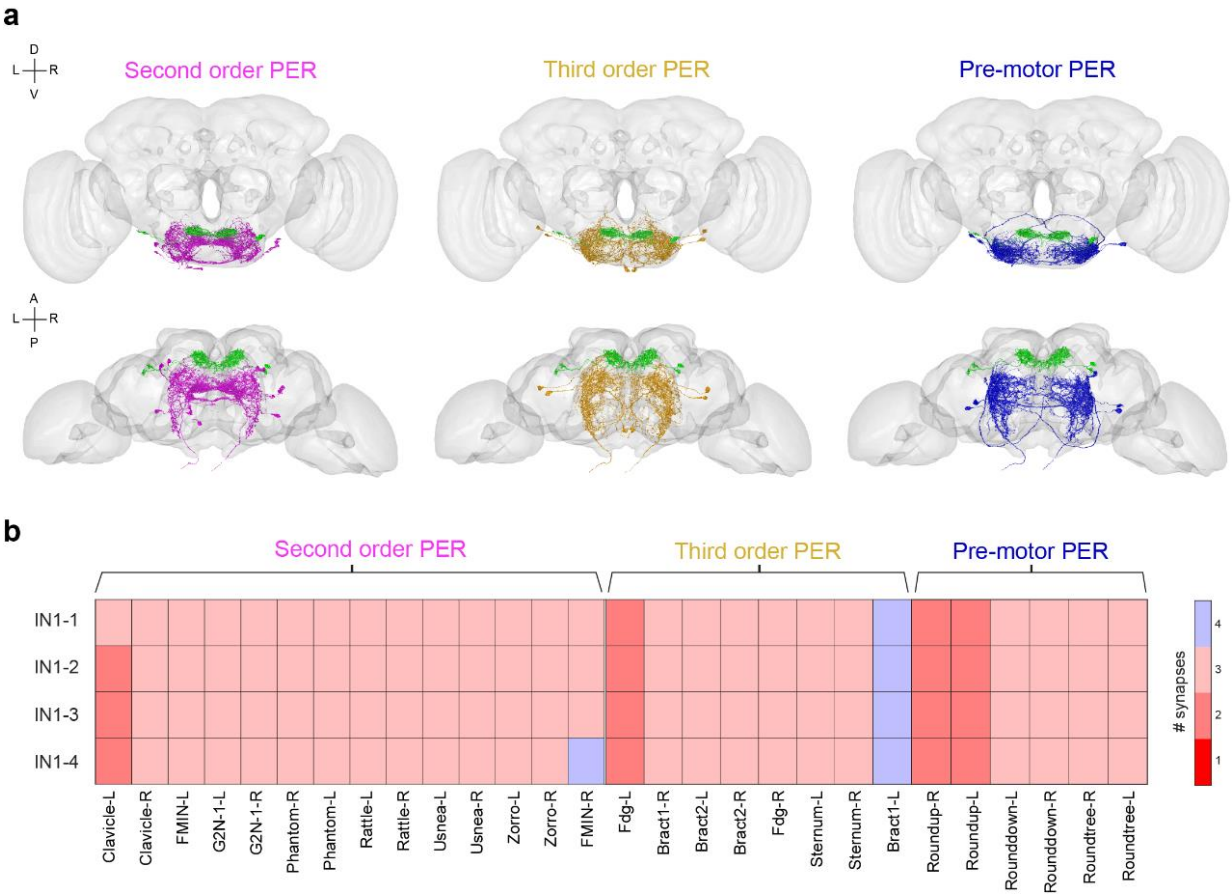

Extended Data Fig. 2. 6| EM analysis of IN1s and their synaptic connectivity with different classes of PER neurons

a, EM reconstruction of putative IN1s (green) with different classes of PER neurons in the FAFB connectome (magenta, second order PER; yellow, third order PER; blue, pre-motor PER). The front view (top) and top view (bottom) are shown. (L, left; R, right; D, dorsal; V, ventral; A, anterior; P, posterior).

b, Heatmap showing the connectivity network between IN1s and different classes of PER neurons. IN1s are at least two synapses away from PER neurons in the SEZ. A threshold of 5 synapses is used to determine connectivity between pairs of neurons. Neurons with cell bodies in the left hemisphere are labeled with -L, and neurons with cell bodies in the right hemisphere are labeled with -R.

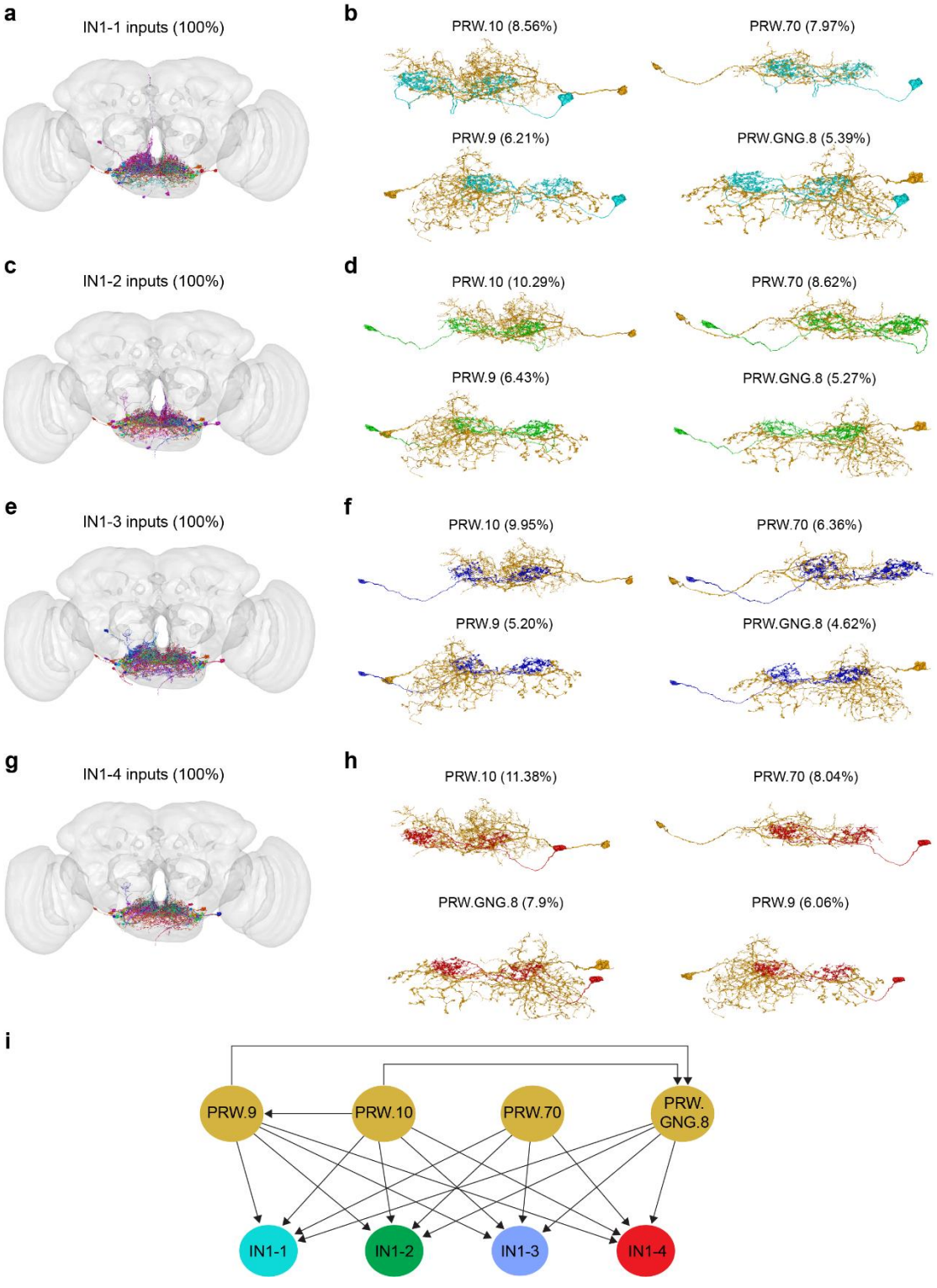
a
IN1-1 inputs (100%)
b
PRW.10 (8.56%)
PRW.70 (7.97%)
PRW.9 (6.21%)
PRW.GNG.8 (5.39%)
c
IN1-2 inputs (100%)
d
PRW.10 (10.29%)
PRW.70 (8.62%)
PRW.9 (6.43%)
PRW.GNG.8 (5.27%)
e
IN1-3 inputs (100%)
f
PRW.10 (9.95%)
PRW.70 (6.36%)
PRW.9 (5.20%)
PRW.GNG.8 (4.62%)
g
IN1-4 inputs (100%)
h
PRW.10 (11.38%)
PRW.70 (8.04%)
PRW.GNG.8 (7.9%)
PRW.9 (6.06%)
i
PRW.9
PRW.10
PRW.70
PRW.
GNG.8
IN1-1
IN1-2
IN1-3
IN1-4

Extended Data Fig. 2. 7| EM analysis of IN1 presynaptic neurons.

a-h, EM reconstruction of putative IN1s (cyan, IN1-1; green, IN1-2; violet, IN1-3; red, IN1-4) with their presynaptic inputs (**a, c, e, g**). Anatomy of the top four presynaptic inputs to IN1-1 (**b**), IN1-2 (**d**), IN1-3 (**f**), or IN1-4 (**h**) in the FAFB brain dataset are shown. The input neurons are ordered based on their % synaptic input to IN1s. The Codex IDs of input neurons and the percentage of synaptic inputs they provide to IN1s are indicated on top of each panel. A threshold of five synapses is used to determine connectivity between neurons. **i**, Synaptic connectivity of IN1s and their inputs. Arrows indicate the direction of connections (from presynaptic to postsynaptic neurons). Synaptic connections between IN1s are not shown in this graph. Please see Extended Data Fig. 2.5d for connections between IN1s.

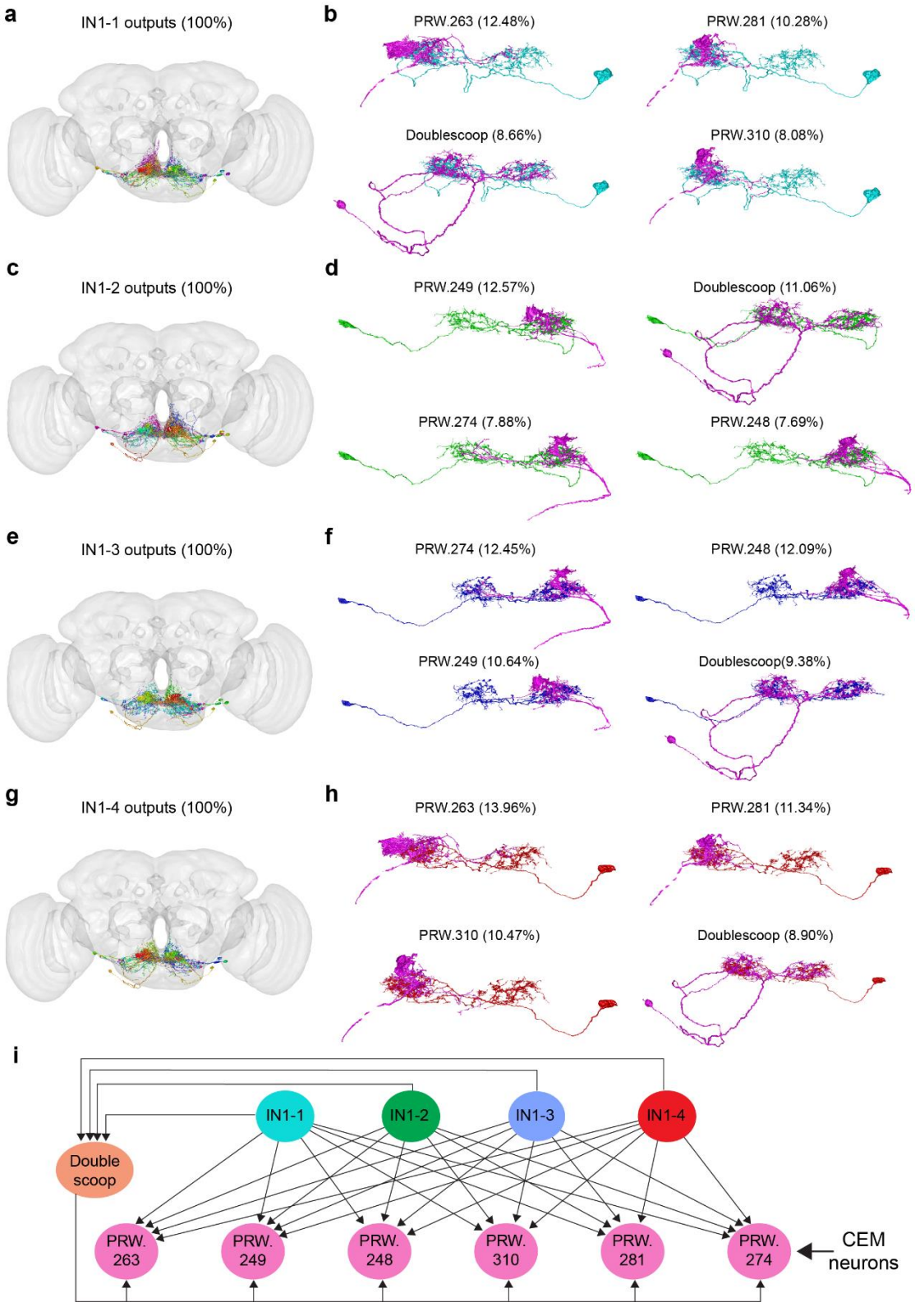
a
IN1-1 outputs (100%)
b
PRW.263 (12.48%)
PRW.281 (10.28%)
Doublescoop (8.66%)
PRW.310 (8.08%)
c
IN1-2 outputs (100%)
d
PRW.249 (12.57%)
Doublescoop (11.06%)
PRW.274 (7.88%)
PRW.248 (7.69%)
e
IN1-3 outputs (100%)
f
PRW.274 (12.45%)
PRW.248 (12.09%)
PRW.249 (10.64%)
Doublescoop(9.38%)
g
IN1-4 outputs (100%)
h
PRW.263 (13.96%)
PRW.281 (11.34%)
PRW.310 (10.47%)
Doublescoop (8.90%)
i
IN1-1
IN1-2
IN1-3
IN1-4
Double scoop
PRW. 263
PRW. 249
PRW. 248
PRW. 310
PRW. 281
PRW. 274
CEM neurons

Extended Data Fig. 2. 8| EM analysis of IN1 postsynaptic neurons.

a-h, EM reconstruction of putative IN1s (cyan, IN1-1; green, IN1-2; violet, IN1-3; red, IN1-4) with their postsynaptic outputs (**a, c, e, g**). Anatomy of the top four postsynaptic outputs for IN1-1 (**b**), IN1-2 (**d**), IN1-3 (**f**), or IN1-4 (**h**) in the FAFB brain dataset are shown. The Codex IDs of output neurons and the percentage of synaptic outputs IN1s provide to them are indicated on top of each panel. A threshold of five synapses is used to determine connectivity between neurons. **i**, Synaptic connectivity of IN1s and their outputs. Arrows indicate the direction of connections (from presynaptic to postsynaptic neurons). The six neurons (pink) shown in the bottom row (PRW.263, PRW.249, PRW.248, PRW.310, PRW.281, and PRW.274) are the crop-innervating enteric motor neurons (CEM neurons). Synaptic connections between IN1s are not shown in this graph. Please see Extended Data Fig. 2.5d for connections between IN1s.

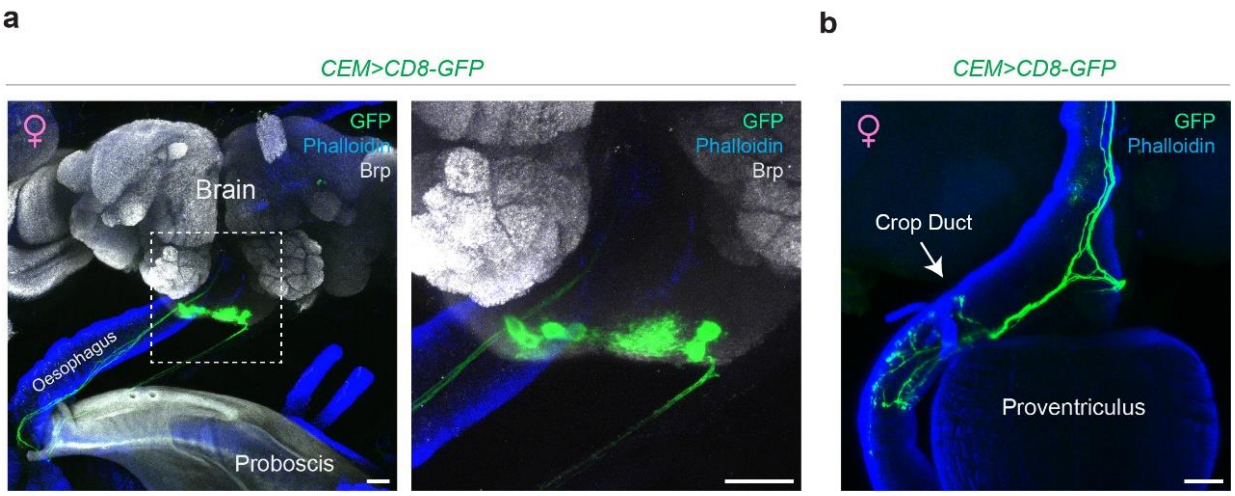

Extended Data Fig. 2. 9| CEM neurons are present in both sexes.

a, Confocal images of CEM neurons (green) in the female brain and their descending projections towards the esophagus (blue) (scale bars = 25µm).

b, Synaptic terminals of CEM neurons (green) innervating the crop duct (blue) in a female fly. (scale bar = 25µm).

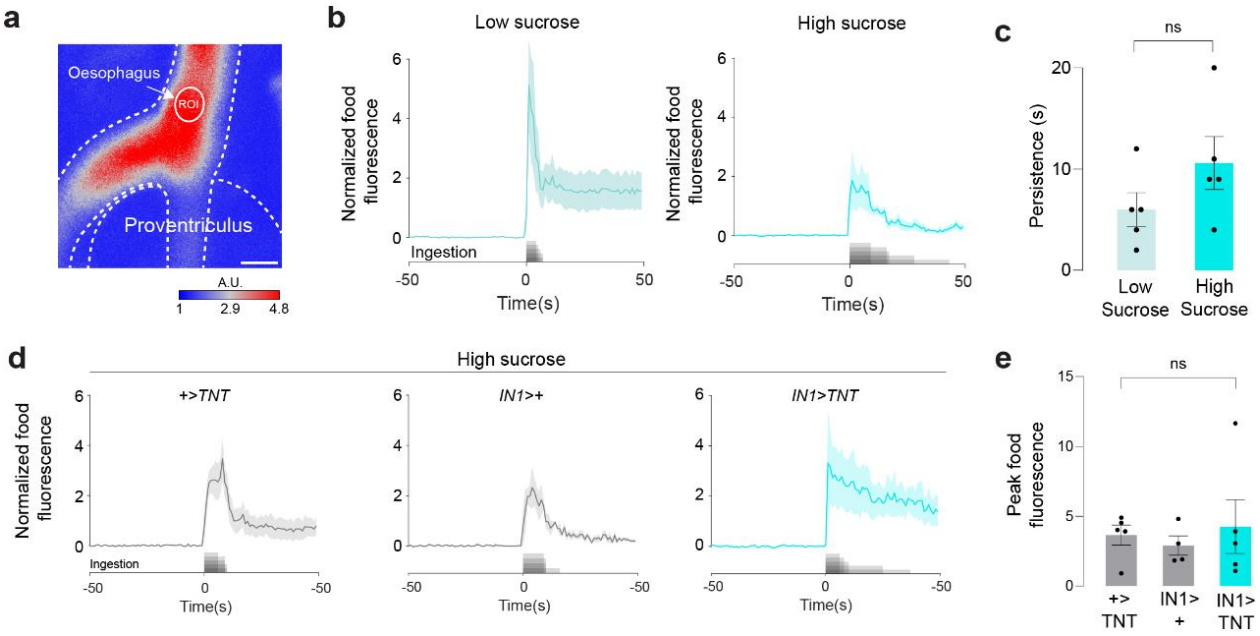

Extended Data Fig. 2. 10| Inhibition of IN1s does not block entry of sucrose into the esophagus.

a, A representative image showing the ROI in the esophagus during ingestion of fluorescein food (scale bar=25μm. A.U., arbitrary unit).

b, Normalized food fluorescence in the esophagus before and after ingestion of low (~100mM) (left) and high (~1M) (right) sucrose (n = 5 male flies, mean ± SEM). The sugar stimulus was provided *ad libitum*.

c, Persistence of normalized food fluorescence in the esophagus when flies are ingesting low (~100mM) or high (~1M) sucrose (n = 5 male flies, mean ± SEM, Unpaired t-test with Welch's correction, p = 0.18).

d, Normalized food fluorescence in the esophagus before and after ingestion of high sucrose (~1M) in flies with indicated genotypes (n = 4-5 flies per group; mean ± SEM).

e, Peak food fluorescence in the esophagus after ingestion of high sucrose (~1M) in flies with indicated genotypes (n = 4-5 male flies; mean ± SEM). The amount of food entering the esophagus is not altered when IN1 neurons are inhibited (n = 4-5 male flies, mean ± SEM, one-way ANOVA, p = 0.78).

Methods

Fly husbandry and genotypes

For all experiments, we used male flies 3 days post-eclosion unless otherwise noted. Flies were housed in a 25° C incubator with 60-65% humidity. Flies were grown on a conventional cornmeal-agar-molasses medium under a 12/12 light/dark cycle (lights on at 9 A.M.). When tested as controls, UAS or GAL4 stocks were tested as hemizygotes after crossing to w^{1118}. IN1-split-GAL4 and IN1-split-LexA were generated in this study. IN1-split-GAL4 was generated by recombining 57F03-GAL4-DBD and 83F01-GAL4-AD on the 3rd chromosome. IN1-split-LexA was generated by recombining 57F03-LexA-DBD and 83F01-GAL4-AD on the 3rd chromosome. $Gr43a^{GAL4}$ and $Gr43a^{LEXA}$ were generously provided by Dr. Hubert Amrein(Miyamoto et al., 2012) (Texas A&M University). Ppk28-GAL4(Cameron et al., 2010) was generously provided by Dr. Micheal Gordon (The University of British Columbia). ChAT-Gal80(Kitamoto, 2002) was generously provided by Dr. Toshihiro Kitamoto (University of Iowa). Gr5a-GAL4(Wang et al., 2004) and Gr66a-GAL4(Wang et al., 2004) were generously provided by Dr. Kristin Scott (University of California, Berkeley). 10XUAS-Syn21-Chrimson88-tdT-3.1, LexAop2-Syn21-opGCaMP6s(Strother et al., 2017) was generously provided by Dr. Michael Reiser (HHMI Janelia). 10xUAS-IVS-Syn21-Chrimson::tdT-3.1(Hoopfer et al., 2015) was generously provided by Dr. David Anderson (Caltech). LexAop-Chrimson-TdTomato(Tuthill & Wilson, 2016) was generously provided by Dr. John Tuthill (University of Washington). The following stocks were obtained from the BDSC: w^{1118} (5905); Gr43a-GAL4 (57637); Gr64f-GAL4 (57669); Gr64a-GAL4 (57661); Gr64d-GAL4 (57665); TMC-GAL4 (66557); Ir25a-GAL4 (41728); UAS-TNT-E (28837); UAS-CD8-GFP 3rd chr. (32185); UAS-CD8-GFP 2nd chr. (32186); UAS-CD8-RFP, LexAop-CD8-GFP (32229); UAS-GCaMP6s 2nd chr (42746); UAS-GCaMP6s 3rd chr (42749);

UAS-GCaMP8s (92594); 15D05-GAL4 (48686); 17A11-GAL4 (48752); 20G03-GAL4 (48907); 24D12-GAL4 (49080); 25F11-GAL4 (49133); 37A08-GAL4 (49946); 38B05-GAL4 (49985); 44F09-GAL4 (50215); 70C02-GAL4 (39521); 15D05-Gla4.DBD (69218); R15D05-GAL4.AD (70556); R17A11-GAL4.DBD (68924); R20C05-GAL4.AD (70905); R20C10-GAL4.AD (70491); R20G03-GAL4.AD (70109); R20G03-GAL4.DBD (69047); R24D12-GAL4.AD (75677); R24D12-GAL4.DBD (68750); R25F11-GAL4.AD (70623); R25F11-GAL4.DBD (69578); R37A08-GAL4.AD (71028); R38B05-GAL4.DBD (69200); R44F09-GAL4.AD (71061); R70B03-GAL4.DBD (75656); R70C02-GAL4.DBD (69783); R84D10-GAL4.AD (70834).

Transgenic fly production

57F03-LexA-DBD, 57F03-GAL4-DBD, and 83F01-GAL4-AD were generated in this study using Gateway recombination cloning. The 83F01 enhancer fragment was obtained from Dr. Gerry Rubin (HHMI Janelia) in a Gateway donor vector[64]. 57F03 enhancer is the same enhancer used to generate 57F03-GAL80 and 57F03-LexA(Yapici et al., 2016). We used the following Gateway destination vectors: ZpLexADBD_pBGUw (provided by Dr. Barry Dickson, Queensland Brain Institute), pBPZpGAL4DBDUw (Addgene plasmid #26233), pBPp65ADZpUw (Addgene plasmid #26234). The Transgenic fly lines were generated with the phiC31-based integration system[65] (Best Gene Inc). The 57F03-GAL4-DBD and 57F03-LexA-DBD transgenes were inserted into the attP2 genomic locus, and the 83F01-GAL4-AD transgene was inserted into the VK00005 genomic locus.

Immunohistochemistry and confocal microscopy

All brains, ventral nerve cords, and guts were dissected in 1x phosphate-buffered saline (PBS, diluted from 10 × PBS listed in the resource table). The samples were then stained as previously

described(Yapici et al., 2016). Briefly, immediately after dissection, samples were transferred to a 1.5mL centrifuge tube filled with ~200ul of 1xPBS using a pipette. After all sample collection was completed, the 1xPBS was removed from the centrifuge tube, and samples were incubated in 4% paraformaldehyde (PFA, Electron Microscopy Sciences, Cat# 15711) on an orbital shaker for 15 to 25 minutes. After tissue fixation, samples were washed with PBT for 4x15 minutes. For most immunohistochemistry experiments in this study, we used 0.1% PBT. However, for the experiment involving the VGLUT antibody, we used 0.2% PBT. Next, the samples were incubated with 5% Normal Goat Serum diluted in PBT (NGS-PBT) for approximately 30 minutes, followed by incubation with primary antibodies diluted in NGS-PBT for approximately 2-5 days at 4°C. After the primary antibody incubation, samples were washed with PBT for 5x15 minutes and incubated with secondary antibodies diluted in NGS-PBT for ~24 to 48 hours at 4°C. Once the antibody incubations were completed, samples were washed with PBT at room temperature for 4x15 minutes and incubated with Slowfade medium (ThermoFisher Scientific, Cat. # S36936) on an orbital shaker for ~30 minutes before getting mounted on a microscope slide. The samples were covered by a glass coverslip and sealed using clear nail polish (Clear Nail Polish, Electron Microscopy Sciences, Cat. # 72180). The following primary and secondary antibodies were used: chicken polyclonal anti-GFP, 1:3000 (Abcam Cat# ab13970), rabbit polyclonal anti-DsRed, 1:500 (Takara Bio, Cat# 632496), mouse monoclonal anti-Bruchpilot, 1:20 (DSHB, Cat# Nc82), rabbit anti-VGLUT, 1:500 (kindly provided by Dr. Dion Dickman), rat monoclonal anti-elav, 1:30 (DSHB, Cat# Rat-Elav-7E8A10), Phalloidin (Invitrogen, Cat#A30104), Alexa 546-conjugated goat anti-rabbit IgG, 1:1000 (Invitrogen, Cat# A11035), Cyanine5-conjugated goat anti-mouse IgG, 1:500 (Invitrogen, Cat# A10524), Alexa 633-conjugated goat anti-mouse IgG, 1:500 (Invitrogen, Cat# A-21052), Alexa 488-conjugated goat

anti-chicken IgG, 1:1000 (Invitrogen, Cat# A11039). Samples were mounted with Slowfade medium (ThermoFisher Scientific, Cat. # S36936). For Extended Data Figs. 2.2a-b, samples were collected and immediately embedded in an imaging medium (Tissue-Tek® O.C.T. Compound, Sakura) and sealed using a coverslip. All fluorescent images were taken using a Zeiss LSM880 upright confocal microscope and Zeiss digital image processing software ZEN. Z-stacks were acquired at 1024x1024-pixel resolution with a z-step size of 1 to 5 μm.

Fly preparation before two-photon imaging

For two-photon imaging coupled with optogenetics experiments, two-day-old male flies were fasted with or without ATR (All-*trans*-retinal, Sigma-Aldrich Cat#R2500, concentration = 0.5mM) in a vial containing Kimwipe soaked in 1ml MilliQ water. An aluminium foil was wrapped around the vial to protect the ATR from light exposure. The fasting duration and/or ATR treatment lasted 18 to 26 hours right before the imaging experiment. For two-photon imaging during food ingestion experiments, two-day-old male flies were fasted for 18-26 hours in a vial containing Kimwipe soaked in 1ml MilliQ water. To generate flies that are in a fed state, we transferred the previously fasted flies into a vial with ~1M sucrose with 0.02% (m/v, or 2g/l) brilliant blue (Sigma-Aldrich, Cat# 80717) dye 1-4 hours before the imaging experiment. Flies that showed a blue color in their abdomen were used in the two-photon imaging.

Fly mounting and dissection for calcium imaging in the brain

Flies were prepared as previously described (Yapici et al., 2016). A custom-made fly holder was used for all two-photon *in vivo* imaging experiments. On the day of the experiment, a male fly was anaesthetized briefly with CO_2 and tethered to a piece of transparent tape (Scotch® Transparent Tape) covering the hole in the fly holder. The fly head was secured using a human hair placed across the fly neck. We removed the tibia and tarsal segments of the forelegs during

imaging experiments that involved food delivery. For the optogenetic imaging experiments, the proboscis of the fly was fully extended by fine forceps (Dumont #5, FST, Cat#11254-20) and fixed using UV curable adhesive (Bondic®) in a fully extended position to minimize the movement during imaging. Next, a small hole was cut into the tape, precisely above the head, to allow the head capsule to extend above the plane of the tape. UV curable adhesive was applied to the fly's eyes and anterior and posterior parts of the head to restrict head movement. Once the fly's head was fixed, ~0.35ml of adult hemolymph-like (AHL) saline (108mM NaCl, 5mM KCl, 8.2mM $MgCl_2 \cdot 6H_2O$, 2mM $CaCl_2 \cdot 2H_2O$, 4mM $NaHCO_3$, 1mM $NaH_2PO_4 \cdot 2H_2O$, 5mM Trehalose$\cdot 2H_2O$, 10mM Sucrose, 5mM HEPES, pH adjusted to 7.5) was applied on top, and the head capsule was opened by carefully cutting the cuticle covering the dorsal-anterior porting of the fly head, including the antennae. Finally, we removed the obstructing air sacks and fat bodies using fine forceps to gain better optical access to the fly brain. The fly holder was then placed under the two-photon microscope for imaging.

Fly mounting and dissection for calcium imaging in the gastrointestinal tract

On the day of the experiment, a male fly was anaesthetized briefly with CO_2 and tethered to a piece of transparent tape (Scotch® Transparent Tape), covering the hole in the fly holder. The fly head and body were secured using human hair, one placed across the fly neck, the other onto the abdomen segment, between the midlegs and the hindlegs. The tibia and tarsal segments of the forelegs were then removed to avoid disruption of food delivery during imaging. Similar to brain imaging preparation, a small hole was cut into the tape, precisely above the head plus the thorax segment, to allow the head and the thorax segment to extend above the plane of the tape. UV curable adhesive (Bondic®) was then applied to seal the space between the fly's body and the transparent tape. We checked the ability of flies to extend their proboscis after the fixation to

ensure they can ingest food during imaging. Once the fly's head and thorax were fixed ~0.35ml of AHL saline (108mM NaCl, 5mM KCl, 8.2mM $MgCl_2 \cdot 6H_2O$, 2mM $CaCl_2 \cdot 2H_2O$, 4mM $NaHCO_3$, 1mM $NaH_2PO_4 \cdot 2H_2O$, 5mM Trehalose$\cdot 2H_2O$, 10mM Sucrose, 5mM HEPES, pH adjusted to 7.5) was applied on top of the thorax and the thorax cuticle, muscles, air sacks and fat bodies covering the hypocerebral ganglion were removed to gain optical access to the enteric neurons. The fly holder was then placed under the two-photon microscope for imaging.

Two-photon imaging

All functional imaging experiments were performed using a resonant scanning two-photon microscope (Bergamo II, Thorlabs) equipped with a 16X Plan Fluor Objective (Nikon, N16XLWD-PF) and GaAsP detectors (Hamamatsu). We used ThorImage software (Thorlabs, v4.0.2020.2171) to control the microscope. Two-photon excitation was provided by a Chameleon Ti: Sapphire femtosecond pulsed laser with pre-compensation (Vision II, Coherent) centred at 920 nm. The laser was directed through a resonant scanning galvanometer for fast-scanning volumetric imaging, and a piezo-electric Z-focus controlled the objective. Laser power was measured using a power meter (PM100D with S175C, Thorlabs). Laser power after the objective ranged between ~25-35 mW for brain imaging and ~10-60 mW for enteric imaging. Before the functional imaging trials, we took a whole-brain z-stack to ensure Chrimson-tomato and/or GCaMP6s proteins were adequately expressed in the brain or the enteric neurons. We then focused on the selected region of interest (ROI) and recorded 4-minute (for all trials with optogenetics stimulation) or 8-minute (for all trials without optogenetics stimulation) volumetric time-lapse GCaMP6s, GCaMP8s or fluorescein fluorescence. The starting and ending z-position of the volumetric imaging is determined to cover the whole region of interest. The details of the fast volumetric scanning can be found in the table below:

ROI	z-planes	Scan rate (Hz)	Step size (µm)	Resolution (pixel)	Figure
IN1 projections	8	4.63	10	256×256	Fig. 2.1,2, Extended Data Fig. 2.4
Gr43a cell bodies	8-10	3.95-4.63	10	256×256	Fig. 2.3
EN cell bodies	10	3.95	10	256×256	Fig. 2.4
CEM projections	8-10	3.95-4.56	10-15	256×256	Fig. 2.5
Fluorescent food ingestion	10	2.02-2.03	20	512×512	Fig. 2.6, Extended Data Fig. 2.10

We used an infrared light (JC Infrared Illuminator) and a FLIR Blackfly-S (BFS-U3-16S2M) equipped with a zoom lens (MLM3X-MP, 0.3X-1X, 1:4.5; Computar) and a Near-Infrared bandpass filter (BP810-34, Midwest Optical Systems, INC.) inside the imaging chamber to record the motion of the fly during imaging experiments (Software: SpinView, Spinnaker v. 2.0.0.147, FLIR Systems, Inc.). The video (30 fps) and the two-photon imaging data acquired by ThorImage were synchronized using GPIO connections. The ThorImage and LED optogenetic stimulation were synchronized using ThorSync software (Thorlabs, version 4.1.2020.1131). In the optogenetics calcium imaging trials that do not involve food ingestion, a spherical treadmill supported by an air pump was placed below the fly to minimize stress during imaging. In the imaging trials that involved food ingestion, the ball was removed to generate space for the food delivery device. At the end of each imaging experiment, we assessed the flies' health condition by mechanical stimulation of the leg using forceps. The data collected from flies that did not respond to the mechanical stimulus were excluded from the final data analysis because we considered those flies unhealthy. Furthermore, imaging data from flies that showed substantial

movement in the Z-direction were also discarded on rare occasions because of the severe motion artefacts in the calcium trace.

Optogenetic stimulation during two-photon imaging

Optogenetic stimulation was generated using a 617nm LED, which is integrated into the light path of the two-photon microscope and delivered to the fly brain via the objective. LED light intensity (~0.75mW) was measured after the objective by an optical power meter (PM100D, Thorlabs) equipped with a light intensity sensor (S175, Thorlabs). A long-pass filter (FELH0600, Thorlabs) was used to reduce the background elevation caused by 617nm-LED light during optogenetic stimulation. All optogenetic activation experiments started with ~30s scanning without stimulation to capture baseline GCaMP fluorescence. Next, LED light stimulation was continuously delivered to the fly brain for 1s or 10s. The stimulation was repeated five times at 30s intervals. For the optogenetic stimulation during fluorescent food ingestion (Fig. 2.6f-h), a continuous 30s long optogenetic stimulation was applied at around t=31-61s of the four-minute two-photon imaging trial.

Sugar ingestion in tethered flies

The sucrose solution was prepared by dissolving sucrose (Sigma-Aldrich, Cat# 9378) in MilliQ water. For high-concentration sucrose solution (~1M), 0.34g sucrose was dissolved in 1 ml MilliQ water. For low-concentration sucrose solution food (~100mM), 0.017g sucrose was dissolved in 500µl MilliQ water. In all ingestion experiments with two-photon imaging, except for fluorescent food ingestion, Brilliant Blue (2 g/l) (Sigma-Aldrich, Cat# 80717) was added to the high- or low-concentration sucrose solution. This allowed us to confirm ingestion episodes by inspecting the blue dye presence in the fly gut after the experiments. In fluorescent food ingestion imaging experiments, fluorescein (0.5 g/l) (Dextran Fluorescein, Thermo Fisher, Cat#

D1823) was added to the high- or low-concentration sucrose solution. The sucrose solution was presented to the fly using a pulled glass capillary attached to a microinjector (Drummond Nanoject II Auto, CAT # 3-000-204) to deliver the sucrose solution in precise volumes. To prevent the sucrose solution from wicking down the sides of the capillary, we applied dental wax to the exterior of the glass capillary. We used a micromanipulator to control the Nanojet and the capillary's movement during imaging (Siskiyou, Micromanipulator Controller Mc1000e). The sugar stimulation was present in discrete durations during imaging experiments unless otherwise stated.

Data processing and analysis

Confocal image processing

Confocal images were processed using the FIJI open-source image-processing package (https://imagej.net/software/fiji/) or Imaris (Oxford Instruments, Imaris x64, version 9.9.0). All confocal images shown in this paper, except for the cross-section images in Figs. 2.3i, Fig. 2.4f, and Extended Data Fig. 2.3k, are z-projections of the confocal image stacks. Confocal image stacks of the fly gastrointestinal tract in Figs. 2.3i, Fig. 2.4f, and Extended Data Fig. 2.3k were processed using Imaris to generate the cross-section images in X, Y, and Z directions.

Two-photon functional imaging data processing

All two-photon imaging data processing was completed using custom-made code written in (version R2022b). Two-photon volumetric image frames were projected along the z-axis for each trial and then aligned by translating each frame in the x and y plane using the MATLAB register function. Registration results were manually inspected to avoid the artifacts produced by the movement of ROI as much as possible. If the registration result from MATLAB were not ideal, image stacks were registered for the second round using TurboReg

(https://bigwww.epfl.ch/thevenaz/turboreg) or manually using FIJI (https://imagej.net/software/fiji/). Image stacks that failed the registration process were discarded. Region of interest (ROI) selection was achieved by manually drawing one or multiple mask(s) surrounding the cell bodies or the neuronal projections using MATLAB freehand function. The ROI masks were applied to all z-projected frames, and the average grey value within each ROI was extracted from each frame to generate a time series.

Two photon imaging	**ROI**	**Figure**
IN1	Projections in left or right hemisphere	Fig. 2.1,2, Extended Data Fig. 2.4
Gr43a	Cell bodies	Fig. 2.3
ENs	Cell bodies	Fig. 2.4
CEM	Projections in the gut	Fig. 2.5
Fluorescent food ingestion	Crop duct or oesophagus	Fig. 2.6, Extended Data Fig. 2.10

Optogenetic stimulation trials (Fig. 2.1c-g, Fig. 2.2 a-f, Fig. 2.5d-e, Extended Data Fig. 2.4a-o): During optogenetic stimulation, the LED light induced a slight background elevation observable in the imaging data. This background elevation served as an indicator of stimulation ON and OFF times during data processing. Background subtraction was applied to each imaging frame during data processing to eliminate this noise. To calculate $\Delta F/F_0$ during optogenetic stimulation trials, the fluorescent time series was first chopped into five segments corresponding to the five stimulation episodes. For 1s-stimulation trials, each imaging segment consists of the time +/- 7s pre- and post-stimulation. For 10s-stimulation trials, each imaging segment consists of the time +/- 10s pre- and post-stimulation. To calculate the $\Delta F/F_0$, we first subtracted the background fluorescence value from the ROI fluorescence value for each frame. Next, the baseline fluorescence F_0 was calculated by averaging the fluorescent intensities from 5s (t=-6 to -1 seconds) before the stimulation onset (t=0). Finally, $\Delta F/F_0$ was calculated using the following

formula: $\frac{\Delta F}{F0} = \frac{Ft - F0}{F0}$. (**F0**=fluorescence at baseline, **Ft**=fluorescence at time t). The resulting time series was binned into 0.25s time bins and plotted as ± SEM $\Delta F/F_0$. We averaged the $\Delta F/F_0$ across all trials to calculate the average and SEM.

Sucrose ingestion trials. (Fig. 2.3d, e, Fig. 2.4d, Fig. 2.5f, Fig. 2.6b, d): To calculate $\Delta F/F_0$ during sucrose ingestion trials, ROI fluorescent intensities recorded from +/- 50s pre- and post-ingestion were used unless otherwise stated. Background subtraction was not applied to the fluorescent time series data in these trials. Baseline fluorescence F_0 was calculated by averaging the fluorescent intensities from 10s (t=-10s to 0s) before the ingestion onset. $\Delta F/F_0$ was calculated using the same formula as in the optogenetic stimulation experiments. For EN cell body imaging (Fig. 2.4d), if an imaging trial contained multiple ROIs corresponding to multiple cell bodies, to generate the averaged $\Delta F/F_0$ plot, $\Delta F/F_0$ traces from all ROIs were first averaged within a fly and then averaged across flies. For Gr43a cell body imaging (Fig. 2.3d, e), ROI fluorescent intensities recorded from +/- 30s pre- and post-ingestion were used. In these imaging experiments, we noticed not all Gr43a neurons responded to sucrose ingestion. Only neurons that were activated by sucrose were used in the data analysis. A Gr43a neuron was classified as responsive if the peak $\Delta F/F_0$ signal was 3x greater than the $\Delta F/F_0$ standard deviation above baseline.

Optogenetic stimulation and ingestion (Fig. 2.6g-j): For combined imaging trials with optogenetic stimulation and ingestion, ROI fluorescent intensities recorded from +/- 5s pre- and post-ingestion were used. $\Delta F/F_0$ was calculated following the same steps as for optogenetic stimulation imaging trials, with the F_0 time window set from 3 seconds (t=-3 to 0 seconds) before ingestion onset. Background subtraction was applied to each imaging frame during processing.

Peak $\Delta F/F_0$ (or peak food fluorescence) calculations. Throughout this study, peak $\Delta F/F_0$ is defined as the maximum or minimum value of $\Delta F/F_0$ within a specified time window. Time windows for peak $\Delta F/F_0$ (or peak food fluorescence) calculations are as follows: in Fig. 2.1h and Fig. 2.4b, 0 to 4 seconds after optogenetic stimulation onset; in Fig. 2.3f, the duration of the ingestion bout; in Fig. 2.5g, 0 to 50 seconds after ingestion onset; in Fig. 2.6e and Extended Data Fig. 2.10e, the duration of the ingestion bout; in Fig. 2.6h, j, 0 to 5 seconds after ingestion onset. We plotted the average peak $\Delta F/F_0$ (or peak food fluorescence) and used GraphPad Prism for statistical comparisons.

Persistence calculations. Persistence in Fig. 2.3g, Fig. 2.6c, and Extended Data Fig. 2.10c is the total duration at half maximum (FDHM), calculated as the duration between the points where the peak $\Delta F/F_0$ is half its maximum value. Persistence in Fig. 2.5h is calculated as the total duration where the $\Delta F/F_0$ is lower than half its minimum value after ingestion onset (t=0-10s). We plotted the average peak $\Delta F/F_0$ (or peak food fluorescence) and $\Delta F/F_0$ persistence and used GraphPad Prism for statistical comparisons. We plotted the average persistence and used GraphPad Prism for statistical comparisons.

Data exclusion

Flies that appeared in poor health after imaging and/or had low-quality image data due to motion artifacts or other reasons were excluded from data analysis. These were less than 4% of the flies used in the entire study.

EM analysis

We used the Flywire open-source platform to identify and classify the putative IN1 neurons(Dorkenwald et al., 2023). We first identified putative IN1s based on light microscopy data, projection patterns, and cell body locations. To plot the putative IN1s in a standard brain

mesh, we used the natverse package in R-studio (version R4.3.3), a toolbox for combining and analyzing neuroanatomical data(Bates et al., 2020). Natverse consists of multiple R-packages that allow the analysis of light microscopy and EM datasets across various model organisms, including *Drosophila melanogaster*. We mainly used the R "fafbseg" package to access and analyse the Flywire datasets. Details of the "fafbseg" package can be found at https://natverse.org/fafbseg/. First, we downloaded neuron meshes for each putative IN1 neuron from Flywire into the R environment and visualized them in 3D using the FAFB14 standard brain mesh. Next, we used Flywire to automatically detect synaptic sites across putative IN1 neurons (n=4) and generated the connectivity matrix across IN1 neurons using Codex (Connectome Data Explorer: codex.flywire.ai)(Lin et al., 2024). We also used Codex to identify the input and output neurons of IN1s. The neuron meshes of the IN1 outputs and inputs, as well as the candidate IN1 interacting neurons, such as sugar, bitter GRNs, second and third-order taste neurons, and taste motor neurons, were downloaded from Flywire into the R environment and visualized in 3D using the FAFB14 standard brain mesh. The connectivity heatmaps for these neurons were generated from the data in Pathway analysis in Codex using a costume MATLAB script. The MATLAB script is available at https://github.com/Nilayyapici/Cui_et_al.

Statistical tests

Sample sizes used in this study were based on previous literature in the field. Experimenters were not blinded in most conditions, as almost all data analyses were automated and done using a standardized computer code. All statistical analyses were performed using Prism Software (GraphPad, Version 10.1.1). One-way ANOVA with Bonferroni post hoc multiple comparisons (for data that are mainly normally distributed) or non-parametric Kruskal-Wallis test with Dunn's post hoc multiple comparisons (for data that are not normally distributed) were used to

compare more than two genotypes or conditions (for details, see the legends of each figure). The paired or unpaired t-test (two-tailed) with Welch's correction was used to compare two genotypes or conditions. Data labeled with different letters are statistically different.

Detailed statistic test information for each figure is listed in the table below:

Figure	**Statistic Test**	**F**	**P Value**	**Kruskal-Wallis statistic**
Fig. 2.1h	One-way ANOVA	7.359	<0.0001	N/A
Fig. 2.3f	One-way ANOVA	0.2179	0.8083	N/A
Fig. 2.3g	One-way ANOVA	4.998	0.0347	N/A
Fig. 2.4b	Kruskal-Wallis test	N/A	<0.0001	143.6
Fig. 2.5g	One-way ANOVA	1.62	0.2353	N/A
Fig. 2.5h	One-way ANOVA	11.41	0.001	N/A
Fig. 2.6c	Unpaired t test with Welch's correction	N/A	0.0125	N/A
Fig. 2.6e	One-way ANOVA	14.44	<.001	N/A
Fig. 2.6h	Paired t test	N/A	0.0328	N/A
Fig. 2.6j	Paired t test	N/A	0.1723	N/A
Extended Data Fig. 2. 10c	Unpaired t test with Welch's correction	N/A	0.1836	N/A
Extended Data Fig. 2. 10e	One-way ANOVA	0.2506	0.7827	N/A

REFERENCES

Bai, L., Mesgarzadeh, S., Ramesh, K. S., Huey, E. L., Liu, Y., Gray, L. A., Aitken, T. J., Chen, Y., Beutler, L. R., Ahn, J. S., Madisen, L., Zeng, H., Krasnow, M. A., & Knight, Z. A. (2019). Genetic identification of vagal sensory neurons that control feeding. *Cell*, *179*(5), 1129-1143 e1123. https://doi.org/10.1016/j.cell.2019.10.031

Bates, A. S., Manton, J. D., Jagannathan, S. R., Costa, M., Schlegel, P., Rohlfing, T., & Jefferis, G. S. (2020). The natverse, a versatile toolbox for combining and analysing neuroanatomical data. *eLife*, *9:e53350*. https://doi.org/10.7554/eLife.53350

Borgmann, D., Ciglieri, E., Biglari, N., Brandt, C., Cremer, A. L., Backes, H., Tittgemeyer, M., Wunderlich, F. T., Bruning, J. C., & Fenselau, H. (2021). Gut-brain communication by distinct sensory neurons differently controls feeding and glucose metabolism. *Cell Metab*, *33*(7), 1466-1482 e1467. https://doi.org/10.1016/j.cmet.2021.05.002

Buhmann, J., Sheridan, A., Malin-Mayor, C., Schlegel, P., Gerhard, S., Kazimiers, T., Krause, R., Nguyen, T. M., Heinrich, L., Lee, W. A., Wilson, R., Saalfeld, S., Jefferis, G., Bock, D. D., Turaga, S. C., Cook, M., & Funke, J. (2021). Automatic detection of synaptic partners in a whole-brain Drosophila electron microscopy data set. *Nat Methods*, *18*(7), 771-774. https://doi.org/10.1038/s41592-021-01183-7

Burneo, J. G., Faught, E., Knowlton, R., Morawetz, R., & Kuzniecky, R. (2002). Weight loss associated with vagus nerve stimulation. *Neurology*, *59*(3), 463-464. https://doi.org/10.1212/wnl.59.3.463

Cameron, P., Hiroi, M., Ngai, J., & Scott, K. (2010). The molecular basis for water taste in Drosophila. *Nature*, *465*(7294), 91-95. https://doi.org/10.1038/nature09011

Chen, J., Cheng, M., Wang, L., Zhang, L., Xu, D., Cao, P., Wang, F., Herzog, H., Song, S., & Zhan, C. (2020). A Vagal-NTS Neural Pathway that Stimulates Feeding. *Curr Biol*, *30*(20), 3986-3998 e3985. https://doi.org/10.1016/j.cub.2020.07.084

Chen, T. W., Wardill, T. J., Sun, Y., Pulver, S. R., Renninger, S. L., Baohan, A., Schreiter, E. R., Kerr, R. A., Orger, M. B., Jayaraman, V., Looger, L. L., Svoboda, K., & Kim, D. S. (2013). Ultrasensitive fluorescent proteins for imaging neuronal activity. *Nature*, *499*(7458), 295-300. https://doi.org/10.1038/nature12354

Chen, Y. D., & Dahanukar, A. (2017). Molecular and Cellular Organization of Taste Neurons in Adult Drosophila Pharynx. *Cell Rep*, *21*(10), 2978-2991. https://doi.org/10.1016/j.celrep.2017.11.041

Chyb, S., Dahanukar, A., Wickens, A., & Carlson, J. R. (2003). Drosophila Gr5a encodes a taste receptor tuned to trehalose. *Proc Natl Acad Sci USA*(100), 14526-14530. https://doi.org/10.1073/pnas.2135339100

Cognigni, P., Bailey, A. P., & Miguel-Aliaga, I. (2011). Enteric neurons and systemic signals couple nutritional and reproductive status with intestinal homeostasis. *Cell Metabolism*, *13*(1), 92-104. https://doi.org/10.1016/j.cmet.2010.12.010

Cui, X., Gruzdeva, A., Kim, H., & Yapici, N. (2022). Of flies, mice and neural control of food intake: lessons to learn from both models. In *Current Opinion in Neurobiology* (Vol. 73): Elsevier Ltd.

Dahanukar, A., Lei, Y. T., Kwon, J. Y., & Carlson, J. R. (2007). Two Gr genes underlie sugar reception in Drosophila. *Neuron*, *56*(3), 503-516. https://doi.org/10.1016/j.neuron.2007.10.024

Dethier, V. G. (1976). *The hungry fly: a physiological study of the behavior associated with feeding*. Harvard University Press

Dorkenwald, S., Matsliah, A., Sterling, A. R., Schlegel, P., Yu, S. C., McKellar, C. E., Lin, A., Costa, M., Eichler, K., Yin, Y., Silversmith, W., Schneider-Mizell, C., Jordan, C. S., Brittain, D., Halageri, A., Kuehner, K., Ogedengbe, O., Morey, R., Gager, J., . . . Murthy, M. (2023). Neuronal wiring diagram of an adult brain. *bioRxiv*. https://doi.org/10.1101/2023.06.27.546656

Dorkenwald, S., McKellar, C. E., Macrina, T., Kemnitz, N., Lee, K., Lu, R., Wu, J., Popovych, S., Mitchell, E., Nehoran, B., Jia, Z., Bae, J. A., Mu, S., Ih, D., Castro, M., Ogedengbe, O., Halageri, A., Kuehner, K., Sterling, A. R., . . . Seung, H. S. (2022). FlyWire: online community for whole-brain connectomics. *Nat Methods*, *19*(1), 119-128. https://doi.org/10.1038/s41592-021-01330-0

Dus, M., Lai, J. S. Y., Gunapala, K. M., Min, S., Tayler, T. D., Hergarden, A. C., Geraud, E., Joseph, C. M., & Suh, G. S. B. (2015). Nutrient sensor in the brain directs the action of the brain-gut axis in Drosophila. *Neuron*, *87*(1), 139-151. https://doi.org/10.1016/j.neuron.2015.05.032

Eckstein, N., Bates, A. S., Champion, A., Du, M., Yin, Y., Schlegel, P., Lu, A. K., Rymer, T., Finley-May, S., Paterson, T., Parekh, R., Dorkenwald, S., Matsliah, A., Yu, S. C., McKellar, C., Sterling, A., Eichler, K., Costa, M., Seung, S., . . . Funke, J. (2024). Neurotransmitter classification from electron microscopy images at synaptic sites in Drosophila melanogaster. *Cell*, *187*(10), 2574-2594.e2523. https://doi.org/10.1016/j.cell.2024.03.016

Engert, S., Sterne, G. R., Bock, D. D., & Scott, K. (2022). Drosophila gustatory projections are segregated by taste modality and connectivity. *eLife*, *11:e78110*. https://doi.org/10.7554/eLife.78110

Friend, W. (1981). Diet destination in Culiseta inornata (Williston): effect of feeding conditions on the response to ATP and sucrose. *Annals of the Entomological Society of America*, *74*(1), 151-154.

Fujii, S., Yavuz, A., Slone, J., Jagge, C., Song, X., & Amrein, H. (2015). Drosophila sugar receptors in sweet taste perception, olfaction, and internal nutrient sensing. *Curr Biol*, *25*(5), 621-627. https://doi.org/10.1016/j.cub.2014.12.058

Hadjieconomou, D., King, G., Gaspar, P., Mineo, A., Blackie, L., Ameku, T., Studd, C., de Mendoza, A., Diao, F., White, B. H., Brown, A. E. X., Plaçais, P. Y., Préat, T., & Miguel-Aliaga, I. (2020). Enteric neurons increase maternal food intake during reproduction. *Nature*, *587*(7834), 455-459. https://doi.org/10.1038/s41586-020-2866-8

Han, W., Tellez, L. A., Perkins, M. H., Perez, I. O., Qu, T., Ferreira, J., Ferreira, T. L., Quinn, D., Liu, Z. W., Gao, X. B., Kaelberer, M. M., Bohorquez, D. V., Shammah-Lagnado, S. J., de Lartigue, G., & de Araujo, I. E. (2018). A Neural Circuit for Gut-Induced Reward. *Cell*, *175*(3), 887-888. https://doi.org/10.1016/j.cell.2018.10.018

Hoopfer, E. D., Jung, Y., Inagaki, H. K., Rubin, G. M., & Anderson, D. J. (2015). P1 interneurons promote a persistent internal state that enhances inter-male aggression in Drosophila. *eLife*, *4:e11346*. https://doi.org/10.7554/eLife.11346

Jiao, Y., Moon, S. J., Wang, X., Ren, Q., & Montell, C. (2008). Gr64f is required in combination with other gustatory receptors for sugar detection in Drosophila. *Curr Biol*, *18*(22), 1797-1801. https://doi.org/10.1016/j.cub.2008.10.009

Kaelberer, M. M., Buchanan, K. L., Klein, M. E., Barth, B. B., Montoya, M. M., Shen, X., & Bohórquez, D. V. (2018). A gut-brain neural circuit for nutrient sensory transduction. *Science*, *361*(6408), eaat5236. https://doi.org/doi:10.1126/science.aat5236

Kitamoto, T. (2002). Conditional disruption of synaptic transmission induces male-male courtship behavior in Drosophila. *Proc Natl Acad Sci U S A*, *99*(20), 13232-13237. https://doi.org/10.1073/pnas.202489099

Klapoetke, N. C., Murata, Y., Kim, S. S., Pulver, S. R., Birdsey-Benson, A., Cho, Y. K., Morimoto, T. K., Chuong, A. S., Carpenter, E. J., Tian, Z., Wang, J., Xie, Y., Yan, Z., Zhang, Y., Chow, B. Y., Surek, B., Melkonian, M., Jayaraman, V., Constantine-Paton, M., . . . Boyden, E. S. (2014). Independent optical excitation of distinct neural populations. *Nat Methods*, *11*(3), 338-346. https://doi.org/10.1038/nmeth.2836

Kral, J. G. (1978). Vagotomy for treatment of severe obesity. *Lancet*, *1*(8059), 307-308. https://doi.org/10.1016/s0140-6736(78)90074-0

LeDue, E. E., Chen, Y. C., Jung, A. Y., Dahanukar, A., & Gordon, M. D. (2015). Pharyngeal sense organs drive robust sugar consumption in Drosophila. *Nat Commun*, *6*, 6667. https://doi.org/10.1038/ncomms7667

Lee, Y., Kim, S. H., & Montell, C. (2010). Avoiding DEET through insect gustatory receptors. *Neuron*, *67*(4), 555-561. https://doi.org/10.1016/j.neuron.2010.07.006

Li, M., Tan, H. E., Lu, Z., Tsang, K. S., Chung, A. J., & Zuker, C. S. (2022). Gut-brain circuits for fat preference. *Nature*, *610*(7933), 722-730. https://doi.org/10.1038/s41586-022-05266-z

Li, P. H., Lindsey, L. F., Januszewski, M., Tyka, M., Maitin-Shepard, J., Blakely, T., & Jain, V. (2019). Automated reconstruction of a serial-section EM Drosophila brain with flood-filling networks and local realignment. *Microscopy and Microanalysis*, *25*(S2), 1364-1365.

Lin, A., Yang, R., Dorkenwald, S., Matsliah, A., Sterling, A. R., Schlegel, P., Yu, S.-c., McKellar, C. E., Costa, M., Eichler, K., Bates, A. S., Eckstein, N., Funke, J., Jefferis, G. S. X. E., & Murthy, M. (2024). Network statistics of the whole-brain connectome of Drosophila. *bioRxiv*. https://doi.org/10.1101/2023.07.29.551086

Lowenstein, E. D., Ruffault, P. L., Misios, A., Osman, K. L., Li, H., Greenberg, R. S., Thompson, R., Song, K., Dietrich, S., Li, X., Vladimirov, N., Woehler, A., Brunet, J. F., Zampieri, N., Kuhn, R., Liberles, S. D., Jia, S., Lewin, G. R., Rajewsky, N., . . . Birchmeier, C. (2023). Prox2 and Runx3 vagal sensory neurons regulate esophageal motility. *Neuron*, *111*(14), 2184-2200 e2187. https://doi.org/10.1016/j.neuron.2023.04.025

Luan, H., Peabody, N. C., Vinson, C. R., & White, B. H. (2006). Refined spatial manipulation of neuronal function by combinatorial restriction of transgene expression. *Neuron*, *52*(3), 425-436. https://doi.org/10.1016/j.neuron.2006.08.028

Ma, D., Hu, M., Yang, X., Liu, Q., Ye, F., Cai, W., Wang, Y., Xu, X., Chang, S., Wang, R., Yang, W., Ye, S., Su, N., Fan, M., Xu, H., & Guo, J. (2024). Structural basis for sugar perception by Drosophila gustatory receptors. *Science*, *383*(6685), eadj2609. https://doi.org/10.1126/science.adj2609

Mabuchi, Y., Cui, X., Xie, L., Kim, H., Jiang, T., & Yapici, N. (2023). Visual feedback neurons fine-tune Drosophila male courtship via GABA-mediated inhibition. *Curr Biol*, *33*(18), 3896-3910.e3897. https://doi.org/10.1016/j.cub.2023.08.034

Manzo, A., Silies, M., Gohl, D. M., & Scott, K. (2012). Motor neurons controlling fluid ingestion in Drosophila. *Proc Natl Acad Sci U S A*, *109*(16), 6307-6312. https://doi.org/10.1073/pnas.1120305109

McDougle, M., de Araujo, A., Singh, A., Yang, M., Braga, I., Paille, V., Mendez-Hernandez, R., Vergara, M., Woodie, L. N., Gour, A., Sharma, A., Urs, N., Warren, B., & de Lartigue, G. (2024). Separate gut-brain circuits for fat and sugar reinforcement combine to promote overeating. *Cell Metab*. https://doi.org/10.1016/j.cmet.2023.12.014

Miguel-Aliaga, I., Jasper, H., & Lemaitre, B. (2018). Anatomy and physiology of the digestive tract of Drosophila melanogaster. *Genetics*, *210*(2), 357-396. https://doi.org/10.1534/genetics.118.300224

Min, S., Oh, Y., Verma, P., Whitehead, S. C., Yapici, N., Van Vactor, D., Suh, G. S. B., & Liberles, S. D. (2021). Control of feeding by piezo-mediated gut mechanosensation in Drosophila. *eLife, 10:e63049*. https://doi.org/10.7554/eLife.63049

Miyamoto, T., & Amrein, H. (2014). Diverse roles for the Drosophila fructose sensor Gr43a. *Fly*, *8*(1), 19-25. https://doi.org/10.4161/fly.27241

Miyamoto, T., Slone, J., Song, X., & Amrein, H. (2012). A fructose receptor functions as a nutrient sensor in the drosophila brain. *Cell*, *151*(5), 1113-1125. https://doi.org/10.1016/j.cell.2012.10.024

Moon, S. J., Kottgen, M., Jiao, Y., Xu, H., & Montell, C. (2006). A taste receptor required for the caffeine response in vivo. *Curr Biol*, *16*(18), 1812-1817. https://doi.org/10.1016/j.cub.2006.07.024

Munch, D., Goldschmidt, D., & Ribeiro, C. (2022). The neuronal logic of how internal states control food choice. *Nature*, *607*(7920), 747-755. https://doi.org/10.1038/s41586-022-04909-5

Naslund, E., & Hellstrom, P. M. (2007). Appetite signaling: from gut peptides and enteric nerves to brain. *Physiol Behav*, *92*(1-2), 256-262. https://doi.org/10.1016/j.physbeh.2007.05.017

Oh, Y., Lai, J. S., Min, S., Huang, H. W., Liberles, S. D., Ryoo, H. D., & Suh, G. S. B. (2021). Periphery signals generated by piezo-mediated stomach stretch and neuromedin-mediated glucose load regulate the Drosophila brain nutrient sensor. *Neuron*, *109*(12), 1979-1995.e1976. https://doi.org/10.1016/j.neuron.2021.04.028

Pauls, D., Blechschmidt, C., Frantzmann, F., el Jundi, B., & Selcho, M. (2018). A comprehensive anatomical map of the peripheral octopaminergic/tyraminergic system of. *Scientific Reports*, *8*. https://doi.org/ARTN 15314
10.1038/s41598-018-33686-3

Pfeiffer, B. D., Ngo, T.-T. B., Hibbard, K. L., Murphy, C., Jenett, A., Truman, J. W., & Rubin, G. M. (2010). Refinement of tools for targeted gene expression in Drosophila. *Genetics*, *186*(2), 735-755. https://doi.org/10.1534/genetics.110.119917

Prescott, S. L., & Liberles, S. D. (2022). Internal senses of the vagus nerve. *Neuron*, *110*(4), 579-599. https://doi.org/10.1016/j.neuron.2021.12.020

Puizillout, J.-J. (2005). *Central projections of vagal afferents*. Editions Publibook.

Ran, C., Boettcher, J. C., Kaye, J. A., Gallori, C. E., & Liberles, S. D. (2022). A brainstem map for visceral sensations. *Nature*, *609*(7926), 320-326. https://doi.org/10.1038/s41586-022-05139-5

Schlegel, P., Yin, Y., Bates, A. S., Dorkenwald, S., Eichler, K., Brooks, P., Han, D. S., Gkantia, M., Dos Santos, M., Munnelly, E. J., Badalamente, G., Capdevila, L. S., Sane, V. A., Pleijzier, M. W., Tamimi, I. F. M., Dunne, C. R., Salgarella, I., Javier, A., Fang, S., . . . Jefferis, G. (2023). Whole-brain annotation and multi-connectome cell typing quantifies circuit stereotypy in Drosophila. *bioRxiv*. https://doi.org/10.1101/2023.06.27.546055

Shiu, P. K., Sterne, G. R., Engert, S., Dickson, B. J., & Scott, K. (2022). Taste quality and hunger interactions in a feeding sensorimotor circuit. *eLife*, *11:e79887*. https://doi.org/10.7554/eLife.79887

Shiu, P. K., Sterne, G. R., Spiller, N., Franconville, R., Sandoval, A., Zhou, J., Simha, N., Kang, C. H., Yu, S., Kim, J. S., Dorkenwald, S., Matsliah, A., Schlegel, P., Yu, S.-c., McKellar,

C. E., Sterling, A., Costa, M., Eichler, K., Jefferis, G. S. X. E., . . . Scott, K. (2023). A leaky integrate-and-fire computational model based on the connectome of the entire adult Drosophila brain reveals insights into sensorimotor processing. *bioRxiv*, 2023.2005.2002.539144. https://doi.org/10.1101/2023.05.02.539144

Simpson, S. J., & Bernays, E. A. (1983). The regulation of feeding: locusts and blowflies are not so different from mammals. *Appetite*, *4*(4), 313-346. https://doi.org/10.1016/s0195-6663(83)80024-5

Slone, J., Daniels, J., & Amrein, H. (2007). Sugar receptors in Drosophila. *Curr Biol*, *17*(20), 1809-1816. https://doi.org/10.1016/j.cub.2007.09.027

Sterne, G. R., Otsuna, H., Dickson, B. J., & Scott, K. (2021). Classification and genetic targeting of cell types in the primary taste and premotor center of the adult Drosophila brain. *eLife*, *10:e71679*. https://doi.org/10.7554/eLife.71679

Stoffolano, J. G., & Haselton, A. T. (2013). The adult dipteran crop: A unique and overlooked organ. In *Annual Review of Entomology* (Vol. 58, pp. 205-225): Annual Reviews Inc.

Strother, J. A., Wu, S. T., Wong, A. M., Nern, A., Rogers, E. M., Le, J. Q., Rubin, G. M., & Reiser, M. B. (2017). The emergence of directional selectivity in the visual motion pathway of Drosophila. *Neuron*, *94*(1), 168-182.e110. https://doi.org/10.1016/j.neuron.2017.03.010

Sweeney, S. T., Broadie, K., Keane, J., Niemann, H., & O'Kane, C. J. (1995). Targeted expression of tetanus toxin light chain in Drosophila specifically eliminates synaptic transmission and causes behavioral defects. *Neuron*, *14*(2), 341-351. https://doi.org/10.1016/0896-6273(95)90290-2

Tan, H. E., Sisti, A. C., Jin, H., Vignovich, M., Villavicencio, M., Tsang, K. S., Goffer, Y., & Zuker, C. S. (2020). The gut-brain axis mediates sugar preference. *Nature*, *580*(7804), 511-516. https://doi.org/10.1038/s41586-020-2199-7

Tao, J., Campbell, J. N., Tsai, L. T., Wu, C., Liberles, S. D., & Lowell, B. B. (2021). Highly selective brain-to-gut communication via genetically defined vagus neurons. *Neuron*, *109*(13), 2106-2115 e2104. https://doi.org/10.1016/j.neuron.2021.05.004

Trembley, H. L. (1952). The distribution of certain liquids in the esophageal diverticula and stomach of mosquitoes. *Am J Trop Med Hyg*, *1*(4), 693-710. https://doi.org/10.4269/ajtmh.1952.1.693

Tuthill, J. C., & Wilson, R. I. (2016). Parallel Transformation of Tactile Signals in Central Circuits of Drosophila. *Cell*, *164*(5), 1046-1059. https://doi.org/10.1016/j.cell.2016.01.014

Uchizono, S., Itoh, T. Q., Kim, H., Hamada, N., Kwon, J. Y., & Tanimura, T. (2017). Deciphering the genes for taste receptors for fructose in Drosophila. *Mol Cells*, *40*(10), 731-736. https://doi.org/10.14348/molcells.2017.0016

Wang, P., Jia, Y., Liu, T., Jan, Y. N., & Zhang, W. (2020). Visceral mechano-sensing neurons control Drosophila feeding by using piezo as a sensor. *Neuron*, *108*(4), 640-650.e644. https://doi.org/10.1016/j.neuron.2020.08.017

Wang, Z., Singhvi, A., Kong, P., & Scott, K. (2004). Taste representations in the Drosophila brain. *Cell*, *117*(7), 981-991. https://doi.org/10.1016/j.cell.2004.06.011

Weiss, L. A., Dahanukar, A., Kwon, J. Y., Banerjee, D., & Carlson, J. R. (2011). The molecular and cellular basis of bitter taste in Drosophila. *Neuron*, *69*(2), 258-272. https://doi.org/10.1016/j.neuron.2011.01.001

Williams, E. K., Chang, R. B., Strochlic, D. E., Umans, B. D., Lowell, B. B., & Liberles, S. D. (2016). Sensory Neurons that Detect Stretch and Nutrients in the Digestive System. *Cell*, *166*(1), 209-221. https://doi.org/10.1016/j.cell.2016.05.011

Wu, S. F., Ja, Y. L., Zhang, Y. J., & Yang, C. H. (2019). Sweet neurons inhibit texture discrimination by signaling TMC-expressing mechanosensitive neurons in Drosophila. *eLife*, *8:e46165*. https://doi.org/10.7554/eLife.46165

Yapici, N., Cohn, R., Schusterreiter, C., Ruta, V., & Vosshall, L. B. (2016). A Taste Circuit that Regulates Ingestion by Integrating Food and Hunger Signals. *Cell*, *165*(3), 715-729. https://doi.org/10.1016/j.cell.2016.02.061

Yu, C. D., Xu, Q. J., & Chang, R. B. (2020). Vagal sensory neurons and gut-brain signaling. *Curr Opin Neurobiol*, *62*, 133-140. https://doi.org/10.1016/j.conb.2020.03.006

Zhang, Y. V., Aikin, T. J., Li, Z., & Montell, C. (2016). The Basis of Food Texture Sensation in Drosophila. *Neuron*, *91*(4), 863-877. https://doi.org/10.1016/j.neuron.2016.07.013

Zhao, Q., Yu, C. D., Wang, R., Xu, Q. J., Dai Pra, R., Zhang, L., & Chang, R. B. (2022). A multidimensional coding architecture of the vagal interoceptive system. *Nature*, *603*(7903), 878-884. https://doi.org/10.1038/s41586-022-04515-5

Zheng, Z., Lauritzen, J. S., Perlman, E., Robinson, C. G., Nichols, M., Milkie, D., Torrens, O., Price, J., Fisher, C. B., Sharifi, N., & others. (2018). A complete electron microscopy volume of the brain of adult Drosophila melanogaster. *Cell*, *174*(3), 730-743.

CHAPTER 3

Discussion

Feeding behavior is one of the most ancient animal behaviors, and the regulatory mechanisms governing it have remained foundational to neural system function and, therefore, remained highly evolutionarily conserved within the kingdom Animalia. Unlike in human societies, where food safety is less of a concern once food is properly cooked, animals in their natural environments must be highly selective about what they eat. Consuming food contaminated with pathogens such as toxins, parasites, or microbes can severely reduce their chances of survival and reproduction. Even without the risk of foodborne illness, animals that can efficiently choose and store more nutritious food are more likely to survive predation and achieve higher evolutionary fitness compared to others in their species. Therefore, animals must carefully and adaptively regulate their food preferences and consumption to maximize their fitness in challenging environments.

In this study, we have revealed how fruit flies can precisely regulate their food ingestion using a gut-brain-gut neural circuit. Through this circuit, flies can detect the food they ingested within the foregut lumen and relay this information to IN1s in the brain. After integrating information from enteric sensory neurons with various other inputs, including the flies' metabolic status, IN1 neurons inhibit the enteric motor neurons (CEM) neurons. Inhibition of CEM neurons causes relaxation of the crop duct muscles, allowing the food in the foregut to be transported into the crop for storage. This regulatory mechanism ensures precise control over the ingestion process, balancing the animal's nutritional needs with its physiological state.

In my thesis project, I developed a method to capture the activity of enteric neurons in flies during food ingestion, establishing a foundation for future research in this field. Additionally, we utilized the recently released electron microscopy-based full adult *Drosophila* brain connectome to significantly expedite our neural circuit mapping process. This approach serves as an example for future studies, demonstrating how similar techniques can greatly enhance the efficiency of neural circuit mapping. Biologically, our study demonstrated the importance of brain-gut communication in insects to maintain an adequate regulation of feeding behavior that is essential for their survival. The gut-brain circuit we have uncovered in *Drosophila* closely remarkably resembles mechanisms found in other animals. In mammals, for instance, the vagus nerve acts as a critical pathway connecting the CNS and ENS (Berthoud, 2008; Cui et al., 2022; Watts et al., 2022). Enteroendocrine cells within the gastrointestinal tract are capable of detecting the presence of sugars, proteins, and fats in ingested food, subsequently releasing a variety of signaling molecules that modulate vagus nerve activity, either through activation or inhibition (Berthoud, 2008; Roh & Choi, 2023; Roura, Depoortere, & Navarro, 2019). The vagus nerve then relays this information from the ENS to the CNS by projecting its axons to the nucleus of the solitary tract (NTS) in the brainstem (Chen et al., 2020). Notably, neurons in the caudal regions of the nucleus of the solitary tract (NTS) also project to vagal efferent neurons in the dorsal motor nucleus of the vagus (DMV), regulating parasympathetic gastrointestinal functions such as insulin secretion and gastric emptying (Grill & Hayes, 2012). This establishes a gut-brain-gut sensorimotor neural circuit loop similar to the one we have identified in *Drosophila*.

One important question from our findings is why this neural circuit, which starts and ends in the gut, takes a detour through the brain. Why don’t the enteric sensory neurons and motor

neurons directly connect to form a local circuit? Neural circuits for food intake have been studied in other invertebrates, especially in crustaceans, particularly in lobster and crayfish. In these animals, the well-known central pattern generator (CPG) circuit was revealed in the stomatogastric ganglion (STG) in their ENS (Delcomyn, 1980; Ronald M Harris-Warrick, 1992; Heinzel, 1988). So far, there have been no conclusive studies on whether the crustacean STG is homologous to the Drosophila HCG or on the evolutionary relationship between these structures. However, given their functional similarity, I believe it is reasonable to assume that the crustaceans STG shares at least partial functional homology with the *Drosophila* ENS for the purposes of this study. One of the significant traits of the CPG circuit in the crustacean STG is its independence from the CNS: even when the whole STG is taken out from the animal, eliminating all sensory and motor feedback, the firing patterns of these neurons are similar to those recorded in vivo (Ronald M. Harris-Warrick, 1992). Given the remarkable independence of the crustaceans STG, it is a reasonable question why the *Drosophila* HCG neurons studied in this research must take a detour to the central brain and interact with IN1 to regulate food ingestion.

I would like to address this question from a physiological perspective. Physiologically, it may be necessary for fruit flies to integrate sensory input from the gut with input from other sensory organs and internal signals about their physiological status. This integration allows them to regulate how long to keep their crop duct open, adjusting the amount of food transported into their crop based on factors such as food composition, the animal's internal needs, and external environmental conditions. For example, if a predator is approaching a fly while it is eating, the fly must swiftly detect that looming visual stimulus and quickly incorporate this visual input into its food intake decision-making circuit. This enables the fly to immediately stop eating and switch to fleeing mode, regardless of how appealing the food is. Considering this scenario can

represent a common threat for adult flies in their natural environment, it is likely that the detour through the brain in the gut-brain-gut circuit enables flies to adapt their feeding behavior to both varying metabolic needs and rapidly changing external environmental challenges.

In the future, we anticipate that further research will shed light on the mechanisms regulating food intake in *Drosophila*, building upon the neural circuit loop we have uncovered. For example, the gastrointestinal tract of the fly is known to secrete a variety of signaling molecules that are involved in food intake regulation (Nassel, 2018). Investigating how this endocrine system interacts with the neural circuit governing food intake presents a promising avenue for further inquiry. We further anticipate that our research may contribute to a deeper understanding of the mechanisms underlying food intake-related disorders in humans, such as diabetes, obesity, and eating disorders like anorexia nervosa, thereby facilitating the development of new and more effective therapies for these diseases.

From a broader perspective, as brain-body communication is becoming a more and more popular research field, not only the brain-gut axis but also more and more axes connecting the brain and other body organs, and the axes connecting different body organs await revelation (Sammons et al., 2024). Eventually, with all these axes characterized, a comprehensive diagram of the brain-body communication network will be established. Such a fully charted brain-body web will significantly enhance our understanding of how the body functions as an integrated system, and tremendously help us to develop novel therapies to combat human diseases.

Last but not least, considering feeding behavior regulation is such a basic and fundamental function of the nervous system in animals, we anticipate the full understanding of feeding behavior regulation mechanisms can lead to the beginning of the total understanding of all the functions of the brain, which includes many other more complicated cognitive functions

such as learning and memory (Morris & Dolan, 2001), spatial navigation, and emotion controls (MacCormack & Lindquist, 2019). I believe that just as completing the corners and edges of a jigsaw puzzle is often the beginning of completing the entire puzzle, our understanding of eating behavior – one of the most fundamental and ancient animal behaviors – can serve as a primer to guide us in the future to unravel more intricate mechanisms of brain function and, ultimately, help us fully understand the mysteries of our mind.

REFERENCES

Berthoud, H. R. (2008). The vagus nerve, food intake and obesity. *Regul Pept, 149*(1-3), 15-25. https://doi.org/10.1016/j.regpep.2007.08.024

Chen, J., Cheng, M., Wang, L., Zhang, L., Xu, D., Cao, P., Wang, F., Herzog, H., Song, S., & Zhan, C. (2020). A Vagal-NTS Neural Pathway that Stimulates Feeding. *Curr Biol, 30*(20), 3986-3998 e3985. https://doi.org/10.1016/j.cub.2020.07.084

Cui, X., Gruzdeva, A., Kim, H., & Yapici, N. (2022). Of flies, mice and neural control of food intake: lessons to learn from both models. In *Current Opinion in Neurobiology* (Vol. 73): Elsevier Ltd.

Delcomyn, F. (1980). Neural basis of rhythmic behavior in animals. *Science, 210*(4469), 492-498. https://doi.org/10.1126/science.7423199

Grill, H. J., & Hayes, M. R. (2012). Hindbrain neurons as an essential hub in the neuroanatomically distributed control of energy balance. *Cell Metab, 16*(3), 296-309. https://doi.org/10.1016/j.cmet.2012.06.015

Harris-Warrick, R. M. (1992). *Dynamic biological networks: the stomatogastric nervous system*. MIT press.

Heinzel, H. G. (1988). Gastric mill activity in the lobster. I. Spontaneous modes of chewing. *J Neurophysiol, 59*(2), 528-550. https://doi.org/10.1152/jn.1988.59.2.528

MacCormack, J. K., & Lindquist, K. A. (2019). Feeling hangry? When hunger is conceptualized as emotion. *Emotion, 19*(2), 301-319. https://doi.org/10.1037/emo0000422

Morris, J. S., & Dolan, R. J. (2001). Involvement of human amygdala and orbitofrontal cortex in hunger-enhanced memory for food stimuli. *J Neurosci, 21*(14), 5304-5310. https://doi.org/10.1523/JNEUROSCI.21-14-05304.2001

Nassel, D. R. (2018). Substrates for Neuronal Cotransmission With Neuropeptides and Small Molecule Neurotransmitters in Drosophila. *Front Cell Neurosci*, *12*, 83. https://doi.org/10.3389/fncel.2018.00083

Roh, E., & Choi, K. M. (2023). Hormonal Gut-Brain Signaling for the Treatment of Obesity. *Int J Mol Sci*, *24*(4). https://doi.org/10.3390/ijms24043384

Roura, E., Depoortere, I., & Navarro, M. (2019). Review: Chemosensing of nutrients and non-nutrients in the human and porcine gastrointestinal tract. *Animal*, *13*(11), 2714-2726. https://doi.org/10.1017/S1751731119001794

Sammons, M., Popescu, M. C., Chi, J., Liberles, S. D., Gogolla, N., & Rolls, A. (2024). Brain-body physiology: Local, reflex, and central communication. *Cell*, *187*(21), 5877-5890. https://doi.org/10.1016/j.cell.2024.08.050

Watts, A. G., Kanoski, S. E., Sanchez-Watts, G., & Langhans, W. (2022). THE PHYSIOLOGICAL CONTROL OF EATING: SIGNALS, NEURONS, AND NETWORKS. In *Physiological Reviews* (Vol. 102, pp. 689-813): American Physiological Society.